



National Library
of Canada

Bibliothèque nationale
du Canada

Canadian Theses Service

Services des thèses canadiennes

Ottawa, Canada
K1A 0N4

CANADIAN THESES

THÈSES CANADIENNES

NOTICE

The quality of this microfiche is heavily dependent upon the quality of the original thesis submitted for microfilming. Every effort has been made to ensure the highest quality of reproduction possible.

If pages are missing, contact the university which granted the degree.

Some pages may have indistinct print especially if the original pages were typed with a poor typewriter ribbon or if the university sent us an inferior photocopy.

Previously copyrighted materials (journal articles, published tests, etc.) are not filmed.

Reproduction in full or in part of this film is governed by the Canadian Copyright Act, R.S.C. 1970, c. C-30.

**THIS DISSERTATION
HAS BEEN MICROFILMED
EXACTLY AS RECEIVED**

AVIS

La qualité de cette microfiche dépend grandement de la qualité de la thèse soumise au microfilmage. Nous avons tout fait pour assurer une qualité supérieure de reproduction.

S'il manque des pages, veuillez communiquer avec l'université qui a conféré le grade.

La qualité d'impression de certaines pages peut laisser à désirer, surtout si les pages originales ont été dactylographiées à l'aide d'un ruban usé ou si l'université nous a fait parvenir une photocopie de qualité inférieure.

Les documents qui font déjà l'objet d'un droit d'auteur (articles de revue, examens publiés, etc.) ne sont pas microfilmés.

La reproduction, même partielle, de ce microfilm est soumise à la Loi canadienne sur le droit d'auteur, SRC 1970, c. C-30.

**LA THÈSE A ÉTÉ
MICROFILMÉE TELLE QUE
NOUS L'AVONS REÇUE**

THE UNIVERSITY OF ALBERTA

MAGNETIC RELAXATION STUDIES OF MOLECULAR ROTATION IN LIQUIDS

by

DO HYUNG LEE

A THESIS

SUBMITTED TO THE FACULTY OF GRADUATE STUDIES AND RESEARCH

IN PARTIAL FULFILMENT OF THE REQUIREMENTS FOR THE DEGREE

OF DOCTOR OF PHILOSOPHY

DEPARTMENT OF CHEMISTRY

EDMONTON, ALBERTA

SPRING 1987,

Permission has been granted to the National Library of Canada to microfilm this thesis and to lend or sell copies of the film.

The author (copyright owner) has reserved other publication rights, and neither the thesis nor extensive extracts from it may be printed or otherwise reproduced without his/her written permission.

L'autorisation a été accordée à la Bibliothèque nationale du Canada de microfilmer cette thèse et de prêter ou de vendre des exemplaires du film.

L'auteur (titulaire du droit d'auteur) se réserve les autres droits de publication; ni la thèse ni de longs extraits de celle-ci ne doivent être imprimés, ou autrement reproduits sans son autorisation écrite.

ISBN 0-315-37638-4



University of Alberta
Edmonton

Department of Chemistry
Faculty of Science

Canada T6G 2G2

Chemistry Building, Telephone (403) 432-3254

February 13, 1987

To: Faculty of Graduate Studies and Research

From: R. E. D. McClung,
Department of Chemistry

Re: Copywrite Permission for Ph. D. Thesis of D. H. Lee

I hereby give my permission for the inclusion of material from the articles:

"The Fokker-Planck-Langevin Model for Rotational Brownian Motion IV. Asymmetric Top Molecules." by D. H. Lee and R. E. D. McClung. (Accepted for publication in Chemical Physics, 1987)

"The Fokker-Planck-Langevin Model for Rotational Brownian Motion V. Comparison with Magnetic Relaxation Data for Asymmetric Top Molecules." by D. H. Lee and R. E. D. McClung. (Accepted for publication in Journal of Magnetic Resonance, 1987).

"Nuclear Relaxation and Molecular Motion in 1,3,5-Trifluorobenzene- d_3 in Liquid Solution." by D. H. Lee and R. E. D. McClung. (Submitted for publication in Chemical Physics, 1987)

In the Ph. D. thesis of Do H. Lee. Permission is also granted for microfilming of this material by the National Library of Canada.

Sincerely

THE UNIVERSITY OF ALBERTA

RELEASE FORM

NAME OF AUTHOR DO HYUNG LEE

TITLE OF THESIS MAGNETIC RELAXATION STUDIES OF MOLECULAR ROTATION
IN LIQUIDS

DEGREE FOR WHICH THESIS WAS PRESENTED DOCTOR OF PHILOSOPHY

YEAR THIS DEGREE GRANTED 1987

Permission is hereby granted to THE UNIVERSITY OF ALBERTA
LIBRARY to reproduce single copies of this thesis and to lend or
sell such copies for private, scholarly or scientific research
purposes only.

The author reserves other publication rights, and neither the
thesis nor extensive extracts from it may be printed or otherwise
reproduced without the author's written permission.

(Signed) *D. H. Lee*

PERMANENT ADDRESS:

*773. Kyong Joo,
Kyeong Boek, Korea*

DATED *Dec. 18*, 19 *86*

THE UNIVERSITY OF ALBERTA
FACULTY OF GRADUATE STUDIES AND RESEARCH

The undersigned certify that they have read, and recommend to the
Faculty of Graduate Studies and Research, for acceptance, a thesis
entitled MAGNETIC RELAXATION STUDIES OF MOLECULAR ROTATION IN LIQUIDS
submitted by DO HYUNG LEE
in partial fulfilment of the requirements for the degree of
DOCTOR OF PHILOSOPHY

R. McElroy
Supervisor

George Stetsky
to him

S. Huzenaye

James Embury

R. Paul
External Examiner

DATE Feb 13, 1987

ABSTRACT

The theoretical formulation of the Fokker-Planck-Langevin (FPL) model for the rotational dynamics of asymmetric top molecules and applications of the FPL model and the J-diffusion limit of the extended diffusion (EDJ) model to the asymmetric top molecules, fluorobenzene- d_5 and chlorine dioxide, and the symmetric top molecule, 1,3,5-trifluorobenzene- d_3 (TFB), are presented. Numerical calculations of the FPL reorientational correlation functions, correlation times, and spin-rotational functions show that these properties are sensitive to frictional anisotropy which is a distinct feature of the FPL model. The comparison of the FPL reorientational correlation times and spin-rotational functions for the case of an isotropic friction tensor with the corresponding EDJ correlation times and functions shows that the predictions of the two models are significantly different only in the region where free rotation and precessional effects become important.

The rotational motion of fluorobenzene- d_5 is found to be better described in terms of the FPL model, including the effects of frictional anisotropy, than in terms of the EDJ model from a comparison of the relationships between the reorientational correlation times and the angular momentum correlation times predicted by the two models with the experimental results obtained from nuclear relaxation measurements. The ESR linewidths of chlorine dioxide in various solvents are found to be in agreement with the predictions of the FPL model in strongly interacting solvents, but

the agreement is poor in very weakly interacting solvents.

In the application of the FPL and EDJ models to the rotational motion of TFB in various solvents, it is found that the observed variations of the reorientational correlation times with the angular momentum correlation times in most solutions are well explained in terms of the FPL model by taking into account the effect of frictional anisotropy, but not in terms of the EDJ model. The viscosity and temperature dependence of the reorientational correlation times are analyzed in terms of a modified Debye equation and the variation of the anisotropic interaction parameter, κ , with solvent is discussed in terms of molecular size and dipole moment of solvent molecules.

ACKNOWLEDGEMENTS

I would like to thank Professor R.E.D. McClung for his helpful guidance and encouragement during the course of this work.

I would also like to thank Dr. B. John for his useful advice and a great deal of practical assistance.

TABLE OF CONTENTS

CHAPTER	PAGE
I. INTRODUCTION.....	1
References.....	11
II. THE FOKKER-PLANCK-LANGEVIN MODEL FOR ROTATIONAL BROWNIAN MOTION. IV. ASYMMETRIC TOP MOLECULES.....	14
1. Introduction.....	14
2. Theory.....	19
A. Rotational Fokker-Planck equation and its general solution.....	19
B. Reorientational correlation functions and correlation times.....	25
C. Spin-rotation relaxation times.....	28
D. Angular velocity correlation functions.....	32
3. Numerical Calculations.....	33
A. FPL model.....	33
B. EDJ model.....	47
4. Discussion.....	51
5. Conclusion.....	59
References.....	61
III. THE FOKKER-PLANCK-LANGEVIN MODEL FOR ROTATIONAL BROWNIAN MOTION. V. COMPARISON WITH MAGNETIC RELAXATION DATA FOR ASYMMETRIC TOP MOLECULES.....	64
1. Introduction.....	64

2.	Theory.....	65
A.	FPL model.....	65
B.	EDJ model.....	68
3.	Results and Discussion.....	71
A.	Fluorobenzene- d_5	71
B.	Chlorine dioxide.....	78
4.	Conclusion.....	89
	References.....	90
IV.	NUCLEAR RELAXATION AND MOLECULAR MOTION OF 1,3,5-TRI- FLUOROBENZENE- d_3 IN LIQUID SOLUTIONS.....	92
	1. Introduction.....	92
2.	Experimental.....	103
3.	Results.....	105
4.	Discussion.....	113
A.	Relationship between τ_θ and τ_J	113
B.	Relationship between τ_θ , D , and solution viscosity.....	118
5.	Conclusion.....	127
	References.....	129
V.	GENERAL DISCUSSION.....	135
	References.....	140
APPENDIX I	EDJ MODEL FOR ASYMMETRIC TOP MOLECULES.....	142
	References.....	152
APPENDIX II	INSTRUMENTATION FOR NMR EXPERIMENTS.....	153
	References.....	158

LIST OF TABLES

TABLE	PAGE
II-1 Correspondence between the index pair (k, σ) and cartesian dipole and polarizability tensor components.....	36
IV-1 Analysis of T_{1D} and T_{1F} for TFB in various solvents.....	106
IV-2 Anisotropy parameters of TFB, hydrodynamic radius, and properties of solvents.....	117

LIST OF FIGURES

FIGURE		PAGE
II-1	FPL reorientational correlation functions for asymmetric top molecule.....	37
II-2	Comparison of reorientational self-correlation and cross-correlation times computed with the EDJ model and with the FPL model for $\tau_x = \tau_y = \tau_z$ for asymmetric top molecule.....	39
II-3	Variation of FPL reorientational self-correlation times with frictional anisotropy.....	42
II-4	Spin-rotation functions $F_{\alpha\beta}$ and $F_{\alpha\beta}^{EDJ}$ for asymmetric top molecule.....	45
III-1	Comparison of correlation times from the EDJ model (curve 1), from the FPL model with $\tau_x = \tau_y = \tau_z$ (curve 2), and from the nuclear relaxation times in C_6D_5F liquid (●).....	75
III-2	Comparison of correlation times from FPL model with $\tau_x = 3.5\tau_y = 3.5\tau_z$ (solid curve), and from the nuclear relaxation times in C_6D_5F liquid (●).....	79
III-3	Observed ESR linewidths of ClO_2 in CCl_4 (■), $CHCl_3$ (●) and acetone (X) and linewidths predicted by the FPL model.....	83
III-4	Comparison of τ_J (●) and τ_x (□) for ClO_2 in n-pentane (1), CCl_4 (2), $CHCl_3$ (3), and acetone (4) obtained with	

the EDJ model (τ_j) and the FPL model (τ_x) with

$$\tau_x = \tau_y = \tau_z \dots \dots \dots 87$$

- IV-1 Reorientational and angular momentum correlation times for TFB in 0.15 mol fraction solutions compared with FPL (curve a - $\tau_{||}/\tau_{\perp} = 5$, b - $\tau_{||}/\tau_{\perp} = 2$, c - $\tau_{||}/\tau_{\perp} = 1$, d - $\tau_{||}/\tau_{\perp} = 0.2$) and EDJ (curve e) models. 114

- IV-2 Viscosity-temperature dependence of reorientational correlation times for TFB in 0.15 mol fraction solutions.

▲ - acetonitrile, ● - chloroform, □ - methanol,

□ - tetrachloroethylene. Lines correspond to

1 - $\kappa = 0.27$, $\tau_0 = 0.48$; 2 - $\kappa = 0.23$, $\tau_0 = 0.22$,

3 - $\kappa = 0.20$, $\tau_0 = 0.24$; 4 - $\kappa = 0.16$, $\tau_0 = 0.52$ 119

CHAPTER I

I. INTRODUCTION

The study of molecular reorientation in liquids has been the subject of many theoretical and experimental works. In a description of the rotational motion in liquids, one is concerned with the orientation of a coordinate system fixed in the molecule with respect to a laboratory coordinate system, and with the magnitude and direction of the rotational angular momentum of the molecule. The time dependence of the orientation of the molecule is characterized by the reorientational correlation time τ_0 , and the time dependence of the rotational angular momentum of the molecule is characterized by the angular momentum correlation time τ_J . A knowledge of these correlation times for a given molecule can provide useful information about the nature of molecular rotation in liquids. One usually compares the theoretical relationship between the reorientational correlation time and the angular momentum correlation time predicted by a model for molecular rotation in liquids with the experimental relationship between them. A number of theoretical models for the rotational motion of molecules in liquids have been proposed. The simplest and most commonly used model was developed by Debye [1] for the analysis of the reorientational correlation times arising in dielectric relaxation. The Debye model was developed on the basis

that the molecule of interest behaved like a large spherical particle immersed in a continuous viscous medium and followed a rotational random walk involving steps of small angular displacement. This assumes that τ_J is very short compared to τ_θ . However, it was found that τ_J and τ_θ were of the same order of magnitude in some cases [2-4] so that any interpretation of experimental observations in such cases, using the Debye model, was questionable. When τ_θ and τ_J are of the same order of magnitude, the molecules reorient through large angles during the rotational diffusive steps and the rotational motion is similar to that in dilute gases where the molecules rotate freely during the time intervals between collisions. The concept of these "inertial" effects in the rotational diffusive steps was widely discussed [5-9], but was not incorporated into a theory in an exact fashion until 1966 when Gordon [10] proposed an extension, for linear molecules, of the Debye model, in which he removed the restriction on the size of the rotational steps. Other workers have extended this extended rotational diffusion (ED) model to spherical [11-13], symmetric [13,14], and asymmetric [15,16] top molecules, and to the perpendicular bands of linear molecules [17]. In this ED model, it is assumed that the molecules rotate freely during the rotational diffusive steps and each step is terminated by a random impulsive torque which reflects the Brownian motion of the molecules. This impulsive torque or "collision" randomizes the angular momentum of the molecule. Two limiting cases have been proposed: the J-diffusion (EDJ) and M-diffusion (EDM) limits. In the case of J-

diffusion, both the orientation and magnitude of the angular momentum vector are randomized at each "collision", while in the case of M-diffusion only the orientation is randomized. It has been shown [18] that the EDJ model reduces to the Debye model in the small angle or rotational diffusion limit. In this limit, τ_0 is inversely proportional to τ_J [18, 19]. On the other hand, in the dilute gas limit, both EDJ and EDM models give results similar to that of the perturbed free rotor model [4] in which τ_0 is proportional to τ_J . The predictions of the ED model have been compared with experimental observations for various types of molecules [18]. Many applications have compared the theoretical relationship between τ_0 and τ_J with the experimentally observed variation of τ_0 with τ_J . In most cases, the EDJ model has been found to be in good agreement with the experimental observations [20-26].

The fundamental approximation in the ED model is the assumption of instantaneous "collisions", and it is expected that this assumption will begin to break down in liquids of very high densities. In 1969, Fixman and Rider [13] proposed another model, the Fokker-Planck-Langevin (FPL) model, for molecular rotation in liquids. This model is based on a rotational Fokker-Planck equation for the conditional probability density of the orientation and angular velocity of a molecule and a rotational Langevin equation for the angular velocity. A derivation of the rotational Fokker-Planck equation is presented below. (See ref. 27 for more details.) Let $P(\omega, \Omega, t; \omega_0, \Omega_0)$ represent the conditional probability-density that

a molecule has angular velocity between ω and $\omega + d\omega$ and orientation between Ω and $\Omega + d\Omega$ at time t , given that it had angular velocity between ω_0 and $\omega_0 + d\omega_0$ and orientation between Ω_0 and $\Omega_0 + d\Omega_0$ at time zero. If the rotational motion is assumed to be Markoff process,

$$P(\omega, \Omega, t+\Delta t; \omega_0, \Omega_0) = \int d(\Delta\omega) \int d(\Delta\Omega) \quad (I-1)$$

$$\times P(\omega, \Omega, \Delta t; \omega-\Delta\omega, \Omega-\Delta\Omega) P(\omega-\Delta\omega, \Omega-\Delta\Omega, t; \omega_0, \Omega_0)$$

The last factor in Eq. (I-1) can be expressed as

$$P(\omega-\Delta\omega, \Omega-\Delta\Omega, t; \omega_0, \Omega_0) = \exp(-i\theta \cdot J) \exp(-\Delta\omega \cdot \nabla_\omega) \times P(\omega, \Omega, t; \omega_0, \Omega_0) \quad (I-2)$$

where J is the infinitesimal rotation operator referred to the molecular coordinate system, and $\Delta\Omega$ is a rotation through angle θ about the direction of θ . It is assumed that for small Δt , $P(\omega, \Omega, \Delta t; \omega-\Delta\omega, \Omega-\Delta\Omega)$ is zero unless $\theta = \omega \Delta t$ so that Eq. (I-1) becomes

$$P(\omega, \Omega, t+\Delta t; \omega_0, \Omega_0) = \int d(\Delta\omega) f(\omega, \Delta t; \omega-\Delta\omega) P(\omega-\Delta\omega, \Omega-\Delta\Omega, t; \omega_0, \Omega_0) \quad (I-3)$$

where $f(\omega, \Delta t; \omega - \Delta\omega)$ is the probability density of a change in angular velocity from $\omega - \Delta\omega$ to ω in time Δt . Application of the operator $\exp(i\omega \cdot J \Delta t)$ to Eq. (I-3), expansion of the left-hand side of the resulting equation as a power series in Δt , McLaurin expansion for $\exp(-\Delta\omega \cdot \nabla_\omega)$ and $\exp(i\omega \cdot J \Delta t)$, and neglect of the higher order terms give

$$\left(\frac{\partial}{\partial t} + i\omega \cdot J\right) P(\omega, \Omega, t; \omega_0, \Omega_0) \Delta t = - \sum_{\alpha=x,y,z} \frac{\partial}{\partial \omega_\alpha} [\langle \Delta\omega_\alpha \rangle P] + \frac{1}{2} \sum_{\alpha, \beta=x,y,z} \frac{\partial}{\partial \omega_\alpha} \frac{\partial}{\partial \omega_\beta} [\langle \Delta\omega_\alpha \Delta\omega_\beta \rangle P] \quad (I-4)$$

where $\langle \Delta\omega_\alpha \rangle$ and $\langle \Delta\omega_\alpha \Delta\omega_\beta \rangle$ are ensemble averages with weighting function $f(\omega, \Delta t; \omega - \Delta\omega)$ and P represents $P(\omega, \Omega, t; \omega_0, \Omega_0)$.

In order to evaluate the ensemble averages, the rotational Langevin equation is used to describe the evolution of the angular velocity:

$$\dot{\omega}_\alpha = r_\alpha \omega_\beta \omega_\gamma - \tau_\alpha^{-1} \omega_\alpha + A_\alpha(t) \quad (I-5)$$

where $r_\alpha = (I_\beta - I_\gamma)/I_\alpha$, I_α , I_β , I_γ are the principal moments of inertia, τ_α^{-1} is the friction coefficient of retarding torque, and $A_\alpha(t)$ is associated with rapidly fluctuating Brownian torques.

Integrating Eq. (I-5) over a short time interval Δt , one obtains

$$\Delta\omega_\alpha = (r_\alpha \omega_\beta \omega_\gamma - \tau_\alpha^{-1} \omega_\alpha) \Delta t + \int_t^{t+\Delta t} A_\alpha(t') dt' \quad (I-6)$$

Using Eq. (I-6) and unique properties of ensemble averages of $\Lambda_\alpha(t)$, the ensemble averages in Eq. (I-4) can be evaluated, and one obtains

$$\frac{\partial}{\partial t} P = - \sum_{\alpha=x,y,z} \left\{ i \omega_\alpha J_\alpha - \frac{\partial}{\partial \omega_\alpha} (E_\alpha) - a_\alpha \frac{\partial^2}{\partial \omega_\alpha^2} \right\} P \quad (I-7)$$

where

$$E_\alpha = \tau_\alpha^{-1} \omega_\alpha - r_{\alpha\beta} \omega_\beta \omega_\gamma \quad (I-8)$$

$$a_\alpha = (k_B T / I_\alpha) \tau_\alpha^{-1} \quad (I-9)$$

Eq. (I-7) is a rotational Fokker-Planck equation which is the basis of the FPL model. In the FPL model the rotational motion of a molecule is approximated by that of an appropriately shaped solid object immersed in a continuous viscous fluid. The angular velocity of the molecule is assumed to be modulated by slowly varying viscosity dependent retarding torques, and by rapidly fluctuating Brownian torques which reflect the molecular nature of the liquid.

There is a marked difference in the basic physical pictures in the ED and FPL models. In the ED model, only the rapidly fluctuating Brownian torques are considered, and they are assumed to manifest themselves as instantaneous collisions which produce large random changes in the angular velocity. In the FPL model, on the other hand, a large number of fluctuations in the Brownian torques are

7

required to change the angular velocity significantly, while the retarding torques act continuously causing the angular velocity to reduce to its ensemble average value of zero.

Fixman and Rider [13] have derived exact expressions for the reorientational correlation functions and spectral densities for linear and spherical top molecules. The correlation functions were expressed as infinite series whose terms were simple exponential functions of time, and the series were found to converge rapidly so that accurate numerical values were obtained with a small number of terms in the truncated series. Hubbard [27,28] has also considered the FPL model and has attempted to obtain the general solution for the conditional probability density from the Fokker-Planck equation, but his perturbation approach has a limited range of validity. He obtained approximate expressions for the reorientational correlation time associated with nuclear dipole-dipole interactions and nuclear quadrupolar interactions, and the correlation time for the spin-rotational interactions for spherical top molecules. Evans [29,30] has also derived approximate expressions for the FPL reorientational correlation functions and correlation times for spherical and symmetric top molecules by a cumulant expansion technique. The results of these approximate methods were valid only for strong intermolecular interactions. The FPL model has also been discussed by Powles and Rickayzen [31] but they were concerned only with the reorientational correlation times which arise in dielectric relaxation and intramolecular dipolar magnetic relaxation of linear and spherical molecules.

General expressions for the reorientational correlation functions, correlation times, memory functions, and spectral densities for linear, spherical [32], and symmetric top [33] molecules and the correlation times for spin-rotation interactions in spherical [32] and symmetric top [33] molecules have been derived using the eigenfunction expansion technique employed by Fixman and Rider [13]. For symmetric top molecules, a new feature is present in the FPL model: anisotropy in the motional modulation of the angular velocity components, which is referred to as frictional anisotropy [33]. The numerical calculation of the reorientational correlation functions, correlation times, spectral densities and the correlation times for spin-rotation interactions showed that these properties were significantly affected by frictional anisotropy [33].

Several workers [34-37] have examined the applicability of the FPL model for linear and spherical top molecules by comparing with the experimental results of Raman studies of CF_4 [34] and SF_6 [35], infrared studies of N_2O [36] and CO [38], and nuclear magnetic relaxation studies of CCl_4 [39]. It was found that the FPL model described the rotational motion of these linear and spherical molecules reasonably well. In addition, the FPL model has been compared with the EDJ model and it was found that both models, although they are based on very different physical pictures of the rotational dynamics, appeared to give similar characterizations of the rotational motion of molecules in liquids [35-37].

In this work, we extend the FPL model to asymmetric top molecules and examine the applicability of the EDJ and FPL models for asymmetric and symmetric top molecules by comparing the predictions of the models with experimental results from magnetic relaxation studies of C_6D_5F [23], ClO_2 [40], and 1,3,5-trifluorobenzene- d_3 (TFB).

In Chapter II, the exact series expansion for the angular velocity-orientation conditional probability density is obtained from the rotational Fokker-Planck equation for asymmetric top molecules. From this general expansion, expressions for the reorientational correlation functions, correlation times, spectral densities and the correlation times for spin-rotation interactions are derived. The effects of frictional anisotropy on these properties are investigated by numerical calculations. Furthermore, the FPL model is compared with the EDJ model for asymmetric top molecules.

In Chapter III, the applicability of the FPL and EDJ models for asymmetric top molecules is tested by comparing correlation times obtained from magnetic relaxation data for asymmetric top molecules C_6D_5F [23] and ClO_2 [40] with the predictions of the two models.

In Chapter IV, 2D and ^{19}F spin-lattice relaxation measurements on the symmetric top molecule TFB in 0.15 mole fraction solutions in various solvents over the temperature range 270 - 400 K are reported. The applicability of the FPL and EDJ models in describing the rotational motion of symmetric top molecules in liquids is tested by comparing the correlation times obtained in the nuclear relaxation

study with the correlation times predicted by the two models. The anisotropic interaction parameters κ [40,41] for TFB in each solvent are obtained from the viscosity-temperature dependence of the reorientational correlation times, and the variation of κ with solvent is discussed.

References

1. P. Debye, **Polar Molecules** (Reinhold, New York, 1929), pp. 77ff.
2. W.R. Hackleman and P.S. Hubbard, *J. Chem. Phys.* **39** (1963) 2688.
3. P. Rigny and J. Virlet, *J. Chem. Phys.* **47** (1967) 4645.
4. M. Bloom, F. Bridges, and W.N. Hardy, *Can. J. Phys.* **45** (1967) 3533.
5. W.A. Steele, *J. Chem. Phys.* **38** (1963) 2404.
6. W.A. Steele, *J. Chem. Phys.* **38** (1963) 2411.
7. W.B. Moniz, W.A. Steele, and J.A. Dixon, *J. Chem. Phys.* **38** (1963) 2418.
8. D.E. Woessner, *J. Chem. Phys.* **40** (1964) 2341.
9. H. Shimizu, *J. Chem. Phys.* **43** (1965) 2453.
10. R.G. Gordon, *J. Chem. Phys.* **44** (1966) 1830.
11. R.E.D. McClung, *J. Chem. Phys.* **51** (1969) 3842.
12. R.E.D. McClung, *J. Chem. Phys.* **55** (1971) 3459.
13. M. Fixman and K. Rider, *J. Chem. Phys.* **51** (1969) 2425.
14. R.E.D. McClung, *J. Chem. Phys.* **57** (1972) 5478.
15. J.C. Leicknam, Y. Guissani, and S. Bratos, *J. Chem. Phys.* **68** (1978) 3380.
16. T.E. Bull, *J. Chem. Phys.* **81** (1984) 3181.
17. C. Dreyfus and T. Nguyen Tan, *J. Chem. Phys.* **62** (1975) 2492.
18. R.E.D. McClung, *Adv. Mol. Relaxation Process* **10** (1977) 83.
19. P.S. Hubbard, *Phys. Rev.* **131** (1963) 1155.

20. T.C. Farrar, A.A. Maryott, and M.S. Malmberg, J. Chem. Phys. 54 (1971) 64.
21. K.T. Gillen, D.C. Douglass, M.S. Malmberg, and A.A. Maryott, J. Chem. Phys. 57 (1972) 5170.
22. R.A. Assink, J. DeZwaan, and J. Jonas, J. Chem. Phys. 56 (1972) 4975.
23. R.A. Assink and J. Jonas, J. Chem. Phys. 57 (1972) 3329.
24. J. DeZwaan, R.J. Finney, and J. Jonas, J. Chem. Phys. 60 (1974) 3223.
25. T.E. Bull, J. Chem. Phys. 59 (1973) 6173.
26. T.E. Bull, J. Chem. Phys. 62 (1975) 222.
27. P.S. Hubbard, Phys. Rev. A6 (1972) 2421.
28. P.S. Hubbard, Phys. Rev. A8 (1974) 1429.
29. G.T. Evans, J. Chem. Phys. 65 (1976) 3030.
30. G.T. Evans, J. Chem. Phys. 67 (1977) 2911.
31. J.G. Powles and G. Rickayzen, Mol. Phys. 33 (1977) 1207.
32. R.E.D. McClung, J. Chem. Phys. 73 (1980) 2435.
33. R.E.D. McClung, J. Chem. Phys. 75 (1981) 5503.
34. S. Perry, V.H. Schiemann, M. Wolfe, and J. Jonas, J. Phys. Chem. 85 (1981) 2805.
35. T.W. Zerda, J. Schroeder, and J. Jonas, J. Chem. Phys. 75 (1981) 1612.
36. G. Lévi, J.P. Marsault, F. Marsault-Hérail, and R.E.D. McClung, J. Chem. Phys. 73 (1980) 2443.
37. P.S. Hubbard, Phys. Rev. A9 (1974) 481.

38. J.P. Marsault, F. Marsault-Hérail, and G. Lévi, J. Chem. Phys. 62 (1975) 893.
39. K.T. Gillen, J.H. Noggle, and T.K. Leipert, Chem. Phys. Lett. 17 (1972) 505.
40. R.E.D. McClung and D. Kivelson, J. Chem. Phys. 49 (1968) 3380.
41. D. Kivelson, M.G. Kivelson, and I. Oppenheim, J. Chem. Phys. 52 (1970) 1810.

CHAPTER II

THE FOKKER-PLANCK-LANGEVIN MODEL FOR ROTATIONAL BROWNIAN

MOTION. IV. ASYMMETRIC TOP MOLECULES¹

1. Introduction

The rotational motion of molecules in liquids can be characterized by two important parameters: the reorientational correlation time τ_θ , and the angular momentum correlation time τ_J . The relationship between these two correlation times can be used to test the applicability of theoretical models for molecular rotation in liquids. A number of theoretical models have been proposed. The simplest and most commonly used model is the Debye small angle diffusion model [1] which is based on the assumption that the rotational motion of a molecule consists of a progression of uncorrelated rotational diffusive steps of short duration. In other words, the duration of each rotational diffusive step is short compared to the time required for a molecule to make a complete revolution so that, in a single diffusive step, the molecular orientation would change only infinitesimally. This assumption also implies that the correlation time τ_J for the angular momentum of a molecule is short compared to the reorientational correlation time τ_θ . In this model, the conditional probability that a molecule has orientation $\Omega(t)$ at time t , given that it had orientation $\Omega(0)$ at

¹A version of this chapter has been accepted for publication. D.H. Lee and R.E.D. McClung, 1986. Chemical Physics.

time zero, obeys a rotational diffusion equation.

In 1966, Gordon [2] extended the Debye model by removing the restriction on the duration of the rotational diffusive steps for linear molecules. Other workers have extended Gordon's model to spherical [3,4,5], symmetric [4,6], and asymmetric top [7,8] molecules, and to the perpendicular bands of linear molecules [9]. In this Extended Diffusion (ED) model, the molecules are assumed to rotate freely during the rotational diffusion steps and each step is terminated by a random impulsive torque which reflects the Brownian motion of the molecules. This impulsive torque or "collision" randomizes the angular momentum of the molecule. Two limiting cases have been proposed: the J-diffusion (EDJ) and M-diffusion (EDM) limits. In the case of J-diffusion, both the orientation and magnitude of the angular momentum vector are randomized at each "collision", while in the case of M-diffusion only the orientation is randomized. The durations of the rotational diffusive steps are random and follow a Poisson distribution. Many experimental investigations [10-19] have suggested that the rotational motion in liquids is well described by the EDJ model.

In 1969, Fixman and Rider [4] proposed the Fokker-Planck-Langevin (FPL) model for the molecular rotation in liquids. This model is based on a rotational Fokker-Planck equation for the conditional probability density of the molecular orientation and angular velocity. The FPL model is a frictional model in which the molecule is taken to be an appropriately shaped solid object immersed

in a continuous viscous fluid. The angular velocity of the molecule is assumed to follow a rotational Langevin equation so that the angular velocity is modulated by slowly varying viscosity dependent retarding torques, which cause the angular velocity to reduce to its ensemble average value of zero, and by rapidly fluctuating Brownian torques which reflect the molecular nature of the viscous medium. Hence the molecules in the FPL model experience intermolecular torques at all times and each fluctuation in the Brownian torque produces only a slight change in the angular velocity. A large number of fluctuations in the Brownian torque are required for significant change in the angular velocity. Fixman and Rider [4] have derived exact expressions for some of the reorientational correlation functions and spectral densities for linear and spherical top molecules. The correlation functions were expressed as infinite series whose terms were simple exponential functions of time, and the series were found to converge rapidly so that accurate numerical values were obtained with only a small number of terms in the truncated series. Hubbard [20,21] has also considered the FPL model and has attempted to obtain the general solution for the conditional probability density from the Fokker-Planck equation, but his perturbation approach has a limited range of validity. He obtained approximate expressions for the reorientational correlation time associated with nuclear dipole-dipole interactions and nuclear quadrupolar interactions, and the correlation time for the spin-rotational interactions for spherical top molecule. Evans [22,23]

has also derived approximate expressions for the FPL reorientational correlation functions and correlation times for spherical and symmetric top molecules by a cumulant expansion technique. The results of these approximate methods were deemed valid only for strong intermolecular interactions. Powles and Rickayzen [24] have extended the approach of Fixman and Rider and have derived continued fraction expressions for the reorientational correlation times which arise in dielectric relaxation and intramolecular dipolar magnetic relaxation of linear and spherical molecules.

In ref. [25], general series expansions for the angular velocity-orientation conditional probability densities for linear and spherical top molecules were derived using the eigenfunction expansion technique employed by Fixman and Rider [4]. The reorientation correlation functions, memory functions, correlation times, and spectral densities for linear and spherical molecules and the correlation times for anisotropic spin-rotational interactions in spherical molecules derived from the FPL model were compared [26] with the corresponding results from the ED model [27].

Some experimental infrared and Raman data have been compared with the theoretical results from the two models [26, 28, 29]. Raman studies of CF_4 [28] and SF_6 [29] showed that the reorientational motions of these spherical molecules are better described by the FPL model rather than the EDJ model over a wide range of density. The infrared studies [26] of N_2O in N_2 and CO in N_2 showed that both models were consistent with the experimental correlation functions at

low temperatures (high densities), but neither the EDJ nor the FPL was consistent with the CO/N_2 and $\text{N}_2\text{O}/\text{N}_2$ data at low densities. In $\text{N}_2\text{O}/\text{O}_2$ solution, both models gave satisfactory fits of the experimental data. Hubbard [30] has compared the correlation times obtained from the FPL model for spherical molecules with the experimental correlation times obtained from nuclear relaxation studies of CCl_4 and ClO_3F . He found that the FPL model agreed less well with the experimental data for ClO_3F than did the EDJ model, but the experimental data for CCl_4 were consistent with both models within experimental uncertainties. From these results, one may tentatively conclude that the FPL model and the EDJ model, although they are based on very different physical pictures of the rotational dynamics, appear to give surprisingly similar characterizations of the rotational motion of molecules in liquids.

Recently the FPL model was extended to symmetric top molecules [31] and the general expressions for the reorientational correlation functions, correlation times, spectral densities, angular velocity correlation functions, and the correlation times for spin-rotational interactions were derived. A new feature present in the FPL model for symmetric top molecules is the possibility for the introduction of anisotropy in the motional modulation of the angular velocity components. The numerical results of the reorientational correlation functions, correlation times, spectral densities and the correlation times for spin-rotation interactions showed that these properties were influenced significantly by the anisotropy in the motional modulation of the angular velocity components [31].

In the present paper the exact series expansion for the angular velocity-orientation conditional probability density is obtained for asymmetric top molecules, general expressions for the reorientational correlation functions, correlation times, spectral densities and the correlation times for spin-rotation interactions are derived, and the numerical results of some of these properties are compared with the corresponding results of the EDJ model [8], and the effect of frictional anisotropy on these properties are investigated.

2. Theory

A. Rotational Fokker-Planck Equation and its General Solution

The conditional probability density $P(\omega, \Omega, t | \omega_0, \Omega_0)$, that a molecule will have angular velocity between ω and $\omega + d\omega$ and orientation between Ω and $\Omega + d\Omega$ at time t , given that it had angular velocity between ω_0 and $\omega_0 + d\omega_0$ and orientation between Ω_0 and $\Omega_0 + d\Omega_0$ at time zero, is governed by the rotational Fokker-Planck equation

$$\frac{\partial P}{\partial t} = - \mathcal{L}P \quad (\text{II-1})$$

where the Liouville operator \mathcal{L} for an asymmetric top molecule is given by [31]

$$\mathcal{L} = \sum_{\alpha=x,y,z} \left\{ i\omega_{\alpha} J_{\alpha} - \frac{\partial}{\partial \omega_{\alpha}} (E_{\alpha}) - a_{\alpha} \frac{\partial^2}{\partial \omega_{\alpha}^2} \right\} \quad (\text{II-2})$$

Here ω_α is the component of the angular velocity along the principal molecular axis α , J_α is the α component of the infinitesimal rotation operator referred to the molecule fixed principal coordinate system,

$$E_\alpha = \tau_\alpha^{-1} \omega_\alpha - r_{\alpha-\alpha} \omega_\alpha \omega_\beta \quad (II-3)$$

$$r_{\alpha,\alpha} = (I_\beta - I_\gamma)/I_\alpha \omega_\alpha \quad (II-4)$$

and

$$a_\alpha = (k_B T/I_\alpha) \tau_\alpha^{-1} \quad (II-5)$$

where (α, β, γ) represents a cyclic permutation of (x, y, z) , I_α is the moment of inertia along the principal axis α , τ_α^{-1} is the coefficient in the viscous retarding torque term in the rotational Langevin equation for ω_α , k_B is the Boltzmann constant and T is the absolute temperature. The introduction of reduced angular velocity variables

$$\omega_\alpha^* = \omega_\alpha (I_\alpha/k_B T)^{1/2} \quad (II-6)$$

and reduced time variables

$$t^* = t(k_B T/I_z)^{1/2} \quad (II-7)$$

$$\tau_\alpha^* = \tau_\alpha (k_B T/I_z)^{1/2}$$

leads to the following form for the \mathbf{Z} operator:

$$\begin{aligned} \mathbf{Z} = \sum_{\alpha=x,y,z} \left\{ -(\tau_{\alpha}^*)^{-1} \left[\frac{\partial^2}{\partial \omega_{\alpha}^{*2}} + \omega_{\alpha}^* \frac{\partial}{\partial \omega_{\alpha}^*} + 1 \right] \right. \\ \left. + i (I_z/I_{\alpha})^{1/2} \omega_{\alpha}^* J_{\alpha} \right. \\ \left. + R_{\alpha} \omega_{\alpha}^* \omega_{\beta}^* \omega_{\gamma}^* \frac{\partial}{\partial \omega_{\alpha}^*} \right\} \end{aligned} \quad (\text{II-8})$$

where

$$R_{\alpha} = (I_{\beta} I_{\gamma}) / (I_x I_y)^{1/2} \quad (\text{II-9})$$

We shall henceforth omit the $*$'s on the angular velocity and time variables, and imply the use of reduced units for these variables throughout.

The general solution of the rotational Fokker-Planck equation is given by [25]

$$P(\omega, \Omega, t | \omega_0, \Omega_0) = \sum_{\lambda, \lambda'} \Psi_{\lambda}(\omega, \Omega) \Psi_{\lambda'}^*(\omega_0, \Omega_0) W(\omega_0, \Omega_0) \Phi_{\lambda\lambda'}(t) \quad (\text{II-10})$$

where $\{\Psi_{\lambda}(\omega, \Omega)\}$ are a complete set of basis functions which are orthonormal under the weighting function $W(\omega, \Omega)$, and

$$\Phi_{\lambda\lambda'}(t) = \sum_{\lambda''} U_{\lambda\lambda''} U_{\lambda''\lambda'}^{-1} \exp(-\Lambda_{\lambda''} t) \quad (\text{II-11})$$

with Λ and U being the eigenvalues and eigenvectors of the matrix

representation of the Liouville operator \mathbf{Z} in the Ψ basis. The basis functions $\{\Psi_\lambda\}$ are chosen to give a relatively simple representation of \mathbf{Z} .

For the asymmetric top problem, we choose to represent the Ω -dependent part of $\Psi[\omega, \Omega]$ in terms of the symmetrized solutions to the Schrödinger equation for the symmetric rotor:

$$S_{JKM\sigma}[\Omega] = \left(\frac{2J+1}{8\pi}\right)^{1/2} \begin{cases} D_{M,0}^{(J)*}[\Omega] & \text{for } \sigma=s, K=0 \\ \{D_{M,K}^{(J)*}[\Omega] + D_{M,-K}^{(J)*}[\Omega]\}/\sqrt{2} & \text{for } \sigma=s, K=1,2,\dots,J \\ \{D_{M,K}^{(J)*}[\Omega] - D_{M,-K}^{(J)*}[\Omega]\}/\sqrt{2} & \text{for } \sigma=a, K=1,2,\dots,J \end{cases} \quad (\text{II-12})$$

where $D^{(J)}[\Omega]$ is the Wigner rotation matrix [32] for spherical tensors of rank J . The functions $S_{JKM\sigma}[\Omega]$ are eigenfunctions of J^2 with eigenvalue $J(J+1)$ and of the z -component of the infinitesimal rotational operator in the laboratory coordinate system with eigenvalue M . However, they are not eigenfunctions of J_z , the z -component of the infinitesimal rotation operator in the molecular frame and they have the following behavior under the molecular components of the infinitesimal rotation operator:

$$J_x S_{JKM\sigma} = \frac{1}{2} \sqrt{J(J+1)-K(K+1)} [1 + (\sqrt{2}-1)\delta_{K,0}] S_{J,K+1,M,\sigma} + \frac{1}{2} \sqrt{J(J+1)-K(K-1)} [1 + (\sqrt{2}-1)\delta_{K,1}\delta_{\sigma,s} - \delta_{K,1}\delta_{\sigma,a}] S_{J,K-1,M,\sigma} \quad (\text{II-13})$$

$$\begin{aligned}
J_y S_{J,K,M,\sigma} &= \frac{1}{2} \sqrt{J(J+1)-K(K+1)} [1 + (\sqrt{2}-1)\delta_{K,0}] S_{J,K+1,M,\sigma^*} \\
&- \frac{1}{2} \sqrt{J(J+1)-K(K-1)} [1 + (\sqrt{2}-1)\delta_{K,1}\delta_{\sigma,a} - \delta_{K,1}\delta_{\sigma,s}] S_{J,K-1,M,\sigma^*}
\end{aligned}
\quad (II-14)$$

$$J_z S_{J,K,M,\sigma} = K S_{J,K,M,\sigma^*} \quad (II-15)$$

Here σ^* is the inverse parity of σ (i.e. $\sigma^* = a$ for $\sigma = s$ and vice-versa). The symmetrized rotor functions are chosen here, rather than spherical components of the tensors describing molecular orientation, to facilitate the use of the Cartesian components. The Cartesian components are preferred in the asymmetric top problem because all three molecular directions are dynamically unique, and there is no advantage to using spherical components.

The ω -dependent part of $\Psi[\omega, Q]$ will be represented in terms of the basis functions $F_l[\omega_x]F_p[\omega_y]F_n[\omega_z]$ where

$$F_q[\omega] = [(q!)(2\pi)^{1/2}]^{-1/2} \exp[-\omega^2/2] He_q[\omega] \quad (II-16)$$

and $He_q[\omega]$ are the Hermite polynomials¹ [33]. The function $F_q[\omega]$ is an eigenfunction of $-\left[\frac{\partial^2}{\partial \omega^2} + \omega \frac{\partial}{\partial \omega} + 1\right]$ with eigenvalue q .

The complete basis, in which Ψ is to be represented, is

$$\Psi_\lambda[\omega, Q] = (i)^{l+n} S_{J,K,M,\sigma} [Q] F_l[\omega_x] F_p[\omega_y] F_n[\omega_z], \quad (II-17)$$

¹ He_q differ from the usual H_q Hermite polynomials [33].

where the index λ represents the set of indices $(J, K, M, \sigma, l, p, n)$, and the factor $(l)^{l+n}$ has been introduced in order that the matrix representation of Z will be real. The functions Ψ_{λ} are orthonormal under the weighting function

$$W(\omega, \Omega) = \exp[(\omega_x^2 + \omega_y^2 + \omega_z^2)/2]. \quad (II-18)$$

In the Ψ_{λ} basis, the Liouville operator Z has the matrix representation:

$$\begin{aligned} & B_{K'\sigma'l'p'n'; K\sigma lpn}^{JM} \\ &= \delta_{K',K} \delta_{\sigma',\sigma} \delta_{l',l} \delta_{p',p} \delta_{n',n} [l/l_x + p/l_y + n/l_z] \\ &+ \delta_{\sigma',\sigma} \delta_{p',p} \delta_{n',n} (l_x/l_x)^{1/2} \{ (J(J+1) - KK')^{1/2}/2 \} \{ (l+1)^{1/2} \delta_{l',l+1} - l^{1/2} \delta_{l',l-1} \} \\ &\times \{ [1 + (\sqrt{2}-1) \delta_{K,0}] \delta_{K',K+1} + [1 + (\sqrt{2}-1) \delta_{K,1} \delta_{\sigma,\sigma} - \delta_{K,1} \delta_{\sigma,\sigma}] \delta_{K',K-1} \} \\ &+ \delta_{\sigma',\sigma} \delta_{l',l} \delta_{n',n} (l_z/l_y)^{1/2} \{ (J(J+1) - KK')^{1/2}/2 \} \{ (p+1)^{1/2} \delta_{p',p+1} - p^{1/2} \delta_{p',p-1} \} \\ &\times \{ -[1 + (\sqrt{2}-1) \delta_{K,0}] \delta_{K',K+1} + [1 + (\sqrt{2}-1) \delta_{K,1} \delta_{\sigma,\sigma} - \delta_{K,1} \delta_{\sigma,\sigma}] \delta_{K',K-1} \} \\ &+ \delta_{K',K} \delta_{\sigma',\sigma} \delta_{l',l} \delta_{p',p} \times \{ (n+1)^{1/2} \delta_{n',n+1} - n^{1/2} \delta_{n',n-1} \} \\ &+ \delta_{K',K} \delta_{\sigma',\sigma} \left[R_x \{ [l(p+1)(n+1)]^{1/2} \delta_{l',l-1} \delta_{p',p+1} \delta_{n',n+1} \right. \\ &\quad - [(l+1)pn]^{1/2} \delta_{l',l+1} \delta_{p',p-1} \delta_{n',n-1} \} \\ &\quad + R_y \{ -[(l+1)p(n+1)]^{1/2} \delta_{l',l+1} \delta_{p',p-1} \delta_{n',n+1} \\ &\quad \quad + [l(p+1)n]^{1/2} \delta_{l',l-1} \delta_{p',p+1} \delta_{n',n-1} \} \\ &\quad + R_z \{ [l(l+1)(p+1)n]^{1/2} \delta_{l',l+1} \delta_{p',p+1} \delta_{n',n-1} \\ &\quad \quad \left. - [lp(n+1)]^{1/2} \delta_{l',l-1} \delta_{p',p-1} \delta_{n',n+1} \} \right]. \end{aligned} \quad (II-19)$$

B. Reorientational correlation functions and correlation times.

The reorientational correlation functions which are of interest in the description of infrared and Raman band shapes, for dielectric relaxation, and for nuclear relaxation via intramolecular dipole-dipole and nuclear quadrupole interactions are

$$G_{kk}^{(j)}(t) = \langle D_{mk}^{(j)}[\Omega(t)] D_{mk}^{(j)*}[\Omega(0)] \rangle / \langle |D_{mk}^{(j)}[\Omega(0)]|^2 \rangle \quad (\text{II-20})$$

where $D^{(j)}[\Omega]$ is the Wigner rotation matrix which describes the transformation of the components of a spherical tensor of rank j , when a rotational transformation through Euler angles Ω is applied. $\Omega(0)$ and $\Omega(t)$ are the Euler angles which relate the laboratory and molecular coordinate systems at times 0 and t , respectively. The brackets denote an equilibrium ensemble average.

In FPL model, this correlation function can be written as

$$G_{kk}^{(j)}(t) = (2j+1) \int d\omega \int d\Omega \int d\omega_0 \int d\Omega_0 P(\omega_0, \Omega_0) P(\omega, \Omega, t | \omega_0, \Omega_0) D_{mk}^{(j)}[\Omega] D_{mk}^{(j)*}[\Omega_0] \quad (\text{II-21})$$

where

$$P(\omega_0, \Omega_0) = (2\pi)^{-1/2} (16\pi^3)^{-1} \exp[-(\omega_{x_0}^2 + \omega_{y_0}^2 + \omega_{z_0}^2)/2] \quad (\text{II-22})$$

is the probability density for the molecule having angular velocity between ω_0 and $\omega_0 + d\omega_0$ and orientation between Ω_0 and $\Omega_0 + d\Omega_0$ at time zero.

For asymmetric top molecules, Eq. (II-21) becomes

$$\begin{aligned}
 G_{kk'}^{(j)}(t) = & \frac{2j+1}{(2\pi)^{1/2}(16\pi^3)} \sum_{\substack{J,M,K,\sigma,\lambda,p,n \\ K',\sigma',\lambda',p',n'}}^{JM} \Phi_{K\sigma\lambda p n; K'\sigma'\lambda'p'n'}^{JM}(t) \\
 & \times \int d\Omega S_{JKM\sigma}(\Omega) D_{mk}^{(j)}(\Omega) \int d\Omega_0 S_{JK'M\sigma'}^*(\Omega_0) D_{mk'}^{(j)*}(\Omega_0) \\
 & \times \int d\omega_x F_\lambda(\omega_x) \int d\omega_y F_p(\omega_y) \int d\omega_z F_n(\omega_z) \int d\omega_{x_0} F_{\lambda'}(\omega_{x_0}) \\
 & \times \int d\omega_{y_0} F_{p'}(\omega_{y_0}) \int d\omega_{z_0} F_{n'}(\omega_{z_0}) \quad (II-23)
 \end{aligned}$$

The integrals in Eq. (II-23) can be evaluated using the relationships

$$\begin{aligned}
 \int d\omega F_q(\omega) &= \int d\omega F_q(\omega) \{ (2\pi)^{1/4} F_0(\omega) \exp(\omega^2/2) \} \\
 &= (2\pi)^{1/4} \delta_{q,0} \quad (II-24)
 \end{aligned}$$

and

$$\begin{aligned}
 & \int d\Omega S_{JKM\sigma}(\Omega) D_{mk}^{(j)}(\Omega) \\
 &= \left(\frac{8\pi^2}{2j+1} \right)^{1/2} \delta_{J,j} \delta_{M,m} \delta_{K,k} |k| \left\{ \delta_{k,0} \delta_{\sigma,s} + (2)^{-1/2} (1 - \delta_{k,0}) (\delta_{\sigma,s} + \text{sgn}(k) \delta_{\sigma,a}) \right\} \quad (II-25)
 \end{aligned}$$

where

$$\text{sgn}(k) = \begin{cases} +1 & , \quad k > 0 \\ 0 & , \quad k = 0 \\ -1 & , \quad k < 0 \end{cases} \quad (\text{II-26})$$

The correlation functions are given by

$$G_{kk'}^j(t) = \sum_{\sigma, \sigma'} C_{\sigma, \sigma'}(k, k') \Phi_{[k]_{\sigma 000}, [k']_{\sigma' 000}}^{jm}(t) \quad (\text{II-27})$$

where the functions $C_{\sigma, \sigma'}(k, k')$ are defined by

$$C_{s, s}(k, k') = \left[\frac{1}{2} + \left(\frac{1}{\sqrt{2}} - \frac{1}{2} \right) (\delta_{k', 0} + \delta_{k, 0}) \right. \\ \left. + (1 - \sqrt{2}) \delta_{k, 0} \delta_{k', 0} \right] [1 + \delta_{k, 0} \delta_{k', 0}]$$

$$C_{s, a}(k, k') = \left[\frac{1}{2} + \left(\frac{1}{\sqrt{2}} - \frac{1}{2} \right) \sigma_{k, 0} \right] \text{sgn}(k')$$

$$C_{a, s}(k, k') = \left[\frac{1}{2} + \left(\frac{1}{\sqrt{2}} - \frac{1}{2} \right) \delta_{k', 0} \right] \text{sgn}(k) \quad (\text{II-28})$$

$$C_{a, a}(k, k') = \frac{1}{2} \text{sgn}(k) \text{sgn}(k')$$

The infrared and Raman bandshapes of asymmetric top molecules are related to the spectral densities.

$$I_{kk'}^j(\omega) = \int_0^\infty G_{kk'}^j(t) \cos \omega t \, dt \quad (\text{II-29})$$

$$= \sum_{\sigma', \sigma''} \text{Re} \{ U_{k|\sigma'000; K\sigma l p n}^{jm} (U^{jm})^{-1}_{K\sigma l p n; |k'| \sigma''000} C_{\sigma', \sigma''}(k, k') / (\Lambda_{K\sigma l p n}^{jm} - i\omega) \}$$

where Λ^{jm} and U^{jm} are the eigenvalues and eigenvectors of the matrix Z^{jm} in Eq. (II-19).

Reorientational correlation times in the FPL model for asymmetric top molecules are given by

$$\tau_{\theta}^{jkk'} = \tau_{kk}^{j00} \left\{ \sum_{\sigma, \sigma'} C_{\sigma, \sigma'}(k, k') (Z^{jm})^{-1}_{k|\sigma 000; |k'| \sigma' 000} \right\} \quad (\text{II-30})$$

C. Spin-rotation relaxation times

The rate of spin relaxation due to motional modulation of spin rotational interactions involves correlation times for correlation functions which involve both orientational and angular momentum variables [29]. In general, the spin rotational interaction is represented by

$$H_{SR} = J \cdot C \cdot S \quad (\text{II-31})$$

where J is the rotational angular momentum of the molecule, C is the spin-rotation interaction tensor, and S is the dimensionless spin angular momentum operator. The components of J are related to the angular velocity components ω_{α} and the principal moments of inertia

I_{α} C is assumed to be diagonal in the principal molecular coordinate system. Then H_{SR} can be written as

$$H_{SR} = (I_{x B} k T)^{1/2} \omega_{x x x} C S_x + (I_{y B} k T)^{1/2} \omega_{y y y} C S_y + (I_{z B} k T)^{1/2} \omega_{z z z} C S_z \quad (II-32)$$

where ω_x , ω_y and ω_z are the reduced angular velocity components.

Since S is quantized in the laboratory coordinate system, it is useful to express S in terms of spherical tensor components

$$\begin{aligned} S_x &= (-S_{+1} + S_{-1})/\sqrt{2} \\ S_y &= i(S_{+1} + S_{-1})/\sqrt{2} \\ S_z &= S_0 \end{aligned} \quad (II-33)$$

and transform the spherical tensor components from the molecular frame to the laboratory frame using the following relation.

$$S = \sum_m S_m D_{mk}^{(1)}[Q] \quad (II-34)$$

Then

$$H_{SR} = \sum_m S_m V_m(t) \quad (II-35)$$

where S_m is the m -th spherical tensor component of the spin angular momentum operator in the laboratory coordinate system, and the lattice functions $V_m(t)$ are given by

$$\begin{aligned}
V_m(t) = & C_x (I_x k_B T)^{1/2} \omega_x (-D_{m,1}^{(1)}[Q] + D_{m,-1}^{(1)}[Q]) / \sqrt{2} \\
& + i C_y (I_y k_B T)^{1/2} \omega_y (D_{m,1}^{(1)}[Q] + D_{m,-1}^{(1)}[Q]) / \sqrt{2} \\
& + C_z (I_z k_B T)^{1/2} \omega_z D_{m,0}^{(1)}
\end{aligned} \quad (II-36)$$

The $V_m(t)$ are time-dependent because they contain the dynamic variables Q , ω_x , ω_y and ω_z . Recognizing the relationship between the Wigner functions and the symmetrized basis functions $S_{JKM}[Q]$ in Eq. (II-12), one may rewrite $V_m(t)$ in the form

$$\begin{aligned}
V_m(t) = & (8\pi^2 k_B T/3)^{1/2} \{ -C_x I_x^{1/2} S_{11ma}^*[Q] \omega_x + i C_y I_y^{1/2} S_{11ms}^*[Q] \omega_y \\
& + C_z I_z^{1/2} S_{10ms}^*[Q] \omega_z \}
\end{aligned} \quad (II-37)$$

The spin relaxation rate due to motional modulation of spin-rotational interactions is given by [34]

$$\frac{1}{T_1} = \frac{2}{\hbar^2} \int_0^\infty \langle V_1(t) V_1^*(0) \rangle dt \quad (II-38)$$

The correlation function $\langle V_1(t) V_1^*(0) \rangle$ can be evaluated by a procedure analogous to that used in the evaluation of $G_{kk}^j(t)$ above. One obtains

$$\begin{aligned}
\langle v_1(t) v_1^*(0) \rangle = & (k_B T/3) \{ C_{xx}^2 I \Phi_{1a100, 1a100}^{11}(t) + C_{yy}^2 I \Phi_{1s010, 1s010}^{11}(t) \\
& + C_{zz}^2 I \Phi_{0s001, 0s001}^{11}(t) \\
& + C_{xy} C_{xy} (I_{xy} I_{xy})^{1/2} [-\Phi_{1a100, 1s010}^{11}(t) - \Phi_{1s010, 1a100}^{11}(t)] \\
& + C_{yz} C_{yz} (I_{yz} I_{yz})^{1/2} [\Phi_{1s010, 0s001}^{11}(t) + \Phi_{0s001, 1s010}^{11}(t)] \\
& + C_{zx} C_{zx} (I_{zx} I_{zx})^{1/2} [-\Phi_{1a100, 0s001}^{11}(t) - \Phi_{0s001, 1a100}^{11}(t)] \} \quad (II-39)
\end{aligned}$$

The spin-rotational relaxation rate may be written as

$$\frac{1}{T_1} = \frac{2k_B T}{3\hbar^2} \sum_{\alpha, \alpha' = x, y, z} C_{\alpha\alpha'}^2 (I_{\alpha\alpha'} I_{\alpha'\alpha})^{1/2} F_{\alpha\alpha'} \quad (II-40)$$

where the functions $F_{\alpha\alpha'}$ are symmetric in the indices α and α' , and are given by

$$\begin{aligned}
F_{xx} &= (Z_{1a100, 1a100}^{11})^{-1} / \tau_x \\
F_{yy} &= (Z_{1s010, 1s010}^{11})^{-1} / \tau_y \\
F_{zz} &= (Z_{0s001, 0s001}^{11})^{-1} / \tau_z \quad (II-41)
\end{aligned}$$

$$F_{xy} = -[(Z^{11})^{-1}_{1a100,1s010} + (Z^{11})^{-1}_{1s010,1a100}]/[2(\tau_x \tau_y)^{1/2}] ,$$

$$F_{yz} = [(Z^{11})^{-1}_{1s010,0s001} + (Z^{11})^{-1}_{0s001,1s010}]/[2(\tau_y \tau_z)^{1/2}] ,$$

$$F_{zx} = -[(Z^{11})^{-1}_{1a100,0s001} + (Z^{11})^{-1}_{0s001,1a100}]/[2(\tau_z \tau_x)^{1/2}] .$$

D. Angular velocity correlation functions

The angular velocity correlation functions are also evaluated in a manner similar to that used for the evaluation of the reorientational correlation functions. One obtains

$$\begin{aligned} \langle \omega_x(t) \omega_x(0) \rangle &= \frac{1}{(2\pi)^{1/2} (16\pi^3)} \sum_{JM} \Phi^{JM} \cdot (t) \\ &\quad \times \int d\Omega S_{JKM\sigma}(\Omega) \int d\Omega_0 S_{JK'M'\sigma'}^*(\Omega_0) \\ &\quad \times \int d\omega_x \omega_x F_{\ell}(\omega_x) \int d\omega_y F_p(\omega_y) \int d\omega_z F_n(\omega_z) \\ &\quad \times \int d\omega_{x_0} \omega_{x_0} F_{\ell}(\omega_{x_0}) \int d\omega_{y_0} F_p(\omega_{y_0}) \int d\omega_{z_0} F_n(\omega_{z_0}) \\ &= \Phi_{0s100,0s100}^{00}(t) \end{aligned} \quad (II-42)$$

In the evaluation of integrals, the relations

$$S_{000s} = 1/(8\pi^2)^{1/2} \quad (II-43)$$

$$F_0[\omega] \exp(\omega^2/2) (2\pi)^{1/4} = 1 \quad , \quad (II-44)$$

$$F_1[\omega] \exp(\omega^2/2) (2\pi)^{1/4} = \omega \quad , \quad (II-45)$$

were used. Similarly,

$$\langle \omega_y(t) \omega_y(0) \rangle = \Phi_{0s010;0s010}^{00}(t) \quad , \quad (II-46)$$

$$\langle \omega_z(t) \omega_z(0) \rangle = \Phi_{0s001;0s001}^{00}(t) \quad . \quad (II-47)$$

3. Numerical Calculations

A. FPL model

Numerical values of the reorientational correlation functions, correlation times and spectral densities and the correlation functions and correlation times for spin-rotational interactions and angular momentum can be obtained from appropriate Z matrices. In general, the Z matrices are of infinite order because the indices l , p and n take on all nonnegative integral values. However, sufficiently accurate values of correlation functions, correlation times and spectral densities can be obtained with truncated Z matrices because of rapid convergence. The rows and columns of the Z matrix are arranged in order of increasingly distant connection to the "1,1" element. Here the "1,1" element is the first element whose

column and row represent the set of indices which correspond to a specific correlation time. The computation of the correlation time is carried out by Gaussian elimination and the results obtained when elements with successively distant connections to the "1,1" element are included are used to judge the precision of the computations. This procedure is essentially a perturbation scheme where the results of successively higher order calculations are compared. The computation is terminated when successive values of the correlation time differ by less than 0.001%, and the truncated Z matrix of corresponding order is used for the computation of the reorientational correlation functions and spectral densities.

Examination of the connectivities of the elements in the Z^{jm} matrix constructed beginning with the set of indices $\{k\sigma 000\}$ for $j = 1, 2, k = 0, \dots, j$ shows that the indices $\{k\sigma 000\}$ and $\{k\alpha 000\}$ belong to different sub-blocks of the Z^{jm} matrix, and that the correlation functions $\Phi_{k\sigma 000, k\alpha 000}^{jm}(t)$ and the associated spectral densities and correlation times vanish identically. Furthermore the indices $\{k \pm 1 \sigma 000\}$ and $\{k \pm 1 \sigma^* 000\}$ belong to sub-blocks of Z^{jm} which do not contain $\{k\sigma 000\}$ so that the only non-vanishing correlation functions are $\Phi_{1\sigma 000, 1\sigma 000}^{1m}(t)$ ($\sigma = s, a$), and $\Phi_{0s 000, 0s 000}^{1m}(t)$ for $j = 1$, and $\Phi_{2\sigma 000, 2\sigma 000}^{2m}(t)$ ($\sigma = s, a$), $\Phi_{1\sigma 000, 1\sigma 000}^{2m}(t)$ ($\sigma = s, a$), $\Phi_{0s 000, 0s 000}^{2m}(t)$, and $\Phi_{2s 000, 0s 000}^{2m}(t)$ for $j = 2$.

Although the spherical tensor correlation functions $G_{k,k}^j(t)$ and spectral densities $I_{k,k}^j(\omega)$ are directly related to observable

spectral band shapes of linear, spherical and symmetric top molecules, they are not entirely appropriate for asymmetric top molecules, where Cartesian variables are preferred. The correlation functions $\Phi_{k\sigma 000; k\sigma 000}^{jm}(t)$ and their Fourier transforms

$$\kappa_{k\sigma 000; k\sigma 000}^{jm}(\omega) = \int_0^\infty \Phi_{k\sigma 000; k\sigma 000}^{jm}(t) \cos(\omega t) dt \quad (\text{II-48})$$

are directly related to the infrared and Raman bandshapes of asymmetric top molecules. The correspondence between the index pairs $\{k, \sigma\}$ and the Cartesian tensor components is given in Table II-1.

The reorientational correlation functions $\Phi_{k\sigma 000; k\sigma 000}^{jm}(t)$ for $j = 1$ and 2 , were computed for various relative magnitudes of τ_x , τ_y and τ_z for a typical asymmetric top molecule, HDO [35] ($I_x = 4.38 \times 10^{-40} \text{ g cm}^2$, $I_y = 3.08 \times 10^{-40} \text{ g cm}^2$, $I_z = 1.19 \times 10^{-40} \text{ g cm}^2$ with x , y , and z axes defined such that $I_x > I_y > I_z$) and the results are shown in Fig. II-1.

Spherical tensor correlation times are useful in the description of nuclear magnetic relaxation via motional modulation of intramolecular dipole-dipole and electric quadrupole interactions, so we have calculated values of the non-vanishing $\tau_\theta^{jkk'}$ for a typical asymmetric top molecule, $\text{C}_6\text{D}_5\text{F}$ [36] ($I_x = 5.43 \times 10^{-38} \text{ g cm}^2$, $I_y = 3.57 \times 10^{-38} \text{ g cm}^2$, $I_z = 1.86 \times 10^{-38} \text{ g cm}^2$) and show their variation with τ_x , for the case $\tau_x = \tau_y = \tau_z$, in Fig. II-2. The variation of $\tau_\theta^{2kk'}$ with τ_x for the cases $\tau_z > \tau_x = \tau_y$ (reorientation of

Table II-1. Correspondence between the index pair $\{k, o\}$ and Cartesian dipole and polarizability tensor components

Infrared Bands $j = 1$

$\{k, o\}$	Dipole moment element
$\{0, s\}$	μ_z
$\{1, s\}$	μ_y
$\{1, a\}$	μ_x

Raman Bands $j = 2$

$\{k, o\}$	Polarizability element
$\{0, s\}$	$\alpha_{xx} + \alpha_{yy} - 2\alpha_{zz}$
$\{1, s\}$	α_{yz}
$\{1, a\}$	α_{xz}
$\{2, s\}$	$\alpha_{xx} - \alpha_{yy}$
$\{2, a\}$	α_{xy}

Fig. II-1. FPL reorientational correlation functions for asymmetric top molecule with moments of inertia $I_x = 4.38 \times 10^{-40} \text{ g cm}^2$,

$$I_y = 3.08 \times 10^{-40} \text{ g cm}^2, \quad I_z = 1.19 \times 10^{-40} \text{ g cm}^2,$$

$\square - \tau_x = 0.1,$	$\tau_y = 0.05,$	$\tau_z = 0.01,$
$\circ - \tau_x = 0.1,$	$\tau_y = 0.05,$	$\tau_z = 0.1,$
$\Delta - \tau_x = 0.1,$	$\tau_y = 0.05,$	$\tau_z = 0.5,$
$+ - \tau_x = 0.1,$	$\tau_y = 0.01,$	$\tau_z = 0.05,$
$\times - \tau_x = 0.1,$	$\tau_y = 0.1,$	$\tau_z = 0.05,$
$\diamond - \tau_x = 0.1,$	$\tau_y = 0.5,$	$\tau_z = 0.05,$
$\Upsilon - \tau_x = 0.01,$	$\tau_y = 0.1,$	$\tau_z = 0.05,$
$\times - \tau_x = 0.1,$	$\tau_y = 0.1,$	$\tau_z = 0.05,$
$\cdot - \tau_x = 0.5,$	$\tau_y = 0.1,$	$\tau_z = 0.05.$

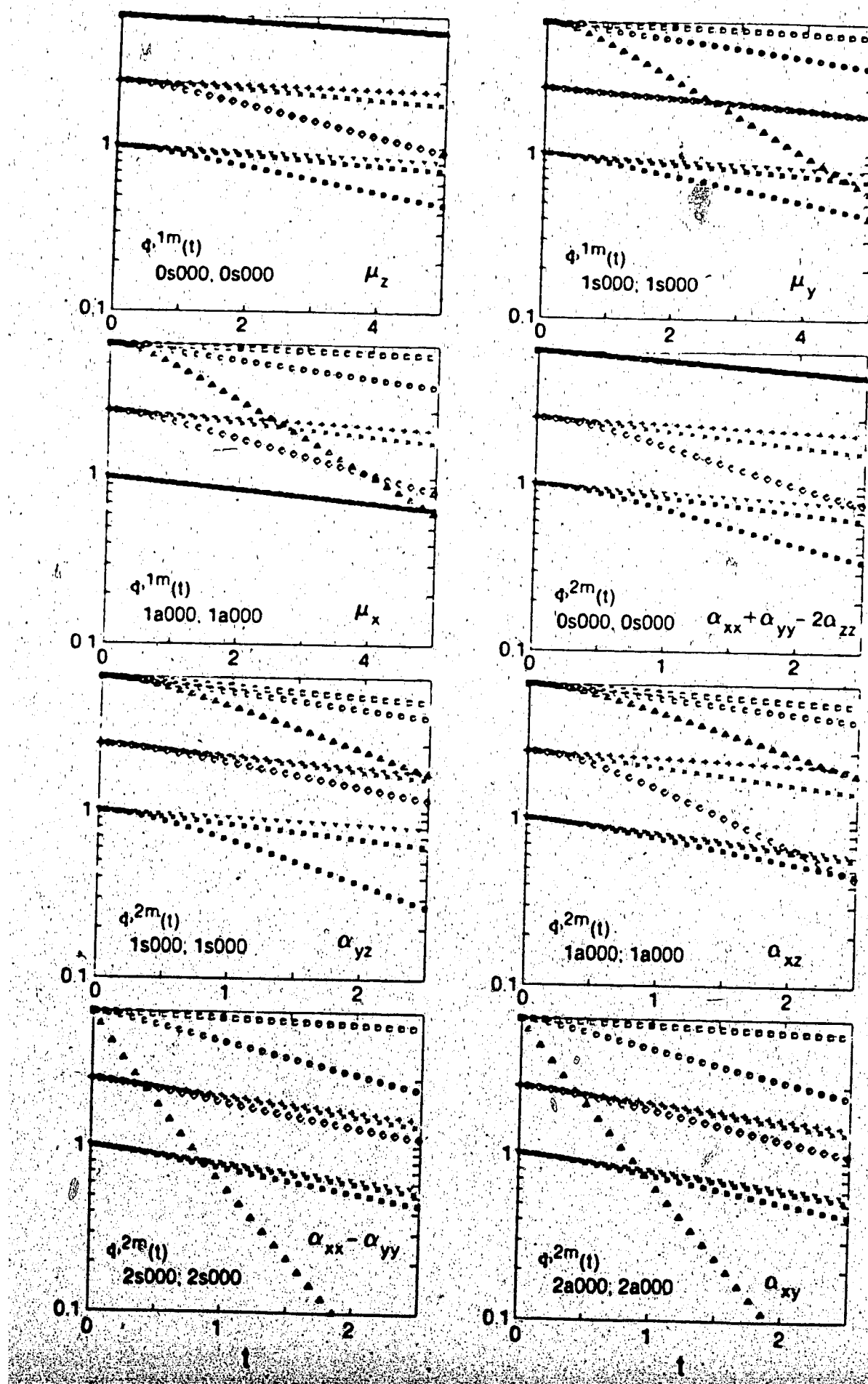
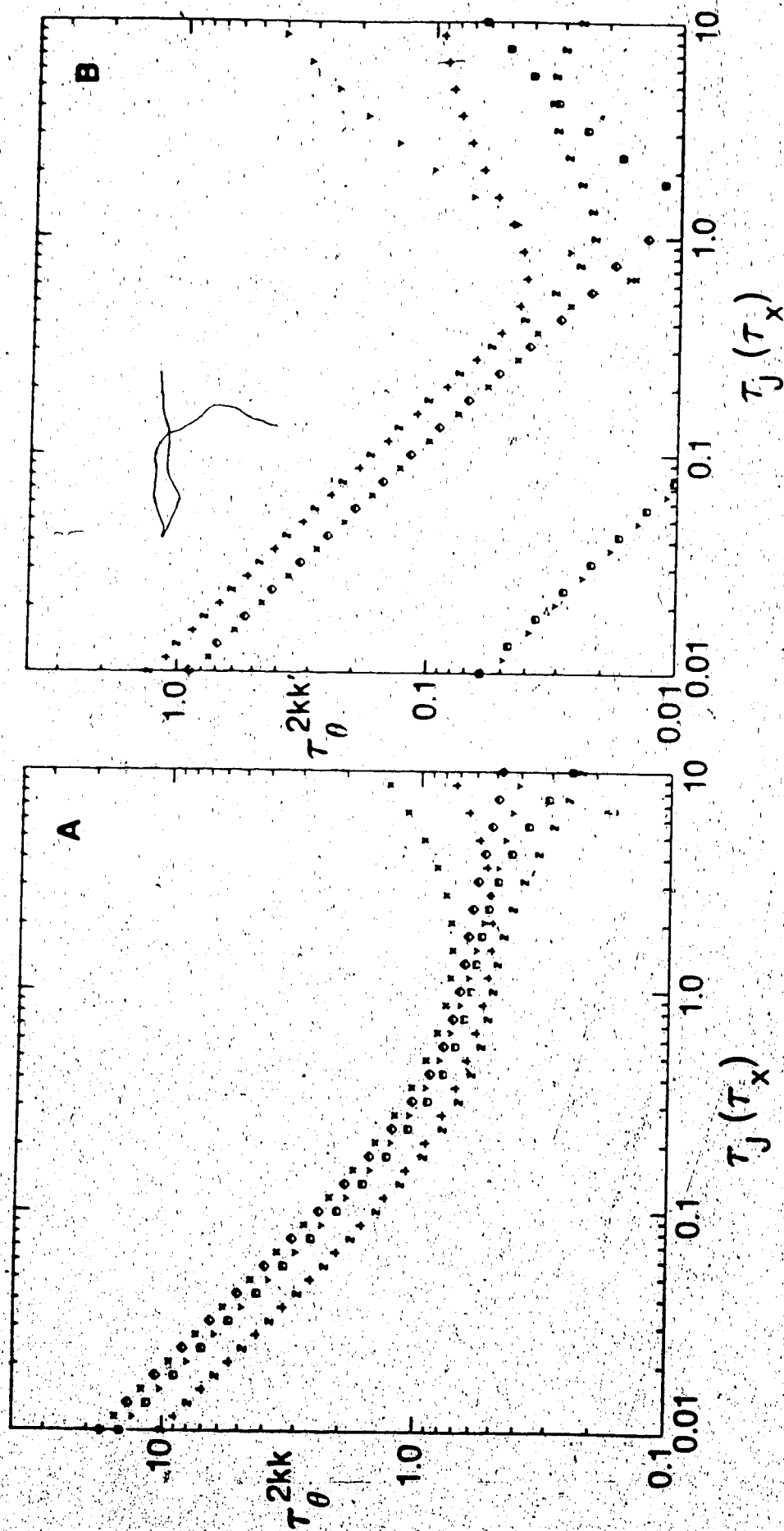


Fig. II-2. Comparison of reorientational self-correlation and cross-correlation times computed with the EDJ model and with the FPL model for $\tau_x = \tau_y = \tau_z$ for asymmetric top with moments of inertia $I_x = 5.43 \times 10^{-38} \text{ g cm}^2$, $I_y = 3.57 \times 10^{-38} \text{ g cm}^2$, $I_z = 1.86 \times 10^{-38} \text{ g cm}^2$.

A.	X - τ_{θ}^{200} (EDJ) ,	\diamond - τ_{θ}^{200} (FPL),
	Y - τ_{θ}^{211} (EDJ) ,	\square - τ_{θ}^{211} (FPL),
	+ - τ_{θ}^{222} (EDJ) ,	\tilde{z} - τ_{θ}^{222} (FPL);
B.	X - τ_{θ}^{21-1} (EDJ) ,	\diamond - τ_{θ}^{21-1} (FPL),
	Y - τ_{θ}^{22-2} (EDJ) ,	\square - τ_{θ}^{22-2} (FPL),
	+ - τ_{θ}^{220} (EDJ) ,	\tilde{z} - τ_{θ}^{220} (FPL).



fluorobenzene restricted by the presence of the large dipole moment along the C-F bond axis which is the z-axis) and $\tau_x > \tau_y = \tau_z$ (reorientation in the plane of the molecule more rapid than out-of-plane reorientation of fluorobenzene) is shown in Fig. II-3.

Rational approximations for $\tau_{\theta}^{jkk'}$ were determined algebraically using Cramer's rule, but the resulting expressions are too complicated to be given here, even for truncated \mathbf{Z} matrices of low order. Instead, only the results to first order are given:

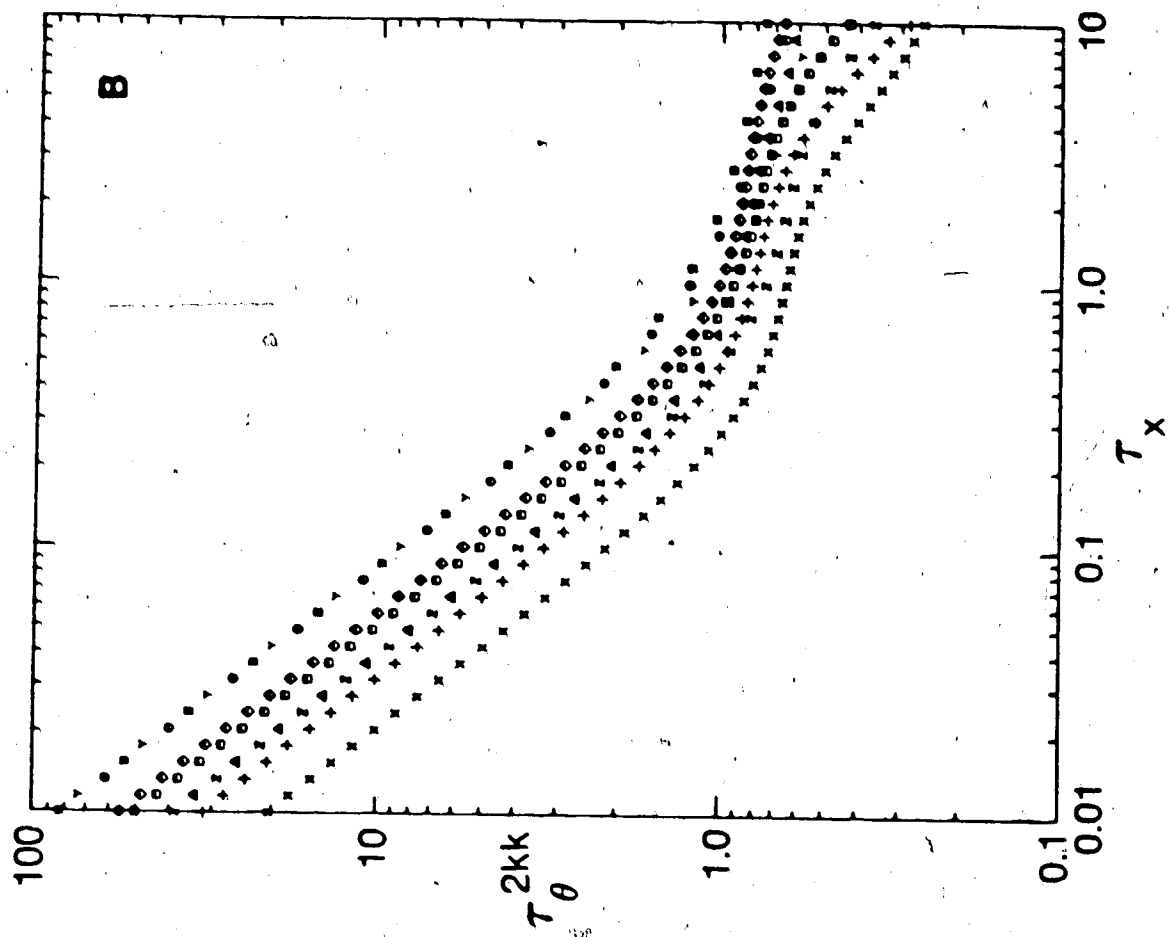
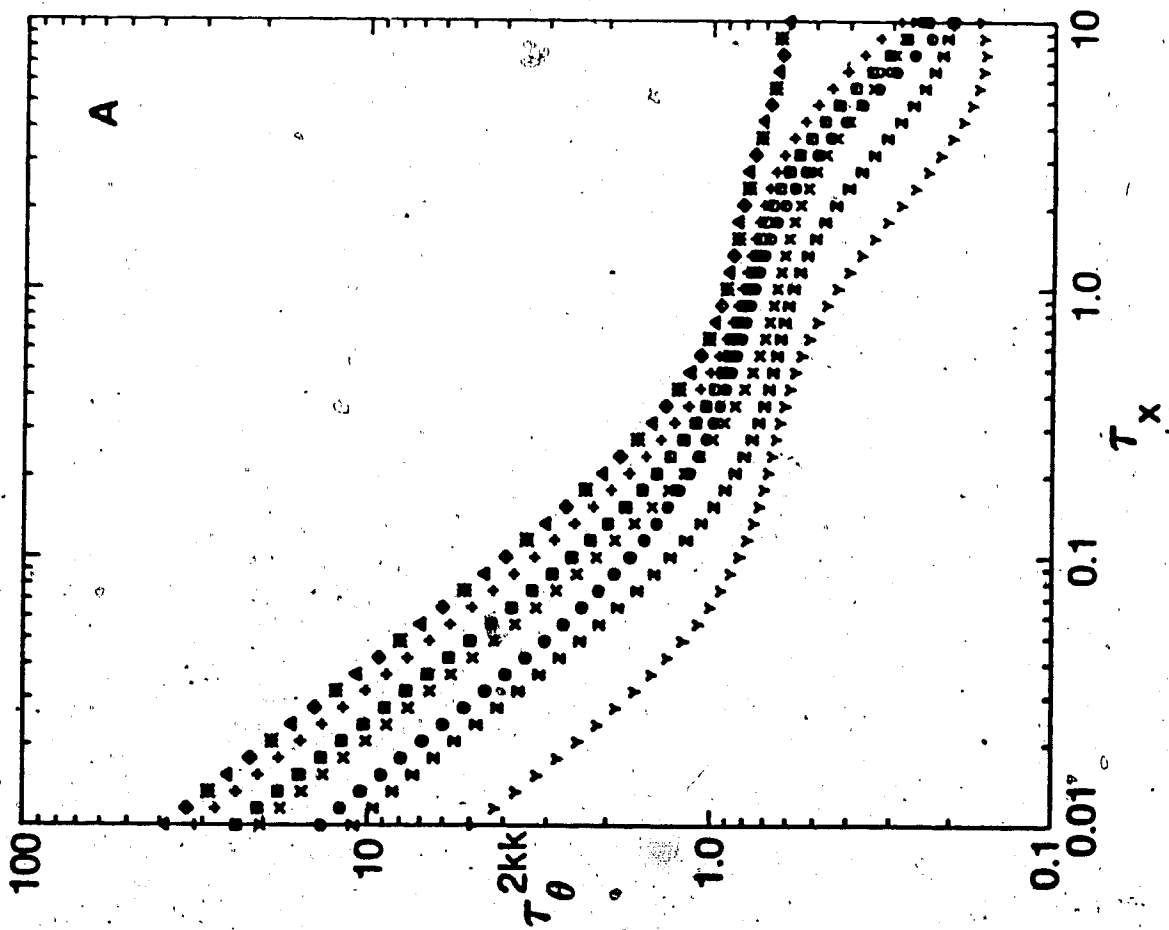
$$\begin{aligned}
 \tau_{\theta}^{100} &\approx \{k_B T(\tau_x/I_x + \tau_y/I_y)\}^{-1} \\
 \tau_{\theta}^{111} &\approx [(\tau_x/I_x + \tau_z/I_z)^{-1} + (\tau_y/I_y + \tau_z/I_z)^{-1}]/(2k_B T) \\
 \tau_{\theta}^{11-1} &\approx [(\tau_x/I_x + \tau_z/I_z)^{-1} - (\tau_y/I_y + \tau_z/I_z)^{-1}]/(2k_B T) \\
 \tau_{\theta}^{200} &\approx \{3k_B T(\tau_x/I_x + \tau_y/I_y)\}^{-1} \\
 \tau_{\theta}^{211} &\approx [(4\tau_x/I_x + \tau_y/I_y + \tau_z/I_z)^{-1} \\
 &\quad + (\tau_x/I_x + 4\tau_y/I_y + \tau_z/I_z)^{-1}]/(2k_B T) \\
 \tau_{\theta}^{222} &\approx \{k_B T(\tau_x/I_x + \tau_y/I_y + 4\tau_z/I_z)\}^{-1} \\
 \tau_{\theta}^{21-1} &\approx [(4\tau_x/I_x + \tau_y/I_y + \tau_z/I_z)^{-1}
 \end{aligned}
 \tag{II-49}$$

Fig. II-3. Variation of FFL reorientational self-correlation times with frictional anisotropy.

$$\begin{aligned}
 \text{A. } \tau_z > \tau_x = \tau_y: \tau_z/\tau_x &= 1 (\Delta - \tau_\theta^{200}, + - \tau_\theta^{211}, \times - \tau_\theta^{222}), \\
 \tau_z/\tau_x &= 2 (\diamond - \tau_\theta^{200}, \square - \tau_\theta^{211}, \text{Z} - \tau_\theta^{222}), \\
 \tau_z/\tau_x &= 5 (* - \tau_\theta^{200}, \circ - \tau_\theta^{211}, \gamma - \tau_\theta^{222}),
 \end{aligned}$$

$$\begin{aligned}
 \text{B. } \tau_x > \tau_y = \tau_z: \tau_x/\tau_y &= 1 (\Delta - \tau_\theta^{200}, + - \tau_\theta^{211}, \times - \tau_\theta^{222}), \\
 \tau_x/\tau_y &= 2 (\diamond - \tau_\theta^{200}, \square - \tau_\theta^{211}, \text{Z} - \tau_\theta^{222}), \\
 \tau_x/\tau_y &= 5 (* - \tau_\theta^{200}, \circ - \tau_\theta^{211}, \gamma - \tau_\theta^{222}).
 \end{aligned}$$

[Moments of inertia as in Fig. II-2].



$$= (\tau_x/I_x + 4\tau_y/I_y + \tau_z/I_z)^{-1} / (k_B T) ,$$

$$\tau_{\theta}^{22-2} \approx 0 ,$$

$$\tau_{\theta}^{220} \approx \{ \sqrt{6} k_B T (\tau_x/I_x - \tau_y/I_y) \}^{-1} ,$$

where τ_x, τ_y, τ_z are in seconds not in reduced units as in other equations.

The variations of the spin-rotation functions, $F_{xx}, F_{yy}, F_{zz}, F_{xy}, F_{yz},$ and F_{zx} , which are defined in Eq. (II-41), for various relative magnitudes of $\tau_x, \tau_y,$ and τ_z are shown in Fig. II-4.

Rational approximations for these functions were also determined algebraically using Cramer's rule and, to lowest order corrections, the results are

$$\begin{aligned} F_{\alpha\alpha} \approx & 1 - k_B T \tau_{\alpha} \{ \tau_{\beta}^2 \tau_{\alpha}^2 (I_{\beta} - I_{\gamma})^2 + \tau_{\alpha}^2 I_{\alpha} (\tau_{\beta}^2 I_{\beta} + \tau_{\gamma}^2 I_{\gamma}) \\ & + \tau_{\alpha} \tau_{\beta} \tau_{\gamma} (\tau_{\alpha} + \tau_{\beta} + \tau_{\gamma}) [(I_{\beta} - I_{\gamma})^2 + I_{\alpha} (I_{\beta} + I_{\gamma})] \} \\ & / [I_x I_y I_z (\tau_x + \tau_y)(\tau_y + \tau_z)(\tau_z + \tau_x)] \end{aligned} \quad (II-50)$$

$$F_{\alpha\beta} \approx k_B T (I_{\alpha} I_{\beta} \tau_{\alpha} \tau_{\beta})^{1/2} \{ I_{\gamma} [\tau_{\alpha}^2 \tau_{\beta}^2 - (\tau_{\alpha}^2 + \tau_{\beta}^2) \tau_{\gamma}^2 - \tau_{\alpha} \tau_{\beta} \tau_{\gamma} (\tau_{\alpha} + \tau_{\beta} + \tau_{\gamma})] \}$$

Fig. II-4. Spin-rotation functions $F_{\alpha\beta}$ and $F_{\alpha\beta}^{\text{EDJ}}$ for asymmetric top molecules

A. $\bigcirc - F_{\alpha\beta}$ for $\tau_x = \tau_y = \tau_z$, $\square - F_{\alpha\beta}^{\text{EDJ}}$

B. $F_{\alpha\beta}$: $\bigcirc - \tau_x = \tau_y = \tau_z$,

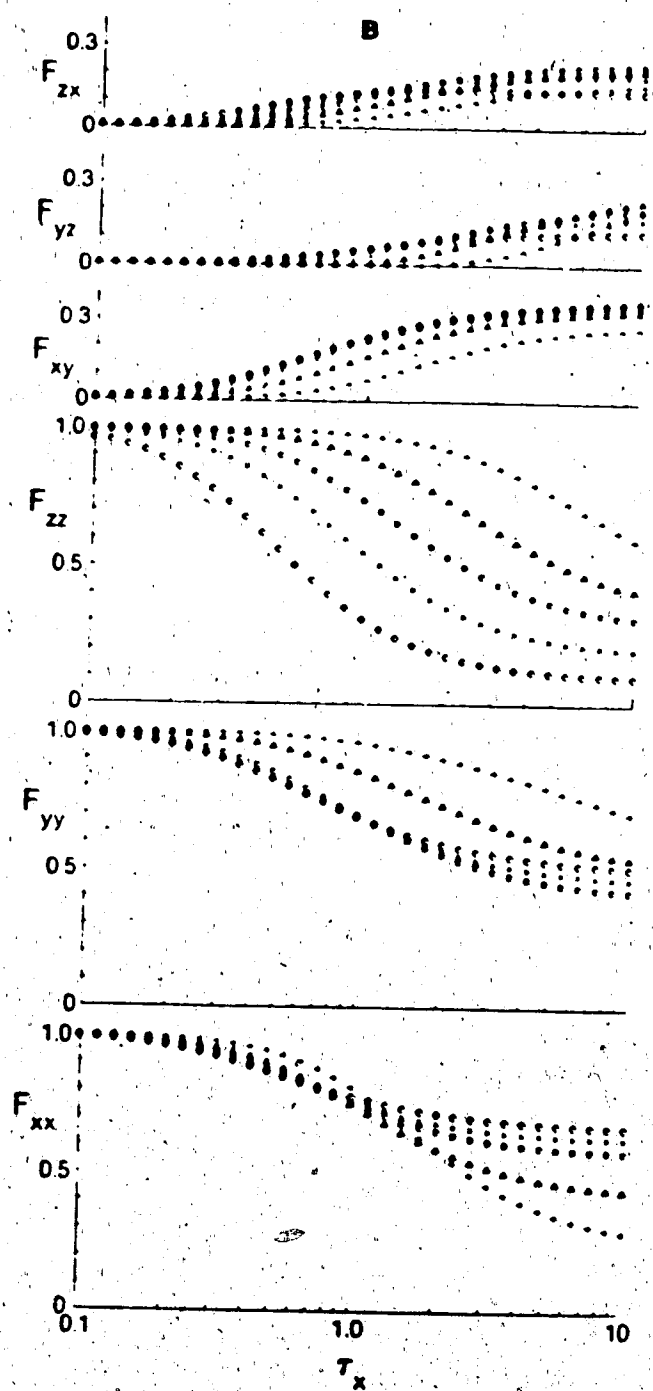
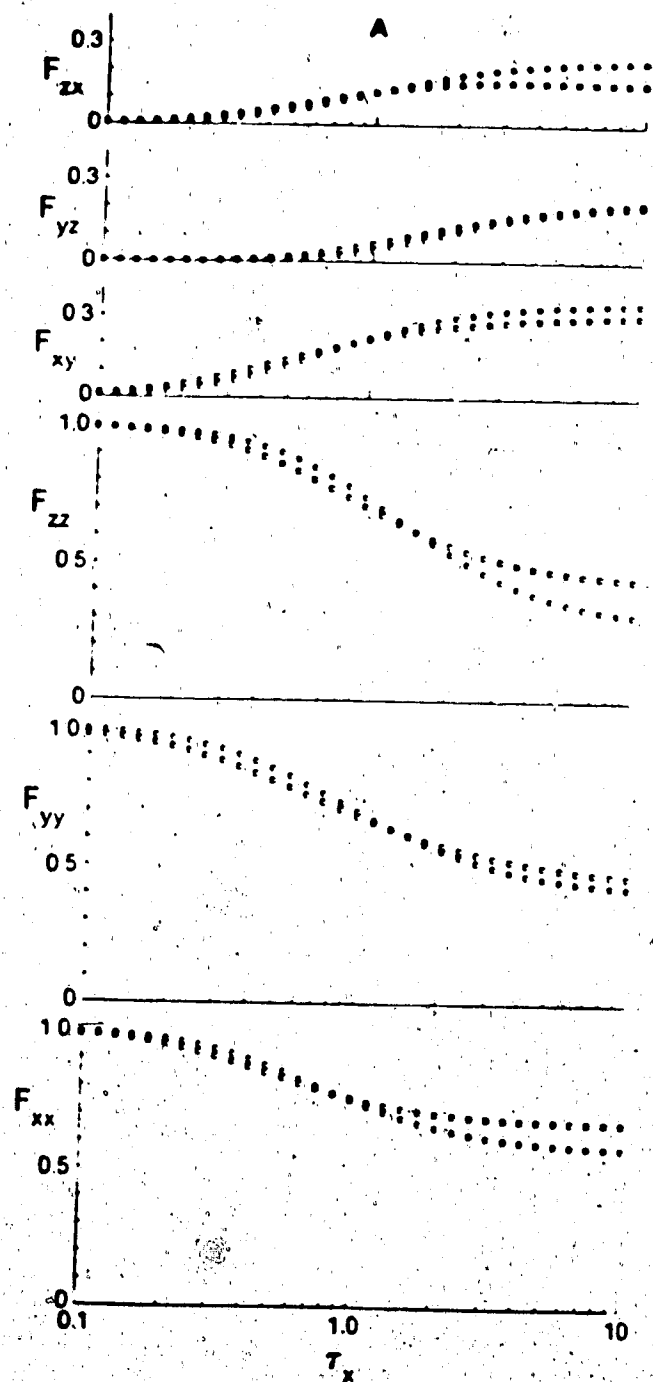
$\Delta - \tau_x = 2\tau_y = 2\tau_z$,

$\dagger - \tau_x = 5\tau_y = 5\tau_z$,

$\times - 2\tau_x = 2\tau_y = \tau_z$,

$\diamond - 5\tau_x = 5\tau_y = \tau_z$.

[Moments of inertia as in Fig. II-2].



$$\frac{+ \tau_{\gamma} (\tau_{\alpha} + \tau_{\beta}) [I_{\alpha} \tau_{\alpha} (\tau_{\beta} + \tau_{\gamma}) + I_{\beta} \tau_{\beta} (\tau_{\alpha} + \tau_{\gamma})]}{I_x I_y I_z (\tau_x + \tau_y) (\tau_y + \tau_z) (\tau_z + \tau_x)}$$

where (α, β, γ) is a cyclic permutation of (x, y, z) . In Eq. (II-50), τ_x, τ_y, τ_z are in seconds, not in reduced units as in other equations.

B. EDJ model

General expressions for the reorientational correlation times and for the spin-rotational relaxation rate for asymmetric top molecules in the EDJ model have been derived by Bull [8]. The reorientational correlation times are given by

$$\tau_{\theta}^{jkk'}(\text{EDJ}) = \left\{ A \left[1 - \frac{1}{\tau_J} A \right]^{-1} \right\}_{kk'} \quad (\text{II-51})$$

where

$$A_{kk'} = \int_0^{\infty} dt \langle D^{(j)}(Q) D^{(j)}(\Delta Q(t)) \rangle_{kk'} \exp(-t/\tau_J) \quad (\text{II-52})$$

Q represents the set of Euler angles describing the transformation from the molecular coordinate system at the beginning of each rotational diffusive step to the "J" frame in which the z-axis lies along the direction of the molecular angular momentum vector, $\Delta Q(t)$ describes the reorientation of the molecule in time t during a single

rotational diffusive step and $\langle \rangle_J$ indicates an ensemble average over the magnitude and direction of the angular momentum vector which are randomized at each "collision". τ_J is the angular momentum correlation time and corresponds to the average time between "collisions".

The spin-rotational relaxation rate for asymmetric top molecules, in the limit of extreme narrowing, is given by [8]

$$\frac{1}{T_1} = \frac{2I_z^2 B^2 \tau_J}{3\hbar^2} \sum_{L,N,k,m} \{ F_{k,m}^{(L,N)} C_k^{(L)*} C_m^{(N)} \} \quad (II-53)$$

where the non-vanishing coefficients $C_k^{(L)}$ are given by

$$C_{\pm 2}^{(2)} = (I_x C_x - I_y C_y) / (2I_z)$$

$$C_0^{(2)} = 2[I_z C_z - (I_x C_x + I_y C_y) / 2] / (\sqrt{6} I_z) \quad (II-54)$$

$$C_0^{(0)} = -(I_x C_x + I_y C_y + I_z C_z) / (\sqrt{3} I_z)$$

C_x, C_y, C_z are the principal values of the spin-rotation interaction tensor, $F_{k,m}^{(L,N)}$ is defined as

$$F_{k,m}^{(L,N)} = (\tau_J I_z^2 B^2)^{-1} \int_0^\infty dt \exp(-t/\tau_J) \sum_a \langle W_{a,k}^{(L)}(t) W_{a,m}^{(N)*}(0) \rangle_J \quad (II-55)$$

and

$$\begin{aligned}
W_{a,k}^{(L)}(t) = & J \left[C(11L, a0a) D_{a,k}^{(L)}[\Delta Q(t)] \left(\frac{I_z}{I_x} + \frac{I_z}{I_y} \right) / 2 \right. \\
& + C(11L, k0k) D_{0,0}^{(1)}[\Delta Q(t)] D_{a,k}^{(1)}[\Delta Q(t)] \left(1 - \frac{I_z}{I_y} \right) \\
& \left. + \sum_r C(11L, r, k-r, k) D_{a,r}^{(1)}[\Delta Q(t)] D_{0,r-k}^{(1)}[\Delta Q(t)] \left(\frac{I_z}{I_y} - \frac{I_z}{I_x} \right) / 2 \right] .
\end{aligned}
\tag{II-56}$$

Here J is the magnitude of the molecular angular momentum, $\Delta Q(t)$ represents the set of Euler angles which relate the molecular coordinate system at time t with the "J" frame, and $C(11L, k, l, k+l)$ are Clebsch-Gordan coefficients [32]. In order to facilitate comparison with the FPL model, it is useful to write the spin-rotational relaxation rate as

$$\frac{1}{T_1} = \frac{2k_B T \tau_J}{3\hbar^2} \sum_{\alpha, \alpha' = x, y, z} C_{\alpha} C_{\alpha'} \left(\frac{I_x I_y}{I_z} \right)^{1/2} F_{\alpha\alpha'}^{EDJ} ,
\tag{II-57}$$

where

$$\begin{aligned}
F_{xx}^{EDJ} = & \left(\frac{1}{2} F_{2,2}^{2,2} - \frac{2}{\sqrt{6}} F_{2,0}^{2,2} + \frac{1}{2} F_{2,-2}^{2,2} - \frac{2}{\sqrt{3}} F_{2,0}^{2,0} + \frac{1}{6} F_{0,0}^{2,2} \right. \\
& \left. + \frac{\sqrt{2}}{3} F_{0,0}^{2,0} + \frac{1}{3} F_{0,0}^{0,0} \right) \frac{I_x}{I_z} ,
\end{aligned}$$

$$F_{xy}^{EDJ} = \left(-F_{2,2}^{2,2} - F_{2,-2}^{2,2} + \frac{1}{3} F_{0,0}^{2,2} + \frac{2\sqrt{2}}{3} F_{0,0}^{2,0} + \frac{2}{3} F_{0,0}^{0,0} \right) \left(\frac{I_x I_y}{I_z} \right)^{1/2} / I_z ,$$

$$F_{xz}^{EDJ} = \left(\frac{4}{\sqrt{6}} F_{2,2}^{2,2} - \frac{2}{\sqrt{3}} F_{2,0}^{2,0} - \frac{2}{3} F_{0,0}^{2,2} - \frac{\sqrt{2}}{3} F_{0,0}^{2,0} + \frac{2}{3} F_{0,0}^{0,0} \right) (I_x/I_z)^{1/2}$$

$$F_{yy}^{EDJ} = \left(\frac{1}{2} F_{2,2}^{2,2} + \frac{2}{\sqrt{6}} F_{2,0}^{2,2} + \frac{1}{2} F_{2,-2}^{2,2} + \frac{2}{\sqrt{3}} F_{2,0}^{2,0} + \frac{1}{6} F_{0,0}^{2,2} \right. \\ \left. + \frac{\sqrt{2}}{3} F_{0,0}^{2,0} + \frac{1}{3} F_{0,0}^{0,0} \right) (I_y/I_z)$$

$$F_{yz}^{EDJ} = \left(\frac{-4}{\sqrt{6}} F_{2,0}^{2,2} + \frac{2}{\sqrt{3}} F_{2,0}^{2,0} - \frac{2}{3} F_{0,0}^{2,2} - \frac{\sqrt{2}}{3} F_{0,0}^{2,0} + \frac{2}{3} F_{0,0}^{0,0} \right) (I_y/I_z)^{1/2}$$

$$F_{zz}^{EDJ} = \frac{2}{3} F_{0,0}^{2,2} - \frac{2\sqrt{2}}{3} F_{0,0}^{2,0} + \frac{1}{3} F_{0,0}^{0,0} \quad \text{○} \quad (II-58)$$

These spin rotation functions, $F_{\alpha\alpha}^{EDJ}$, correspond to the $F_{\alpha\alpha}$ in Eq. (II-41) for the FPL model.

The computation of the reorientational correlation times and the spin rotation functions for fluorobenzene over a wide range of τ_J was performed by evaluating the necessary ensemble averages in Eqs. (II-52) and (II-55) by means of Gaussian quadrature.² The variation of the reorientational correlation times with τ_J is shown together with the corresponding results for the FPL model in Fig. II-2. The spin rotation functions $F_{\alpha\alpha}^{EDJ}$ in Eq. (II-58) are plotted against τ_J in Fig. II-4A along with the corresponding FPL spin rotation functions.

²The calculations were performed using a FORTRAN 77 program supplied by T. E. Bull.

4. Discussion

In Fig. II-1, representative FPL reorientational correlation functions are shown for various relative magnitudes of τ_x , τ_y , and τ_z . The reorientational correlation functions are essentially exponential in character when τ_x , τ_y and τ_z are all less than 0.1. For $j = 1$, the correlation function $\Phi_{0s000;0s000}^{jm}(t)$ is essentially independent of the variation in τ_z . This means that this correlation function, which describes the time correlation of the z-component of the molecular dipole moment, is not affected significantly by the motional modulation of the z-component of the angular momentum. This is compatible with the fact that the reorientation of the unit vector along the z-axis depends only on the rotational motion about the x- and y-axes of the molecule. Similarly, the correlation functions $\Phi_{1a000;1a000}^{1m}(t)$ and $\Phi_{1s000;1s000}^{1m}(t)$ which describe the reorientation of the x- and y- components of the dipole moment respectively, are independent of the variations in τ_x and τ_y respectively. For $j = 2$, $\Phi_{0s000;0s000}^{jm}(t)$ is essentially independent of the variation in τ_z , but other correlation functions vary significantly with all correlation times τ_x , τ_y , and τ_z . $\Phi_{2s000;2s000}^{2m}(t)$ and $\Phi_{2a000;2a000}^{2m}(t)$ show similar, but not identical, dependences on the correlation times τ_x , τ_y and τ_z . The similarity between these two-functions is not unexpected since the correlation times corresponding to the two functions are, to lowest order, identical since the cross-correlation time τ_{θ}^{22-2} , which is the difference between the above correlation times, is zero [see Eq. (II-49)]. Furthermore, the calculated values of τ_{θ}^{22-2} given in Fig. II-2 are much smaller than the self

correlation times τ_θ^{222} . When τ_x , τ_y and τ_z are greater than 0.1 the correlation functions show initial Gaussian time-dependence with exponential tails. However in the case of $\phi_{2s000,2s000}^{2m}(t)$ and $\phi_{2a000,2a000}^{2m}(t)$ for $\tau_x = .1$, $\tau_y = .05$, $\tau_z = .5$, the initial non-exponential character is different from others and may be due to poor accuracy in the evaluation of these correlation functions because they required the largest dimension \mathbf{Z} matrix allowed in our program.

The relations in Eq. (II-49) between the FPL reorientational correlation times $\tau_\theta^{jkk'}$ and the frictional coefficients τ_α^{-1} ($\alpha = x, y, z$) can be written in the general form

$$\tau_\theta^{jkk'} = A^{jkk'} / (k_B T \tau_x) \quad (\text{II-59})$$

where $A^{jkk'}$ depends on the moments of inertia and upon the ratios τ_y/τ_x and τ_z/τ_x , and has the same dimensions as the moments of inertia. Eq. (II-59) can be viewed as a generalization of the relation

$$\tau_\theta = I / (6k_B T \tau_J) \quad (\text{II-60})$$

which Hubbard [34] derived for spherical top molecules using a rotational diffusion model to describe the reorientational motion (correlation time τ_θ) and a Langevin equation to describe the modulation of the angular velocity (correlation time τ_J). In Eq.

(II-60), I is the moment of inertia of the spherical molecule. For symmetric top molecules, the EDJ model gives the relationship [27]

$$\tau_{\theta}^{jkk} = I_x / \{ k_B T_J [j(j+1) - k^2 + k^2 I_x / I_z] \}. \quad (\text{II-61})$$

The relations in Eq. (II-59) for the FPL self-correlation times reduce to this result when $I_x = I_y$ and $\tau_x = \tau_y = \tau_z = \tau_J$.

It is interesting that the cross-correlation times ($\tau_{\theta}^{jkk'}$ for $k \neq k'$) follow Hubbard relations just as the self-correlation times τ_{θ}^{jkk} do. Since the coefficients $A^{jkk'}$ for $k \neq k'$ contain differences between moments of inertia and/or friction coefficients for different axes, the cross-correlation times are expected to be somewhat smaller than the self-correlation times.

The reorientational correlation times, $\tau_{\theta}^{jkk'}$, computed with the FPL model are compared with the corresponding results for the EDJ model in Fig. II-2. In this case, the FPL calculations were done with $\tau_x = \tau_y = \tau_z$, which means that the motional modulation of the angular velocity components is taken to be isotropic as the EDJ model assumes. In Fig. II-2A, the self-correlation times for the FPL model are found to be inversely proportional to τ_x at short τ_x ($\tau_x \leq 0.1$), which is consistent with Eq. (II-49). This behavior is identical with that for the EDJ model in this region. In fact, the two models give identical values of τ_{θ} in the small angle diffusion limit where a Hubbard relationship is expected to be valid. This implies that,

although the basic physical pictures of the two models are very different, the macroscopic results are the same in this limit. As τ_x increases beyond 0.1, deviations from the Hubbard relationship occur and the reorientational correlation times for the FPL model are slightly shorter than the corresponding EDJ correlation times. This general trend is compatible with the comparison between the FPL and EDJ models for linear and spherical top molecules [26]. At much longer τ_x ($\tau_x > 1$), the values of τ_θ in the FPL model are much smaller than the corresponding τ_θ values in the EDJ model. In this region, the calculation of $\tau_\theta^{jkk'}$ for the FPL model requires the largest dimension \mathbf{Z} matrix allowed in our program, so that the accuracy for $\tau_x > 4$ may be poorer than for smaller τ_x . In addition, the validity of the FPL model is questionable in this region because one cannot define a time τ satisfying the condition of $\tau_T \ll \tau \ll \tau_x$ required for the validity of the rotational Langevin equation [37] which is an integral part of the FPL model. Here τ_T represents the correlation time which characterizes the time dependence of the rapidly fluctuating intermolecular torques. In the region $\tau_x > 1$, τ_T is comparable to τ_x since fluctuations in the angular momentum and in the intermolecular torque experienced by the molecule are governed by the rate of bimolecular collisions so that the required condition cannot be fulfilled.

The non-vanishing cross-correlation times for the FPL and EDJ models are shown in Fig. II-2B. The values of these cross-correlation times are smaller than those of the diagonal correlation

times by one to two orders of magnitude. At short τ_x ($\tau_x \leq 0.1$), the cross-correlation times are inversely proportional to τ_x as the self-correlation times are. Even τ_θ^{22-2} , which is zero to lowest order as given in Eq. (II-49), shows an inverse τ_x dependence at short τ_x . As expected, τ_θ^{22-2} is smaller than the other cross-correlation times by more than an order of magnitude. While the FPL and EDJ models give almost identical values for the reorientational cross-correlation times at short τ_x , they differ significantly at long τ_x . This feature is similar to that observed for the self-correlation times. In both models, τ_θ^{220} becomes negative as τ_x increases beyond 1.0, and τ_θ^{22-2} goes through a minimum in the region $0.1 < \tau_x < 1$ and then increases with τ_x in the dilute gas limit.

One of the features of the FPL model which distinguishes it from the EDJ model is that the FPL model allows the introduction of anisotropy in the motional modulation of the angular velocity components as well as the anisotropy in the moments of inertia. The anisotropy in the motional modulation of the angular velocity components is reflected in the relative magnitudes of the parameters τ_x , τ_y , and τ_z of the FPL model. In Fig. II-3, the second rank tensor reorientational self-correlation times, τ_θ^{2kk} , for fluorobenzene- d_5 , a planar asymmetric molecule, are shown for a variety of combinations of τ_x , τ_y and τ_z . In this molecule, the z-axis is chosen to lie along the C-F bond and the x-axis is taken to be perpendicular to the molecular plane. If the molecular shape

effect is dominant in determining the relative magnitudes of τ_x , τ_y , and τ_z , one would expect τ_x to be longer than τ_y or τ_z since rotation of the benzene ring about the x-axis should disturb neighboring molecules less than rotations about the y- and z-axes would.

However, if the intermolecular interactions due to the large electric dipole moment along the C-F bond axis is more important than molecular shape effects, then τ_z might be significantly longer than τ_x or τ_y since rotations about the z-axis do not reorient the electric dipole. Therefore we have considered two different cases:

$\tau_z > \tau_x = \tau_y$ and $\tau_x > \tau_y = \tau_z$. First, for the case $\tau_z > \tau_x = \tau_y$, the variation of the reorientational self-correlation times with τ_x is shown in Fig. II-3A for different values of the ratio, τ_z/τ_x . The reorientational correlation times are found to decrease for a given τ_x as the ratio, τ_z/τ_x , increases as predicted by Eq. (II-49). The variation of the $k \neq 0$ self-correlation times with this ratio is much more significant than the corresponding variation in the $k = 0$ correlation time. As a matter of fact, the variation of the $k = 0$ correlation times with this ratio is almost negligible. This implies that the reorientation of the $k = 0$ component of a spherical tensor is not significantly affected by motional modulation of the z-component of the angular velocity, which is characterized by τ_z . This is compatible with the result for symmetric top molecules [31]. For symmetric top molecules, only variations in $\tau_{\perp} = \tau_x = \tau_y$, which characterize modulation of the angular velocity component perpendicular to the symmetry axis, affect the $k = 0$ correlation

time. Secondly, for the case $\tau_x > \tau_y = \tau_z$, the variation of the reorientational self-correlation times with τ_x is shown in Fig. II-3B for different values of the ratio, τ_x/τ_y . It is shown that the reorientational correlation times increase for a given τ_x as the ratio, τ_x/τ_y , increases as predicted by Eq. (II-49). In this case also, the variation of the $k \neq 0$ self-correlation times with this ratio is larger than that of the $k = 0$ correlation time. In this case, however, the $k = 0$ correlation time varies quite strongly with the ratio, τ_x/τ_y , since the $k = 0$ tensor component is significantly modulated by rotational motion about the y-axis, which is characterized by τ_y .

The variation of the reorientational cross-correlation times for fluorobenzene- d_5 with the relative magnitudes of τ_x , τ_y and τ_z has also been studied, and follows the predictions of Eq. (II-49) for short τ 's. The variation of the cross-correlation times with τ_x for $\tau_x > 1$ is similar in form to that shown in Fig. II-2B for the case $\tau_x = \tau_y = \tau_z$, but shows significant variations with τ_y/τ_x and τ_z/τ_x .

The spin-rotational relaxation rate in the FPL model is expressed in terms of the spin-rotation functions F_{xx} , F_{yy} , F_{zz} , F_{xy} , F_{yz} and F_{zx} [see Eq. (II-40)]. These functions are compared with the corresponding functions for the EDJ model [Eq. (II-58)] in Fig. II-4A. From this comparison, one can see that, in general, the spin-rotation functions for both models exhibit similar dependence on τ_x (or τ_y). When τ_x is less than 1, the FPL spin-rotation functions F_{xx} , F_{yy} , and F_{zz} have slightly higher values than the corresponding

EDJ functions. As τ_x increases beyond 1, the EDJ spin-rotation functions become higher than the corresponding FPL functions. F_{xx} , F_{yy} , and F_{zz} represent the ratios of the autocorrelation times for the functions $\omega_x S_{11ms}^*[\Omega]$, $\omega_y S_{11ms}^*[\Omega]$, and $\omega_z S_{10ms}^*[\Omega]$ to the respective times τ_x , τ_y , and τ_z . [See Eq. (II-37) - (II-41)]. When τ_x , τ_y , and τ_z are short, the time dependence of the angular velocity components ω_α ($\alpha = x, y, z$) contributes much more to the decay of the autocorrelation functions than the time dependence of the reorientational part, S_{1km}^* , does. In other words, the reorientational motion is very slow compared to the fluctuations in the angular velocity so that the autocorrelation functions $F_{\alpha\alpha}$ are predominantly governed by the time dependence of the angular velocity. In fact, the correlation time for the angular velocity component ω_α is equal to τ_α ($\alpha = x, y, z$) in the limit of short τ 's. Hence the autocorrelation times for the products $\omega_x S_{11ms}^*[\Omega]$, $\omega_y S_{11ms}^*[\Omega]$ and $\omega_z S_{10ms}^*[\Omega]$ are essentially identical to τ_x , τ_y and τ_z , respectively and the spin rotation functions F_{xx} , F_{yy} , and F_{zz} are equal to 1. This is in agreement with the result obtained by rational approximation for the spin-rotation functions in Eq. (II-50). In this limit, the spin rotation relaxation rate, Eq. (II-40), can be reduced to

$$\frac{1}{T_1} \sim \frac{2k_B T}{3\hbar^2} (I_x^2 C_x^2 \tau_x + I_y^2 C_y^2 \tau_y + I_z^2 C_z^2 \tau_z) \quad (\text{II-62})$$

The variation of the spin-rotation functions $F_{\alpha\beta}$ ($\alpha, \beta = x, y, z$) for the EPL model with τ_x for various ratios τ_x/τ_y and τ_z/τ_x are shown in Fig. II-4B. The functions are shown to be sensitive to the ratios τ_x/τ_y and τ_z/τ_x even at short τ_x .

In general, the spin-rotational relaxation rate [Eq. (II-40)] will be dominated by the terms $C_x^2 F_{xx}$, $C_y^2 F_{yy}$, $C_z^2 F_{zz}$, but the cross-correlation terms $C_\alpha C_\beta F_{\alpha\beta}$ ($\alpha = x, y, z, \beta \neq \alpha$) may become significant when the times τ_α become long.

5. Conclusions

The general expressions for the reorientational correlation functions, correlation times, and spectral densities for asymmetric top molecules in liquids have been presented using the series expansion for the angular velocity-orientation conditional probability density obtained from the rotational Fokker-Planck equation [25]. In addition, the expression for the spin relaxation rate due to the spin-rotation interaction has been derived. Numerical calculations indicate that these properties are influenced by the anisotropy in the motional modulation of the angular velocity components. For instance, in the case of reorientational self-correlation times τ_0^{jkk} , the $k \neq 0$ correlation times vary strongly with this frictional anisotropy, but the dependence of the $k = 0$ correlation times on the frictional anisotropy is weak. On the other hand, all spin-rotation functions $F_{\alpha\beta}$ ($\alpha, \beta = x, y, z$) have

significant dependence on the frictional anisotropy. The comparison of the FPL reorientational correlation times and spin-rotation functions for the case $\tau_x = \tau_y = \tau_z$ with the corresponding EDJ correlation times and functions leads to the conclusion that the two models give almost indistinguishable descriptions of rotational motion of molecules in liquids in the rotational diffusion limit although the basic physical pictures for the FPL and EDJ models are very different, but the predictions of the two models differ outside this limit.

References

1. P. Debye, **Polar Molecules** (Reinhold, New York, 1929), pp.77ff.
2. R. G. Gordon, J. Chem. Phys. **44** (1966) 1830.
3. R. E. D. McClung, J. Chem. Phys. **51**, (1969) 3842.
4. M. Fixman and K. Rider, J. Chem. Phys. **51**, (1969) 2425.
5. M. Fixman and K. Rider, J. Chem. Phys. **57** (1972) 2548.
6. R. E. D. McClung, J. Chem. Phys. **57**, (1972) 5478.
7. J. C. Leicknam, Y. Guissani, and S. Bratos, J. Chem. Phys. **68** (1978) 3380.
8. T. E. Bull, J. Chem. Phys. **81** (1984) 3181.
9. C. Dreyfus and T. Nguyen Tan, J. Chem. Phys. **62** (1975) 2492.
10. T. C. Farrar, A. A. Maryott and M. S. Malmberg, J. Chem. Phys. **54** (1971) 64.
11. K. T. Gillen, J. H. Noggle and T. K. Leipert, Chem. Phys. Lett. **17** (1972) 505.
12. R. R. Sharp, J. Chem. Phys. **57** (1972) 5321.
13. R. R. Sharp, J. Chem. Phys. **60** (1974) 1149.
14. J. H. Campbell, S. J. Seymour and J. Jonas, J. Chem. Phys. **59** (1973) 4151.
15. K. T. Gillen, D. C. Douglass, M. S. Malmberg and A. A. Maryott, J. Chem. Phys. **57** (1972) 5170.
16. R. E. D. McClung, Chem. Phys. Lett. **19** (1972) 304.
17. T. C. Farrar, A. A. Maryott and M. S. Malmberg, Ber. Bunsen Gesell. **75** (1971) 246.

18. T. E. Bull, J. Chem. Phys. 59 (1973) 6173.
19. T. E. Bull, J. Chem. Phys. 62 (1975) 222.
20. P. S. Hubbard, Phys. Rev. A6 (1972) 2421.
21. P. S. Hubbard, Phys. Rev. A8 (1974) 1429.
22. G. T. Evans, J. Chem. Phys. 65 (1976) 3030.
23. G. T. Evans, J. Chem. Phys. 67 (1977) 2911.
24. J. G. Powles and G. Rickayzen, Mol. Phys. 33 (1977) 1207.
25. R. E. D. McClung, J. Chem. Phys. 73 (1980) 2435.
26. G. Levi, J. P. Marsault, F. Marsault-Heraill, and R. E. D. McClung, J. Chem. Phys. 73 (1980) 2443.
27. R. E. D. McClung, Adv. Mol. Relaxation Processes 10 (1977) 83.
28. S. Perry, V. H. Schiemann, M. Wolfe and J. Jonas, J. Phys. Chem. 85 (1981) 2805.
29. T. W. Zerda, J. Schroeder, and J. Jonas, J. Chem. Phys. 75 (1981) 1612.
30. P. S. Hubbard, Phys. Rev. A9 (1974) 481.
31. R. E. D. McClung, J. Chem. Phys. 75 (1981) 5503.
32. M. E. Rose, Elementary Theory of Angular Momentum (Wiley, New York, 1957).
33. M. Abramowitz and I. A. Stegun, Handbook of Mathematical Functions (Dover, New York, 1965) Chap. 22.
34. P. S. Hubbard, Phys. Rev. 131 (1963) 1155.
35. S. Weisbaum, Y. Beers, and G. Herrmann, J. Chem. Phys. 23 (1955) 1601.
36. R. A. Assink and J. Jonas, J. Chem. Phys. 57 (1972) 3329.

37. F. Reif, **Fundamentals of Statistical and Thermal Physics**
(McGraw-Hill, New York, 1965), Chap. 15. The corresponding
translational problem is discussed.

CHAPTER III

THE FOKKER-PLANCK-LANGEVIN MODEL FOR ROTATIONAL BROWNIAN MOTION. V. COMPARISON WITH MAGNETIC RELAXATION DATA FOR ASYMMETRIC TOP MOLECULES

1. Introduction

Molecular rotation in liquids has been studied by a number of experimental techniques - nuclear and electron spin relaxation, infrared and Raman bandshapes, light scattering, and neutron scattering. The interpretation of the experimental measurements is usually made in the context of one or more models or conceptual pictures of molecular dynamics in fluids. The extended diffusion (ED) [1-8] and the Fokker-Planck-Langevin (FPL) [6,9-15] models have often been employed in the interpretation of experimental measurements. Recently, the mathematical frameworks for the J-diffusion limit of the ED model (EDJ) [16] and for the FPL model [17] for asymmetric top molecules have been developed, and detailed comparisons with experimental data on asymmetric top molecules are now possible.

The relaxation times of the ^{19}F and ^2D nuclei in fluorobenzene- d_5 ($\text{C}_6\text{D}_5\text{F}$) have been reported by Assink and Jonas [18]. They compared the reorientational and angular momentum correlation times

¹A version of this chapter has been accepted for publication. D.H. Lee and R.E.D. McClung, 1986. Journal of Magnetic Resonance.

obtained from the nuclear relaxation data with the predictions of the ED model for spherical top molecules, and found that the rotational motion of C_6D_5F was described reasonably well by the EDJ, but not by the EDM (M-diffusion limit of ED) model.

Electron spin relaxation measurements on chlorine dioxide (ClO_2) have been reported by McClung and Kivelson [19]. The ESR linewidths are determined by the motional modulation of spin-rotational interactions, and were analyzed using an approximate solution to the Langevin equation for the angular velocities. It was reported that, particularly in non-polar solvents, the precessional motion of the rotational angular momentum of the ClO_2 molecule contributed significantly to the observed linewidths. The FPL model for asymmetric top molecules is a complete extension of the approximate rotational Langevin equation approach used in the ClO_2 work [19], and allows a non-approximate analysis of the linewidths.

In this paper, we examine the suitability of the EDJ and FPL models in the characterization of the rotational motions of the asymmetric top molecules C_6D_5F and ClO_2 .

2. Theory

A. FPL model

We review briefly the FPL model [17] for asymmetric top molecules. This FPL model is a frictional model for molecular rotation in liquids and is based on a rotational Fokker-Planck equation for the conditional probability density of the orientation

and the angular velocity of the molecule and a rotational Langevin equation for the angular velocity [9,20]. In this model, the angular velocity of the rotating molecule is modulated by slowly varying viscosity dependent retarding torques and by rapidly fluctuating Brownian torques which reflect the molecular nature of the liquid.

In the FPL model, the reorientational correlation times $\tau_{\theta}^{jkk'}$, which are used in the description of infrared and Raman bandshapes, dielectric relaxation, and magnetic relaxation via intramolecular dipole-dipole and nuclear quadrupole interactions, are given by [17]

$$\tau_{\theta}^{jkk'} = \sum_{\sigma, \sigma' = s, a} C_{\sigma, \sigma'}(k, k') (Z^{jm})^{-1} |k|_{\sigma 000} |k'|_{\sigma' 000} \quad , \quad (\text{III-1})$$

where the functions $C_{\sigma, \sigma'}(k, k')$ are defined by

$$C_{s, s}(k, k') = \left[\frac{1}{2} + \left(\frac{1}{\sqrt{2}} - \frac{1}{2} \right) (\delta_{k,0} + \delta_{k',0}) \right]$$

$$+ (1 - \sqrt{2}) \delta_{k,0} \delta_{k',0} [1 + \delta_{k,0} \delta_{k',0}]$$

$$C_{s, a}(k, k') = \left[\frac{1}{2} + \left(\frac{1}{\sqrt{2}} - \frac{1}{2} \right) \delta_{k,0} \right] \text{sgn}(k') \quad ,$$

$$C_{a, s}(k, k') = \left[\frac{1}{2} + \left(\frac{1}{\sqrt{2}} - \frac{1}{2} \right) \delta_{k',0} \right] \text{sgn}(k) \quad , \quad (\text{III-2})$$

$$C_{a,a}(k,k') = \frac{1}{2} \operatorname{sgn}(k) \operatorname{sgn}(k')$$

and

$$\operatorname{sgn}(k) = \begin{array}{ll} +1 & , \quad k > 0 \\ 0 & , \quad k = 0 \\ -1 & , \quad k < 0 \end{array}$$

(III-3)

Here Z^{jm} is the matrix representation of the Liouville operator of the rotational Fokker-Planck equation in the appropriate basis [17], and the subscript indices $|k|\sigma 000$ and $|k'|\sigma' 000$ represent the row and column of the inverse of the Z matrix.

In the FPL model, the spin relaxation rate due to motional modulation of spin-rotational interactions is given by [17]

$$\frac{1}{T_{1SR}} = \frac{1}{T_{2SR}} = (2k_B T / 3\hbar^2) \sum_{\alpha, \alpha' = x, y, z} C_{\alpha} C_{\alpha'} (I_{\alpha} I_{\alpha'} \tau_{\alpha} \tau_{\alpha'})^{1/2} F_{\alpha\alpha'} \quad (\text{III-4})$$

where C_{α} are the principal values of the spin-rotation coupling tensor, I_{α} are the moments of inertia, and τ_{α} are the parameters of the FPL model which are the inverses of the friction coefficients of the retarding torques in the rotational Langevin equation. The parameter τ_{α} is identical to the correlation time for the α -component of the angular momentum in the limit of short τ_{α} . The functions $F_{\alpha\alpha'}$ are symmetric in the indices α and α' , and are given by

$$F_{xx} = (Z^{11})^{-1}_{1a100, 1a100} / \tau_x$$

$$F_{yy} = (Z^{11})^{-1}_{1s010, 1s010} / \tau_y \quad (\text{III-5})$$

$$F_{zz} = (Z^{11})^{-1}_{0s001, 0s001} / \tau_z$$

$$F_{xy} = -[(Z^{11})^{-1}_{1a100, 1s010} + (Z^{11})^{-1}_{1s010, 1a100}] / [2(\tau_x \tau_y)^{1/2}]$$

$$F_{yz} = [(Z^{11})^{-1}_{1s010, 0s001} + (Z^{11})^{-1}_{0s001, 1s010}] / [2(\tau_y \tau_z)^{1/2}]$$

$$F_{zx} = -[(Z^{11})^{-1}_{1a100, 0s001} + (Z^{11})^{-1}_{0s001, 1a100}] / [2(\tau_z \tau_x)^{1/2}]$$

B. EDJ model

The EDJ model assumes that the molecules perform free rotations which are interrupted by strong "collisions" of short duration [1]. The effects of intermolecular interactions are represented by these strong instantaneous collisions during which the molecule remains fixed, but the angular velocity is changed. In the EDJ model, both the magnitude and the direction of the angular velocity are randomized at every "collision". The mean time between these collisional events is equal to the angular momentum correlation time τ_j . Note that all components of the angular momentum have the same correlation time.

The reorientational correlation times for asymmetric top molecules, in the EDJ model, are given by [16]

$$\tau_{\theta}^{jkk'}(\text{EDJ}) = \left\{ A \left[1 - \frac{1}{\tau_J} A \right]^{-1} \right\}_{kk'} \quad (\text{III-6})$$

where 1 is the unit matrix and A is the matrix whose elements are given by

$$A_{kk'} = \int_0^\infty dt \langle D^{(j)}[Q] D^{(j)}[\Delta Q(t)] \rangle_{kk'} \exp(-t/\tau_J) \quad (\text{III-7})$$

where the $D^{(j)}$ are the Wigner rotation matrices [21], Q represents the set of Euler angles describing the transformation from the molecular coordinate system at the beginning of each rotational diffusive step to the "J" frame in which the z-axis lies along the direction of the molecular angular momentum vector, $\Delta Q(t)$ describes the reorientation of the molecule in time t during a single rotational diffusive step, and the brackets $\langle \rangle$ denote an ensemble average over the magnitude and direction of the angular momentum which are randomized at each "collision". τ_J is the angular momentum correlation time and corresponds to the average time between "collisions".

The spin relaxation rate due to motional modulation of spin-rotational interaction is given by [16]

$$\frac{1}{T_{1SR}} = \frac{1}{T_{2SR}} = (2k_B T I_Z \tau_J / 3\hbar^2) \sum_{L,N,k,p} C_k^{(L)*} C_P^{(N)} F_{k,p}^{(L,N)} \quad (\text{III-8})$$

where $C_k^{(L)}$ are related to the principal values C_α of the spin-rotation coupling tensor by

$$C_{\pm 2}^{(2)} = (I_x C_{xx} - I_y C_{yy}) / (2I_z)$$

$$C_0^{(2)} = 2[I_z C_{zz} - (I_x C_{xx} + I_y C_{yy})/2] / (\sqrt{6}I_z) \quad (\text{III-9})$$

$$C_0^{(0)} = -(I_x C_{xx} + I_y C_{yy} + I_z C_{zz}) / (\sqrt{3}I_z)$$

No other components are involved in spin-rotational relaxation. The $F_{k,p}^{(L,N)}$ are spin-rotation correlation factors defined as [16]

$$F_{k,p}^{(L,N)} = (\tau_J I_z k_B T)^{-1} \int_0^\infty dt \exp(-t/\tau_J) \int_a \langle w_{a,k}^{(L)}(t) w_{a,p}^{(N)}(0) \rangle_J \quad (\text{III-10})$$

where

$$\begin{aligned} w_{a,k}^{(L)}(t) = & J [C(11L; a0a) D_{a,k}^{(L)}[\Delta Q(t)] (I_z/I_x + I_z/I_y)/2 \\ & + C(11L; k0k) D_{0,0}^{(1)}[\Delta Q(t)] D_{a,k}^{(1)}[\Delta Q(t)] (1 - I_z/I_y) \\ & + C(11L; r, k-r, k) D_{a,r}^{(1)}[\Delta Q(t)] D_{0,r-k}^{(1)}[\Delta Q(t)] (I_z/I_y - I_z/I_x)/2] \end{aligned} \quad (\text{III-11})$$

and the $C(11L; 1 j 1+j)$ are Clebsch-Gordan coefficients [22], J is the magnitude of the molecular angular momentum, and $\Delta Q(t)$ represents the set of Euler angles which relate the molecular coordinate system at time t with the "J" frame.

3. Results and Discussion

A. Fluorobenzene- d_5

In order to examine the validity of the FPL and EDJ models in the interpretation of experimental observations, we compare the theoretical relationship between the angular momentum correlation time and the reorientational correlation time predicted by each model with the experimental results obtained from magnetic relaxation time measurements. The spin lattice relaxation times of the 2D and ^{19}F nuclei in C_6D_5F have been reported by Assink and Jonas [18] for a wide range of temperature and pressure. They interpreted the experimental data in terms of the ED model derived for spherical top molecules and approximated the non-sphericity of the C_6D_5F molecule by taking the average, I , of the principal moments of inertia. The angular momentum correlation times, τ_J , were determined from the spin-rotational contributions, $1/T_{1SR}$, to the ^{19}F relaxation using the relationship

$$\frac{1}{T_{1SR}} = (2Ik_B T / 3\hbar^2) (C_x^2 + C_y^2 + C_z^2) \tau_J \quad (III-12)$$

which is valid in the limit of rotational diffusion. Using this approximate approach, Assink and Jonas [18] found that the rotational motion of C_6D_5F was reasonably consistent with the EDJ model, but not with the EDM model as judged by comparison of the observed relationship between the reorientational correlation times and the angular momentum correlation times with the relationships predicted by the two models. In this work, we wish to reanalyze the C_6D_5F magnetic relaxation data using the EDJ and FPL models for asymmetric top molecules.

The spin relaxation rate of 2D is exclusively determined by the motional modulation of the nuclear quadrupolar interactions. The 2D spin-lattice relaxation time is related to an effective reorientational correlation time, $\tau_0^{(2)}(eff)$, by

$$\frac{1}{T_{1D}} = \frac{3}{8} \left(\frac{e^2 q Q}{h} \right)^2 \left(1 + \frac{1}{3} \eta^2 \right) \tau_0^{(2)}(eff) \quad , \quad (III-13)$$

where $(e^2 q Q/h)$ is 2π times the quadrupole coupling constant and η is the asymmetry parameter. The deuterium quadrupole coupling constant for C_6D_5F has not been measured, so it is assumed to be 180 KHz, which is the value obtained for perdeutero benzene [23] and for 1,3,5-tri-fluorobenzene- d_3 [24]. The asymmetry parameters [23,24] for these molecules were found to be negligibly small, so we have taken η to be zero for C_6D_5F . Since C_6D_5F contains five deuterium nuclei, the effective reorientational correlation time is the average of the reorientational correlation times for the five 2D nuclei:

$$\tau_{\theta}^{(2)}(\text{eff}) = \frac{1}{5} \sum_{i=1}^5 \tau_{\theta}^{(2)}(D_i) \quad , \quad (\text{III-14})$$

where the reorientational correlation time, $\tau_{\theta}^{(2)}(D_i)$, for the i -th deuterium is given by

$$\tau_{\theta}^{(2)}(D_i) = \sum_{k,k'} \tau_{\theta}^{2kk'} D_{k0}^{(2)*} [\phi_i, \theta_i, 0] D_{k'0}^{(2)} [\phi_i, \theta_i, 0]. \quad (\text{III-15})$$

In Eq. (III-15), $[\phi_i, \theta_i, 0]$ represents the set of Euler angles which interrelates the "quadrupolar" frame in which the electric field gradient tensor is diagonalized and the molecular coordinate system in which the inertia tensor is diagonal. The electric field gradient tensor is assumed to be diagonalized in the frame where the C-D_i bond lies along the z-axis. The third of the Euler angles is zero because of the assumed axial symmetry of the electric field gradient. In Eq. (III-15), the Wigner rotation matrices are [21]

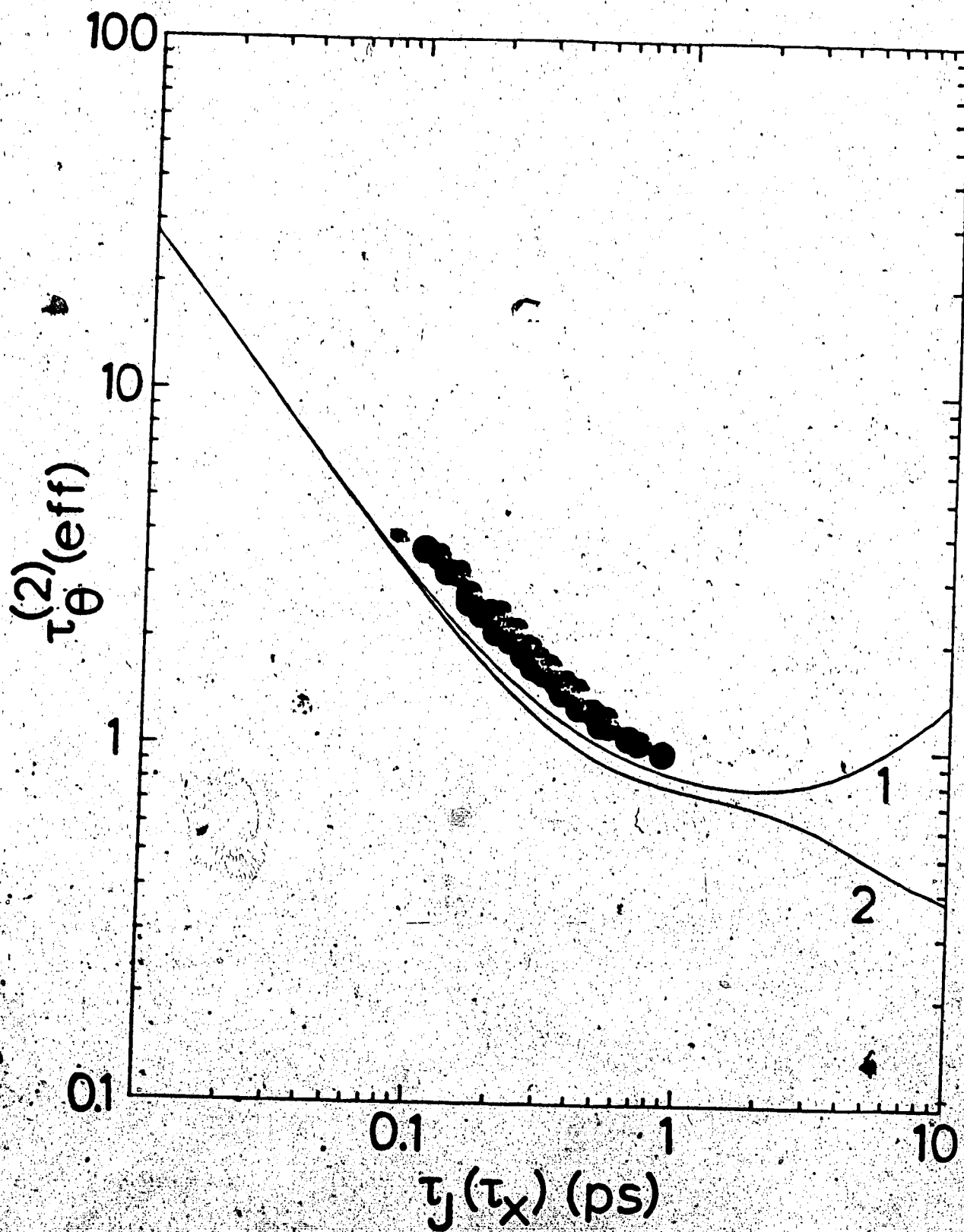
$$D_{0,0}^{(2)}[\phi, \theta, 0] = \frac{1}{2}(3\cos^2\theta - 1)$$

$$D_{\pm 1,0}^{(2)}[\phi, \theta, 0] = \mp \left(\frac{3}{2}\right)^{1/2} \sin\theta \cos\theta \exp(\mp i\phi) \quad , \quad (\text{III-16})$$

$$D_{\pm 2,0}^{(2)}[\phi, \theta, 0] = \left(\frac{3}{8}\right)^{1/2} \sin^2\theta \exp(\mp 2i\phi)$$

The experimental values of $\tau_0^{(2)}(\text{eff})$ were obtained from the T_{1D} data [18] using Eq. (III-13). The angular momentum correlation time, τ_J , which serves as the only variable parameter of the EDJ model, was obtained from T_{1F} at each temperature [18]. In general, the relaxation of ^{19}F is determined by several relaxation mechanisms: intermolecular dipole-dipole interactions, intramolecular dipole-dipole interactions, chemical shift anisotropy, and spin-rotation interactions. Since the angular momentum correlation times are directly related to the spin-rotation interactions it is necessary to make corrections for other contributions to ^{19}F relaxation in order to determine the angular momentum correlation times. After making corrections as described in [18], the experimental angular momentum correlation times for the EDJ model were obtained from Eq. (III-8). In this work, we have used the same principal values of the spin-rotation coupling tensor as Assink and Jonas [18] ($C_x = 1.2 \times 10^4 \text{ s}^{-1}$, $C_y = 1.7 \times 10^4 \text{ s}^{-1}$, $C_z = 0.5 \times 10^4 \text{ s}^{-1}$) which are expected to be reliable since they have been determined by molecular beam measurements [25]. The relationship between $\tau_0^{(2)}(\text{eff})$ and τ_J obtained from the experimental data and the relationships predicted by the EDJ and FPL models are shown in Fig. III-1. The FPL curve was obtained using $\tau_x = \tau_y = \tau_z$. One can obtain values of τ_x (assuming $\tau_x = \tau_y = \tau_z$) from the experimental T_{1F} data using Eq. (III-4), and these do not differ significantly from the values of τ_J obtained using Eq. (III-8). Fig. III-1 shows that both EDJ and FPL models

Fig. III-1. Comparison of correlation times from the EDJ model (curve 1), from the FPL model with $\tau_x = \tau_y = \tau_z$ (curve 2), and from the nuclear relaxation times in C_6D_5F liquid (●).



agree qualitatively with the experimental results in that the observed decrease in $\tau_0^{(2)}(\text{eff})$ with increasing τ_J (or τ_X) is paralleled in both models. Both models give similar predictions in the range of $\tau_J(\tau_X)$ spanned by the experimental data, but both models predict values of $\tau_0^{(2)}(\text{eff})$ which are 10-20% smaller than the values obtained from the nuclear relaxation data. Since the EDJ model and the FPL model with $\tau_X = \tau_Y = \tau_Z$ assume isotropic modulation of the angular velocity components, it is useful to investigate the effects of frictional anisotropy which can be introduced into the FPL model.

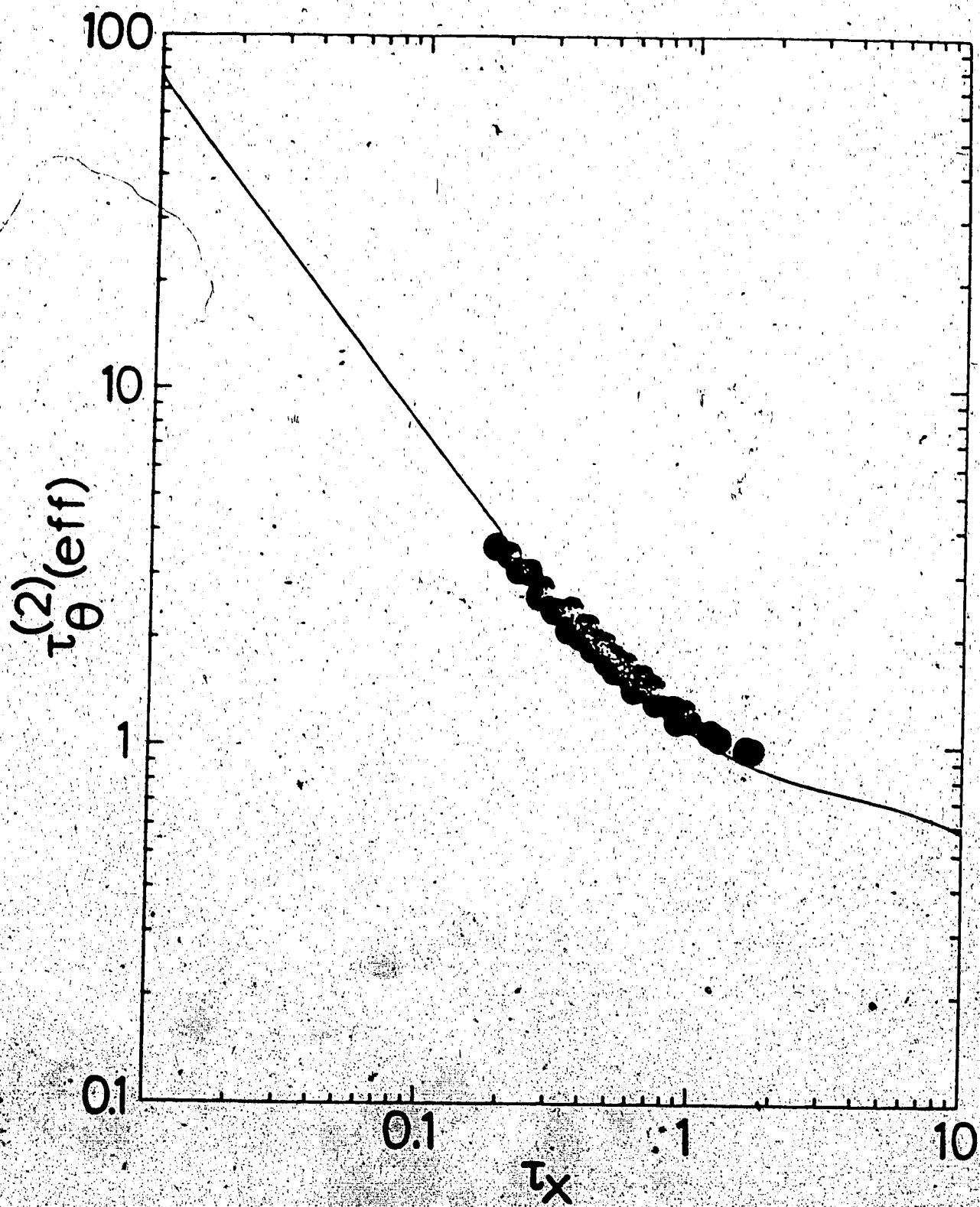
The anisotropy in the motional modulation of the angular velocity components is reflected in the relative magnitudes of the parameters τ_X , τ_Y and τ_Z of the FPL model. We compared the relationship between $\tau_0^{(2)}(\text{eff})$ and τ_X obtained from the experimental data with the corresponding relationship predicted by the FPL model for different relative magnitudes of τ_X , τ_Y and τ_Z . The theoretical relationship between $\tau_0^{(2)}(\text{eff})$ and τ_X is obtained from Eqs. (III-1), (III-14) and (III-15) for a given relative magnitude of τ_X , τ_Y and τ_Z . In $\text{C}_6\text{D}_5\text{F}$, the z-axis is chosen to lie along the C-F bond and the x-axis is taken to be perpendicular to the molecular plane. If molecular shape effects are dominant in determining the relative magnitudes of τ_X , τ_Y and τ_Z , one would expect τ_X to be longer than τ_Y or τ_Z since rotation of the benzene ring about the x-axis should be less hindered by interactions with neighboring molecules than rotation about y- or z-axes. However, if the intermolecular interactions arising from the electric dipole moment along the C-F

bond axis are more important than molecular shape effects, then τ_z might be significantly longer than τ_x or τ_y . Based on these molecular shape and electric dipole moment considerations, we have considered two different cases: $\tau_z > \tau_x = \tau_y$ and $\tau_x > \tau_y = \tau_z$. First, for the case $\tau_z > \tau_x = \tau_y$, we compared the theoretical relationships between $\tau_0^{(2)}(\text{eff})$ and τ_x with the corresponding experimental results for several ratios, τ_z/τ_x , in the range $1 < \tau_z/\tau_x \leq 5$. From these comparisons, we found that the agreement between theory and experiment was poorer for $\tau_z > \tau_x = \tau_y$ than for the case $\tau_x = \tau_y = \tau_z$. For the second case $\tau_x > \tau_y = \tau_z$, we varied the ratio τ_x/τ_z in the range $1 < \tau_x/\tau_z \leq 5$ and found that the agreement between experiment and theory was much better than for the case $\tau_x = \tau_y = \tau_z$. We obtained a good fit for $\tau_x/\tau_z = 3.5$ as shown in Fig. III-2. This result implies that the rotational motion of $\text{C}_6\text{D}_5\text{F}$ is significantly affected by the anisotropy in the motional modulation of the angular velocity components and that the relative magnitudes of τ_x , τ_y and τ_z appear to be dominated by molecular shape effects rather than by electrostatic interactions due to the dipole moment of $\text{C}_6\text{D}_5\text{F}$.

B. Chlorine dioxide

We now wish to use the FPL and EDJ models as a basis for the interpretation of the ESR linewidths of ClO_2 in dilute liquid solutions reported by McClung and Kivelson [19]. The electron spin relaxation in ClO_2 is dominated by the spin-rotational contribution,

Fig. III-2. Comparison of correlation times from FPL model with $\tau_x = 3.5 \tau_y = 3.5 \tau_z$ (solid curve), and from the nuclear relaxation times in C_6D_5F liquid (●).



but the observed linewidths are not proportional to T/η (T being the absolute temperature, η the solvent viscosity) as simple theory predicts [26]. In order to explain this nonlinear relationship, an approximate theory, which included motional modulation of the rotational angular momentum, precessional motion of the angular momentum, and reorientational modulation of the spin-rotational interactions, was developed [19]. In this theory, the spin-rotational contribution to the transverse relaxation rate was given by

$$\frac{1}{T_{2SR}} = (2k_B T / 3\hbar^2) \sum_{\alpha=x,y,z} C_\alpha^2 I_\alpha [\tau_{J\alpha}^{-1} + k_B T (\tau_{J\beta} / I_\beta + \tau_{J\gamma} / I_\gamma)]^{-1} \quad (\text{III-17})$$

where $\tau_{J\alpha}$ is the correlation time for the α -component of the angular momentum, and (α, β, γ) is an even permutation of (x, y, z) . The $k_B T (\tau_{J\beta} / I_\beta + \tau_{J\gamma} / I_\gamma)$ term in Eq. (III-17) represents the reorientational effects on the spin-rotational interactions. From a first-order approximate solution to the rotational Langevin equation and a Stokes-Einstein relationship, it can be shown [27] that the angular momentum correlation times are given by

$$\tau_{J\alpha}^{-1} = \frac{(8\pi r^3 \eta)}{I_\alpha} \kappa + \frac{(I_\beta - I_\gamma) k_B T \tau_{J\beta} \tau_{J\gamma}}{I_\alpha I_\beta I_\gamma (\tau_{J\beta} + \tau_{J\gamma})} \quad (\text{III-18})$$

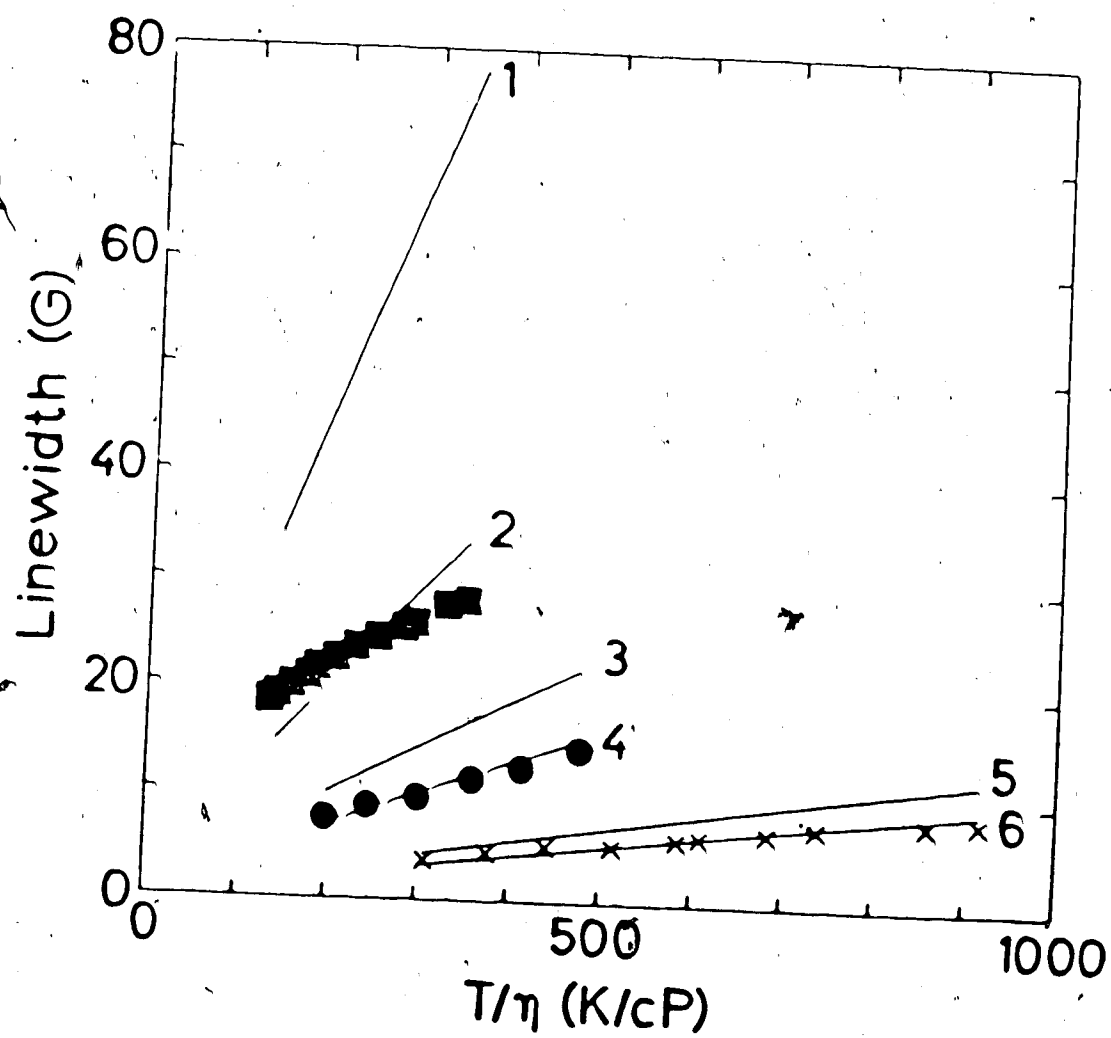
where (α, β, γ) is an even permutation of (x, y, z) , r is the

hydrodynamic radius of ClO_2 and κ is a parameter which characterizes the anisotropic solute-solvent interactions. The first term in Eq. (III-18) describes the viscosity-dependent frictional torques on the solute molecule, and corresponds to the parameter τ_α^{-1} of the FPL model. The FPL model is an exact extension of the approximate theory used by McClung and Kivelson [19]. In order to evaluate the ClO_2 data in terms of the FPL model, and to ascertain the correctness of the conclusions based on the approximate theory, we have computed the spin-rotational contributions to the ClO_2 linewidths with the FPL model using parameters

$$\tau_\alpha = I_\alpha / (8\pi r^3 \eta \kappa) \quad (\text{III-19})$$

with $r = 1.1\text{\AA}$, and the values of κ given in [19] and η given in [27]. In this work we used the same principal values of the spin-rotation coupling tensor ($C_x = -1.362 \times 10^9 \text{ s}^{-1}$, $C_y = 0.028 \times 10^9 \text{ s}^{-1}$, $C_z = -8.725 \times 10^9 \text{ s}^{-1}$) as in the previous work [19]. We have computed the linewidths for three representative cases: ClO_2 in acetone where the anisotropic intermolecular interactions are relatively strong, ClO_2 in chloroform where the intermolecular interactions are intermediate among solvents studied, and ClO_2 in carbon tetrachloride where the intermolecular interactions are very weak. As shown in Fig. III-3, the linewidths calculated with the FPL model using the values of κ given in [19] are much larger than the

Fig. III-3. Observed ESR linewidths of ClO_2 in CCl_4 (■), CHCl_3 (●) and acetone (X) and linewidths predicted by the FPL model ($1 - \kappa = .0178$, $2 - \kappa = .0450$, $3 - \kappa = 0.0986$, $4 - \kappa = 0.148$, $5 - \kappa = 0.372$, $6 - \kappa = 0.500$).



experimental linewidths. Furthermore, the FPL linewidths vary almost linearly with T/η , while the T/η -dependence of the observed linewidths shows significant non-linearity. In order to get better fits to the experimental data, we have increased the values of κ and the results are shown in Fig. III-3. In the cases of ClO_2 in acetone and chloroform, the observed linewidths vary approximately linearly with T/η and the agreement between the FPL model and the experimental data is reasonably good, but, in the case of ClO_2 in CCl_4 , the T/η -dependence of the calculated and experimental linewidths is very different. One must conclude that the FPL model does not account for the observed T/η -dependence of the ESR linewidths of ClO_2 when the anisotropic intermolecular interactions are very weak. The apparent success of the approximate theory of McClung and Kivelson [19] can be attributed to two factors: (1) the use of Eq. (III-17) for $1/T_{2SR}$ which ignores contributions from the cross-correlation terms involving $C_x C_y$, $C_y C_z$ and $C_z C_x$ which are present in Eq. (III-4); and (2) the approximate relationship in Eq. (III-18) which, although only a first order approximation, was employed far beyond the limits of its applicability.

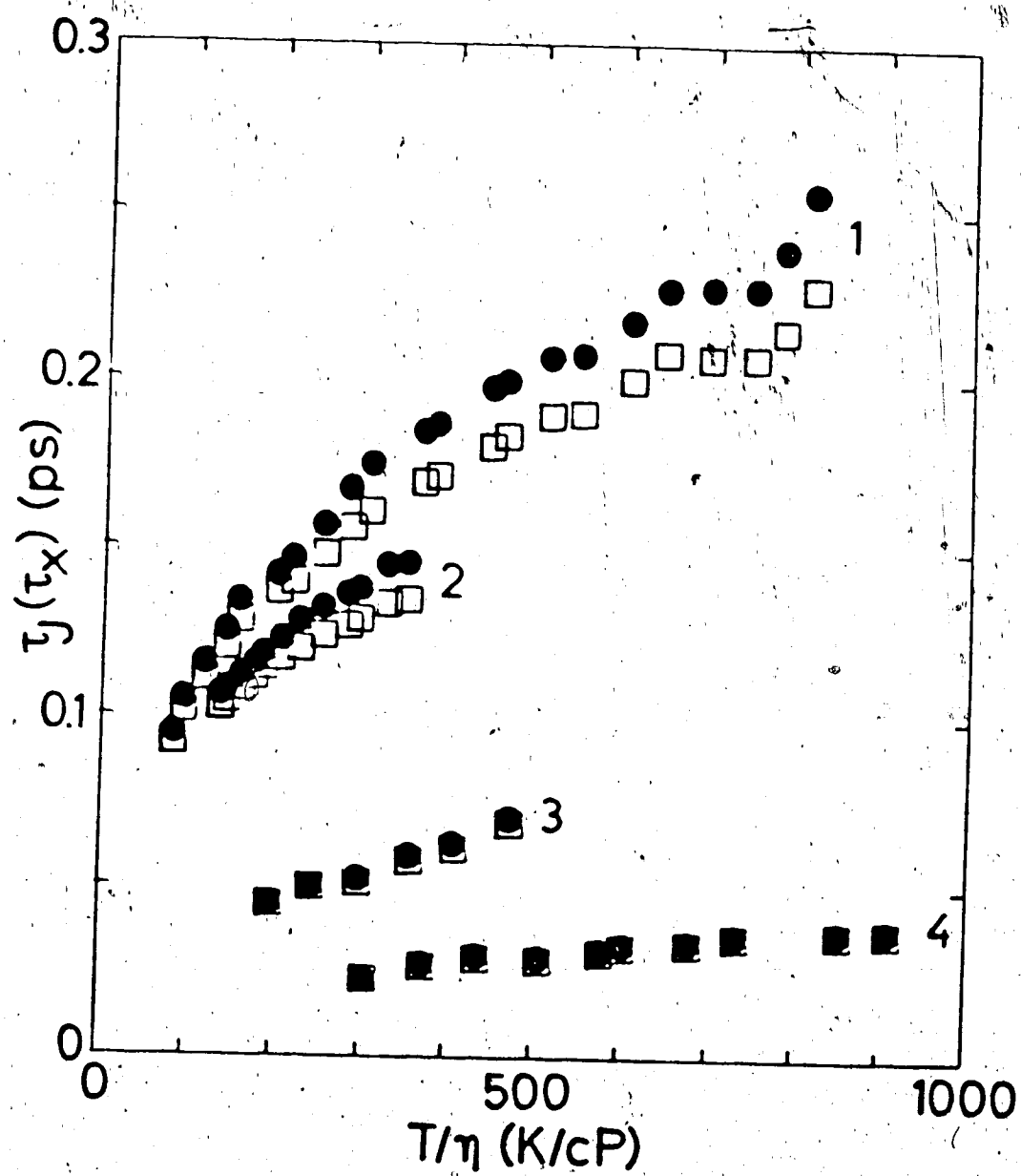
The values of the reduced time parameter $\tau_x^* = \tau_x (k_B T / I_z)^{1/2}$ obtained from the FPL fit of the $\text{ClO}_2/\text{CCl}_4$ linewidth data lie between 1 and 4. The validity of the FPL model in the region $\tau_x > 1$ is questionable because one cannot define a time τ satisfying the condition $\tau_T \ll \tau \ll \tau_x$ which is required for the validity of the rotational Langevin equation, a basic component of the FPL model.

Here τ_T is the correlation time which characterizes the time dependence of the rapidly fluctuating intermolecular torques. In the region where the rotational motion is nearly free ($\tau_x^* > 1$) and fluctuations in angular momentum and intermolecular torque are dominated by the rate of bimolecular collisions, τ_T and τ_x are of comparable magnitude so the required condition is not fulfilled. The applicability of the FPL model to the analysis of the ClO_2 linewidths in non-interacting solvents is therefore uncertain.

It should be noted that the use of Eq. (III-19) attributes all of the anisotropy in the friction coefficients, τ_α^{-1} , to anisotropy of the inertia tensor, since it assumes that κ is isotropic. In general, one might expect κ to be anisotropic, and one might attempt to fit the experimental data with the FPL model allowing the friction coefficients to vary freely. Such fits, which employ 3 variable parameters, were not attempted.

We have also compared the FPL model with the EDJ model for the description of the rotational motion of ClO_2 . The values of τ_x for the FPL model with $\tau_x = \tau_y = \tau_z$ were determined from the experimental ESR linewidths using Eq. (III-4). The corresponding values of τ_J for the EDJ model have been obtained using Eq. (III-8). The results are shown in Fig. III-4. Both models show very similar trends. In the non-polar solvents CCl_4 and n-pentane, however, τ_J is longer than τ_x for a given T/η . In the relatively strongly interacting solvents acetone and chloroform, τ_x and τ_J vary reasonably linearly with T/η , while, in the weakly interacting solvents CCl_4 and n-pentane, the

Fig. III-4. Comparison of τ_J (●) and τ_x (□) for ClO_2 in n-pentane (1), CCl_4 (2), CHCl_3 (3) and acetone (4) obtained with the EDJ model (τ_J) and the FPL model (τ_x) with $\tau_x = \tau_y = \tau_z$.



relationships between τ_x (or τ_J) and T/η are not linear.

4. Conclusion

The rotational motion of the asymmetric top molecules C_6D_5F and ClO_2 has been investigated in terms of the FPL and EDJ models for asymmetric top molecules. It was found that the rotational motion of neat C_6D_5F liquid is better described in terms of the FPL model by incorporating the anisotropy in motional modulation of the angular velocity components than in terms of the EDJ model although the agreement between the EDJ model and experiment is qualitatively correct. The rotational motion of C_6D_5F is rendered anisotropic because of molecular shape effects, while electric dipole interactions are less important. In the case of ClO_2 , the ESR linewidths predicted by the FPL model are in agreement with the observed linewidths in strongly interacting solvents, but the agreement is poor in very weakly interacting solvents. In addition, the angular momentum correlation times for ClO_2 obtained with the EDJ model and with the FPL model with frictional isotropy are very similar.

References

1. R. G. Gordon, J. Chem. Phys. **44** (1966) 1830.
2. R. E. D. McClung, J. Chem. Phys. **51** 3842 (1969); **54** (1971) 3248.
3. R. E. D. McClung, J. Chem. Phys. **55** (1971) 3459.
4. R. E. D. McClung, J. Chem. Phys. **57** (1972) 5478.
5. R. E. D. McClung, Adv. Mol. Relaxation Process **10** (1977) 83.
6. M. Fixman and K. Rider, J. Chem. Phys. **51** (1969) 2425.
7. C. Dreyfus and T. Nguyen Tan, J. Chem. Phys. **62** (1975) 2492.
8. J. C. Leicknam, Y. Guissani and S. Bratos, J. Chem. Phys. **68** (1978) 3380.
9. P. S. Hubbard, Phys. Rev. **A6** (1972) 2421.
10. P. S. Hubbard, Phys. Rev. **A8** (1973) 1429.
11. P. S. Hubbard, Phys. Rev. **A9** (1974) 481.
12. G. T. Evans, J. Chem. Phys. **65** (1976) 3030.
13. J. G. Powles and G. Rickayzen, Mol. Phys. **33** (1977) 1207.
14. R. E. D. McClung, J. Chem. Phys. **73** (1980) 2435.
15. R. E. D. McClung, J. Chem. Phys. **75** (1981) 5503.
16. T. E. Bull, J. Chem. Phys. **81** (1984) 3181.
17. D. H. Lee and R. E. D. McClung, Chem. Physics (submitted for publication).
18. R. A. Assink and J. Jonas, J. Chem. Phys. **57** (1972) 3329.
19. R. E. D. McClung and D. Kivelson, **49** (1968) 3380.

20. The corresponding translational Langevin equation is discussed in F. Reif, **Fundamentals of Statistical and Thermal Physics** (McGraw-Hill, New York, 1965), chap. 15.
21. M. E. Rose, **Elementary Theory of Angular Momentum** (Wiley, New York, 1957) Chap. IV.
22. Reference 21, chap. III.
23. R. G. Barnes and J. W. Bloom, J. Chem. Phys. **57** (1972) 3082.
24. P. K. Bhattachavyya and B. P. Dailey, J. Chem. Phys. **63** (1975) 1336.
25. S. I. Chan and A. S. Dubin, J. Chem. Phys. **45** (1967) 1745.
26. P. W. Atkins and D. Kivelson, J. Chem. Phys. **44** (1966) 169.
27. R. E. D. McClung, Ph.D. dissertation, UCLA, 1967.

CHAPTER IV

NUCLEAR RELAXATION AND MOLECULAR MOTION OF 1,3,5-TRIFLUOROBENZENE- d_3 IN LIQUID SOLUTIONS

1. Introduction

Molecular rotation in liquids has been studied for many molecular systems in various ways [1-28]. Nuclear [1-7] and electron [8-13] spin relaxation, infrared and Raman bandshapes [14-20], light scattering [21-27], and neutron scattering [28] techniques have been used for the study of molecular rotation. Two important correlation times, τ_θ and τ_J , can be used to characterize the rotational motion. τ_θ is the reorientational correlation time which characterizes the time dependence of the orientation of a molecule, and τ_J is the angular momentum correlation time which characterizes the time dependence of the rotational angular momentum of the molecule. A knowledge of these correlation times for a given molecule can provide useful information about the nature of molecular rotation in liquids. A number of theoretical models for molecular rotation in liquids have been proposed. The simplest and most commonly used model was developed by Debye [29] to describe dielectric relaxation. The Debye model was developed on the basis

¹A version of this chapter has been submitted for publication. D.H. Lee and R.E.D. McClung, 1986. Chemical Physics.

that the molecule of interest behaved like a large spherical particle immersed in a continuous, viscous medium and followed a rotational random walk involving steps of small angular displacement. This assumes that the correlation time τ_J for the angular momentum is very short compared to the reorientational correlation time τ_θ . However, it was found that τ_J and τ_θ were of the same order of magnitude in some cases [30-32] so that any interpretation of experimental observations in such cases, using the Debye model, was questionable. When τ_θ and τ_J are of the same order of magnitude, the molecules reorient through large angles during the rotational diffusive steps and the rotational motion is similar to that in dilute gases where the molecules rotate freely during the time intervals between collisions. The concept of these "inertial" effects in the rotational diffusive steps was widely discussed [33-37], but was not incorporated into a theory in an exact fashion until 1966 when Gordon [38] suggested an extension, for linear molecules, of the Debye model which removed the restriction on the size of the rotational steps. Other workers have extended Gordon's model to spherical [39-41], symmetric [41-42], and asymmetric top [43-44] molecules, and to the perpendicular bands of linear molecules [45]. In this extended diffusion model (ED model), the molecules are assumed to rotate freely during the rotational diffusive steps and each step is terminated by a random impulsive torque which reflects the Brownian motion of the molecules. This impulsive torque or "collision" randomizes the angular momentum of the molecule. Two

limiting cases have been proposed: the J-diffusion (EDJ) and M-diffusion (EDM) limits. In the case of J-diffusion, both the orientation and magnitude of the angular momentum vector are randomized at each "collision", while in the case of M-diffusion only the orientation is randomized. It has been shown [46] that the EDJ model reduces to the Debye model in the small angle or rotational diffusion limit ($\tau_J^* \ll 1$), where τ_J^* is the angular momentum correlation time expressed in units of $(k_B T / I_x)^{1/2}$, where k_B is the Boltzman constant, T is the absolute temperature, and I_x is the moment of inertia of the molecule about the x principal axis. In this limit, τ_θ is inversely proportional to τ_J [46,47]. On the other hand, in the dilute gas limit ($\tau_J^* \gg 1$) both EDJ and EDM models give results similar to that of the perturbed free rotor model [32] in which τ_θ is proportional to τ_J . The predictions of the ED model have been compared with experimental observations for various types of molecules [46]. Many applications have compared the theoretical relationship between τ_θ and τ_J with the experimentally observed variation of τ_θ with τ_J . In most cases, the EDJ model has been found to be in good agreement with the experimental observations [1-7]. For instance, Bull has interpreted the ^{19}F and ^2D relaxation times for 1,3,5-trifluorobenzene- d_3 (TFB) in liquid solutions in hexachlorobutadiene [6] and in the pure liquid [7] in terms of the ED model for symmetric top molecules. He found that the reorientational motion of TFB was well described by the EDJ model rather than by the EDM model.

Another model for the rotational motion of molecules in liquids, the Fokker-Planck-Langevin (FPL) model, has been considered by several workers [41,48-53]. This model is based on the view that the rotational motion of a molecule in a liquid can be approximated by that of appropriately shaped solid object immersed in a continuous viscous fluid. The angular velocity of the molecule is modulated by slowly varying viscosity-dependent retarding torques and by rapidly fluctuating Brownian torques which reflect the molecular nature of the liquid. There is a marked difference in the nature of intermolecular torques in the ED and the FPL models. In the ED model, only the rapidly fluctuating Brownian torques are considered, and they are assumed to manifest themselves as random collisions which produce large random changes in the angular velocity. In the FPL model, on the other hand, a large number of fluctuations in the Brownian torques are required to change the angular velocity significantly, while the retarding torques act continuously causing the angular velocity to move towards its ensemble average value of zero. In other words, the molecules in the ED model experience intermittent and very strong torques but the molecules in the FPL model experience retarding torques at all times in addition to the intermittent Brownian torques.

Applications of the FPL model are not abundant, but it has been shown from comparison of theory with the experimental results from Raman studies of CF_4 [54] and SF_6 [55], infrared studies of N_2O [56] and CO [57], and nuclear magnetic relaxation studies of CCl_4 [58] and

C_6D_5F [4] that the FPL model describes the rotational motion of these molecules in liquids reasonably well [54-56,59,60]. In addition, the FPL model has been compared with the EDJ model and it has been shown that both the FPL model and the EDJ model, although they are based on very different physical pictures of the rotational dynamics, appear to give remarkably similar characterizations of the rotational motion of molecules in liquids [55,56,59,60]. For symmetric and asymmetric top molecules, a new feature is present in the FPL model: anisotropy in the motional modulation of the angular velocity components, which is referred to as the frictional anisotropy.

In this paper, we report measurements of the 2D and ^{19}F nuclear relaxation rates of the symmetric top molecule 1,3,5-trifluorobenzene- d_3 (TFB) in 0.15 mol fraction solutions in a number of polar and non-polar solvents over the temperature range 270-400K. The relationship between the correlation times τ_θ and τ_J obtained from the nuclear relaxation data is compared with the theoretical relationships predicted by the EDJ and FPL models. The effect of frictional anisotropy on the anisotropic molecular reorientation is also investigated.

It is common to relate the reorientational correlation time of a solute molecule to the macroscopic viscosity of the solution. Using the Debye model, Bloembergen, Purcell and Pound [61] obtained the "Debye" equation

$$\tau_{\theta} = (4\pi r^3 \eta) / (3k_B T) \quad (IV-1)$$

where r is the hydrodynamic radius of the rotating molecule, and η is the coefficient of shear viscosity of the liquid. Although this Debye equation has been used successfully in some cases [61-64], it has been found that the reorientational correlation times predicted by the Debye equation are larger than those observed experimentally [65-71]. Several workers [72-74] have generalized the Debye theory to ellipsoidal molecules taking into account the effect of anisotropic rotational motion, but this generalization did not result in good agreement between theory and experiment. In order to improve agreement between theory and experiment, a parameter κ has been introduced into the Debye equation by McClung and Kivelson [8] so that

$$\tau_{\theta} = (4\pi r^3 \eta \kappa) / (3k_B T) \quad (IV-2)$$

A molecular interpretation of κ in terms of the relative magnitudes of intermolecular torques and intermolecular forces has been given [75]. In the limit of rotational diffusion, it has been assumed [47] that τ_{θ} can be related to the correlation time $\tau_{J_{\alpha}}$ for the α -component of the angular momentum by

$$\tau_{\theta} \tau_{J_{\alpha}} = I_{\alpha} / 6k_B T \quad (IV-3)$$

where I_α is the moment of inertia about the α principal axis. Hence, from Eqs. (IV-2) and (IV-3), τ_{J_α} is also related to κ and η by

$$\tau_{J_\alpha} = I_\alpha / (8\pi r^3 \kappa \eta) \quad (IV-4)$$

In general, κ is a tensor [75] which can be diagonalized in a molecular coordinate system. However, it has been assumed that κ is isotropic and can be treated as a scalar. In this sense, κ is similar to the rotational microviscosity factor which was introduced empirically by Wirtz and Gierer [66]. Wirtz and Gierer took into account the finite size of the solvent molecules in the description of the rotational motion of a spherical solute molecule recognizing that the surrounding solvent molecules did not form a continuous and homogeneous medium as assumed in the hydrodynamic theory. Their rotational microviscosity factor, which is denoted by κ_w , can be expressed as [9,66]

$$\kappa_w = \{6(r_s/r) + (1 + r_s/r)^{-3}\}^{-1} \quad (IV-5)$$

where r_s is the radius of the solvent molecule and r is the radius of the solute molecule. When $r \gg r_s$, κ_w approaches unity so that the Gierer-Wirtz theory reduces to the Debye hydrodynamic result [Eq. (IV-1)]. When $r \ll r_s$, κ_w approaches zero.

Kivelson et al. [75] have shown that κ is proportional to the ratio of the mean square intermolecular torque on the solute molecule to the mean square intermolecular force on the solute molecule. The intermolecular force depends on the total intermolecular potential, while the intermolecular torque arises exclusively from the anisotropic part of the intermolecular potential. Hence κ represents the degree of anisotropy of the intermolecular potential. Physically, κ is a measure of coupling between the rotational and translational motion. Usually κ is less than 1. When $\kappa = 1$, Eq. (IV-2) reduces to the Debye equation [Eq. (IV-1)] which is a hydrodynamic result derived for the rotational motion of a spherical particle in a continuous viscous liquid with the "stick" boundary condition, which assumes that the surrounding molecules stick to the surface of the rotating molecule so that the tangential velocities of the rotating molecule and the surrounding molecules are equal at the surface of the rotating molecule. If, on the other hand, it is assumed that a "slip" boundary condition (the tangential velocity of solvent molecules is zero at the surface of the sphere) applies, the hydrodynamic result is Eq. (IV-2) with $\kappa = 0$. When the size of the rotating molecule (solute) is very large compared to that of the surrounding molecules (solvent) or when there are strong intermolecular interactions between solute and solvent, the "stick" boundary condition is expected to be appropriate. It is expected that the boundary condition for most liquids and liquid solutions will lie somewhere between "stick" and "slip", and κ will therefore lie between 0 and 1.

Hu and Zwanzig [76] have considered the hydrodynamic model with the "slip" boundary condition where the tangential velocity of the surrounding molecule is zero at the surface of a rotating molecule. They have calculated the rotational friction coefficients for oblate and prolate spheroids with the "slip" boundary condition and have reported values of the ratio, f , of the rotational friction coefficient with the "slip" boundary condition to the corresponding coefficient with the "stick" boundary condition. This ratio, f , depends only on the geometric factor, d_S/d_L , where d_S and d_L are the semiaxis lengths along the short and long axes of the spheroid.

Since most molecular systems lie in the region between the "slip" and "stick" boundary conditions, an empirical stickiness factor, S , defined as

$$S = (\kappa - f)/(1 - f) \quad (\text{IV-6})$$

has been introduced [10,11]. Here κ is the anisotropic interaction parameter and f is the factor introduced by Hu and Zwanzig [76].

According to Hoel and Kivelson [10], the lower limit of S is zero in the purely hydrodynamic case, but, since real molecular liquids do not form continuous and homogeneous media, the lower limit of S could go below zero and become

$-f/(1 - f)$ which corresponds to $\kappa = 0$. In the latter situation the molecular system is said to be under the "subslip" boundary condition. Generally speaking, κ is a measure of total anisotropic

interactions which produce rotational relaxation, f is a measure of the molecular geometric contribution to the anisotropic interactions and S is a measure of all non-geometric anisotropic interactions.

Pecora et al [21-25] have studied the viscosity dependence of the reorientational correlation times of small molecules in a variety of organic solvents at constant temperature. They employed Rayleigh light-scattering techniques to determine the reorientational correlation times and found that the "slip" boundary condition rather than the "stick" boundary condition gave a better description of the rotational motion of small molecules in the absence of strong solute-solvent interactions. They also found that, at constant temperature, the reorientational correlation time was a linear function of viscosity with non-zero intercept, τ_0 :

$$\tau_\theta = (4\pi r^3 \eta) / (3k_B T) + \tau_0 \quad (IV-7)$$

The values of τ_0 obtained were similar to the free rotor correlation times, τ_{FR} , given by Bartoli and Litovitz [77]:

$$\tau_{FR} = 2\pi(41/360)(I/k_B T)^{1/2} \quad (IV-8)$$

where I is the moment of inertia. Fury and Jonas [78] have found that the zero-viscosity reorientation time τ_0 was significant for a number of neat liquid monosubstituted benzenes and symmetric top molecules, but τ_0 was not predicted well by Eq. (IV-8).

Kivelson et al [8,9] have assumed that the hydrodynamic radius, r , in Eq. (IV-2) can be determined from the translational diffusion coefficient, D , via the Stokes-Einstein relation

$$D = k_B T / (6\pi\eta r) \quad (IV-9)$$

This hydrodynamic result is derived for the translational motion of a spherical particle of radius r immersed in a continuous fluid of viscosity η , and assumes the "stick" boundary condition. Eq. (IV-9) has been applied successfully in some systems [8,9,79-81], but in other cases, especially liquids composed of small molecules, the experimental values of the translational diffusion coefficient have been found to be much larger than the theoretical values predicted by the Stokes-Einstein equation [82-85]. Thus, it has been suggested that it is necessary to modify the Stokes-Einstein equation by introducing some empirical correction factor for the translational frictional coefficient taking account of variations between the "stick" and "slip" boundary conditions, and of the discontinuous nature of the molecular liquid when applied to small molecules [85].

In this paper we analyze the reorientational correlation times and the translational diffusion coefficients of TFB in various solvents in terms of Eqs. (IV-7) and (IV-9), discuss the variation of κ and S with solvent, and examine the applicability of Eq. (IV-9) in these systems.

2. Experimental

TFB (98 atom % D) was obtained from MSD Isotopes Company and was dried by storing over molecular sieves (Fisher Scientific Co. Type 3A). Deuterated and non-deuterated solvents used in this work (sources of deuterated solvents are given): methylene chloride (Stohler Isotope Co.), toluene (Aldrich Chemical Co.), tetrachloroethylene (Eastman-Kodak Co.), chloroform (Norell Co.), dimethylformamide (DMF) (Aldrich Chemical Co.), and acetonitrile (Aldrich Chemical Co.), hexamethylphosphoramide (HMPA) (MSD Isotopes Co.), and methanol (General Intermediate of Canada) were dried over molecular sieves (Type 3A). 0.15 mole fraction solutions of TFB in deuterated (^{19}F measurements) and non-deuterated (^2D measurements) solvents were prepared and samples for NMR relaxation measurements were placed into a 9 mm diameter sample tube with the 2 mm diameter capillary section (Wilmad Glass Co.), degassed using three freeze-pump-thaw cycles, and sealed under vacuum.

Nuclear spin-lattice relaxation times, T_1 , were measured using a Bruker SXP 4-100 pulsed NMR spectrometer interfaced to a Nicolet 1180 computer and a Nicolet 293A pulse programmer. The operating frequencies were 13.7 MHz for deuterium and 84.2 MHz for fluorine. The temperature of the sample solution was controlled by means of a Bruker B-ST temperature control unit which controlled the sample temperature to $\pm 0.5\text{K}$. A Doric Trendicator 400 digital thermometer

with a copper-constantan thermocouple was used to measure the sample temperature. The sample was allowed to equilibrate at each temperature for 15-20 minutes after inserting it into the probe.

Relaxation times were measured using the $180^\circ - \tau - 90^\circ$ pulse sequence with a delay time of $\sim 5 T_1$ between successive pulse sequences. The estimated errors in T_1 measurements were 5% for deuterium and 8% for fluorine.

The translational diffusion coefficients of TFB in the solutions were measured using the stationary field gradient spin-echo technique [86-88]. The stationary magnetic field gradient was generated by passing current through a pair of copper coils mounted on the aluminum side plates of the NMR probe. The magnetic field gradient was calibrated using a sample of hexafluorobenzene whose translational diffusion coefficients are known [89]. The estimated error in the translational diffusion coefficient measurements was 6%.

Viscosities of sample solutions were measured with a Cannon-Fenske viscometer in a thermostatic bath. The temperature was controlled to $\pm 0.2^\circ\text{C}$ by an electrical heating controller (Model 226, LFE Corporation). A copper constantan thermocouple placed inside the bath was used to monitor the temperature. The estimated error in the viscosity measurements was about 2%.

3. Results

The ^2D and ^{19}F spin lattice relaxation times $T_{1\text{D}}$ and $T_{1\text{F}}$ of TFB in various solvents (0.15 mol fraction solutions) were measured over the temperature range 270 to 400K with the upper limit being near the boiling point of the solvent. The results are tabulated in Table IV-

1. Viscosities of the solutions and the translational diffusion coefficients of TFB in various solvents are also given in Table IV-1.

The spin relaxation rate of deuterium is almost entirely governed by the nuclear quadrupolar relaxation mechanism, and measurement of $T_{1\text{D}}$ provides an excellent means for determining the reorientational correlation time τ_0 provided that the nuclear quadrupole coupling constant and the asymmetry of the electric field gradient are known. The quadrupole coupling constant (180 KHz) of deuterium in TFB and the asymmetry parameter (0.05) have been determined in a NMR study of a liquid crystal phase [90]. We have determined τ_0 from $T_{1\text{D}}$ using the relationship [91]

$$1/T_{1\text{D}} = (3/8)(e^2qQ/\hbar)^2(1 + \eta^2/3)\tau_0 \quad (\text{IV-10})$$

where e^2qQ/\hbar represents 2π times the quadrupole coupling constant and η is the asymmetry parameter. The τ_0 results are also included in Table IV-1.

The relaxation of fluorine in TFB solutions in deuterated solvents can be considered to arise mainly from the spin-rotation

Table IV-1. Analysis of T_{1D} and T_{1F} for TFB in various solvents

Solvent	Temp. (K)	$1/T_{1D}$ (s^{-1})	$1/T_{1F}$ ($10^{-2}s^{-1}$)	$(1/T_{1F})_{SR}$ ($10^{-2}s^{-1}$)	η (cp)	D ($10^{-5}cm^2s^{-1}$)	τ_θ (ps)	τ_J (ps $\times 10^{-1}$)
Tetrachloro- ethylene	281	1.97	2.34	1.85	0.945	1.90	4.1	0.057
	300	1.61	2.60	2.20	0.766	2.37	3.3	0.064
	332	1.08	3.22	2.94	0.564	3.20	2.2	0.077
	352	0.926	3.57	3.34	0.475	3.75	1.9	0.082
	373	0.862	4.39	4.18	0.412	4.39	1.8	0.097
	394	0.730	5.08	4.90	0.362	4.95	1.5	0.107
Toluene	281	1.88	2.89	2.37	0.644	2.20	3.9	0.073
	300	1.44	3.41	3.02	0.510	2.90	3.0	0.087
	332	0.909	4.41	4.15	0.364	3.90	1.9	0.108
	352	0.826	4.67	4.45	0.301	4.95	1.7	0.109
	374	0.746	5.85	5.65	0.257	5.95	1.5	0.131
	394	0.699	8.06	7.88	0.223	6.60	1.4	0.173
Chloroform	281	1.83	2.90	2.44	0.637	2.20	3.8	0.075
	300	1.46	3.18	2.82	0.523	2.75	3.0	0.082
	332	0.980	3.86	3.61	0.393	3.62	2.0	0.094
	356	0.833	4.61	4.40	0.330	4.43	1.7	0.107
Methylene chloride	290	1.25	3.30	2.97	0.445	2.95	2.6	0.089
	300	1.18	3.48	3.18	0.398	3.35	2.4	0.092
	312	1.01	3.77	3.52	0.353	3.80	2.1	0.098
	317	0.962	4.15	3.91	0.333	4.05	2.0	0.107
	340	0.820	4.95	4.75	0.272	4.95	1.7	0.121
	356	0.746	5.24	5.05	0.239	5.50	1.5	0.123

(Continued)

Table IV-1. (Continued)

Solvent	Temp. (K)	$1/T_{1D}$ (s^{-1})	$1/T_{1F}$ ($10^{-2}s^{-1}$)	$(1/T_{1F})_{SR}$ ($10^{-2}s^{-1}$)	η (cp)	D ($10^{-5}cm^2s^{-1}$)	τ_{θ} (ps)	τ_{β} (ps $\times 10^{-1}$)
DMF	300	2.78	2.72	1.93	0.850	1.53	5.7	0.056
	333	1.61	3.26	2.79	0.606	2.30	3.3	0.073
	355	1.25	3.86	3.50	0.494	2.96	2.6	0.085
	374	1.00	4.37	4.08	0.429	3.47	2.1	0.094
Acetonitrile	281	1.72	2.94	2.48	0.469	2.50	3.6	0.076
	300	1.40	3.40	3.03	0.383	3.20	2.9	0.088
	333	0.990	4.88	4.62	0.284	4.45	2.0	0.120
HMPA	300	10.3	4.42	1.70	3.26	0.612	21.	0.049
	333	4.42	3.17	1.96	1.67	1.30	9.1	0.051
	353	2.95	3.15	2.31	1.16	1.66	6.1	0.057
	374	2.27	3.64	2.97	0.856	1.90	4.7	0.069
Methanol	273	2.07	3.64	2.95	0.808	1.69	4.3	0.094
	282	1.77	3.73	3.12	0.684	1.84	3.7	0.096
	300	1.31	3.85	3.42	0.540	2.79	2.7	0.099
	323	0.934	4.29	3.97	0.397	3.38	1.9	0.107

interactions because the intra- and intermolecular dipolar interactions should be relatively weak. The observed variation of the fluorine relaxation rate with temperature given in Table IV-1 shows the typical characteristics of relaxation dominated by spin-rotation interactions: increase in the relaxation rate with increasing temperature [47]. However, in the case of hexamethylphosphoramide (HMPA) solutions, the relaxation rate of fluorine goes through a minimum between 333 and 353K. This implies that dipole-dipole relaxation mechanism, which has a temperature dependence opposite to that of the spin-rotation interactions, contributes significantly to the relaxation of fluorine in HMPA. In general, the relaxation rate of fluorine has contributions from several relaxation mechanisms and can be written as

$$1/T_{1F} = (1/T_{1F})_{SR} + (1/T_{1F})_{DD}^{inter} + (1/T_{1F})_{DD}^{intra} + (1/T_{1F})_{ACS} \quad (IV-11)$$

where $(1/T_{1F})_{SR}$ represents the contribution due to motional modulation of the spin-rotation interactions, $(1/T_{1F})_{ACS}$ the contribution from rotational modulation of anisotropic chemical shift interactions, and $(1/T_{1F})_{DD}^{intra}$ and $(1/T_{1F})_{DD}^{inter}$ represent the contributions from motional modulation of intra- and intermolecular dipolar interactions.

The intramolecular dipole-dipole contribution to the fluorine relaxation rate is given by [91]

$$(1/T_{1F})_{DD}^{intra} = \left[\frac{3}{2} \gamma_F^4 \frac{h^2}{r_{FF}^6} + \frac{8}{3} \gamma_F^2 \gamma_D^2 h^2 \left(\frac{2}{6} \right) \right] \tau_\theta \quad (IV-12)$$

where γ_F and γ_D are the magnetogyric ratios for ^{19}F and 2D , r_{FF} is the distance between the fluorine atoms in TFB (.466 nm), r_{FD} is the distance between a fluorine atom and an adjacent deuterium atom in TFB (0.259 nm), and τ_θ is the reorientational correlation time. $(1/T_{1F})_{DD}^{intra}$ can be estimated accurately from the known molecular dimensions of TFB and from the reorientational correlation times determined from 2D relaxation time measurements. (The contribution to $(1/T_{1F})_{FF}^{intra}$ due to interactions between ^{19}F and 2D para to each other is neglected).

The intermolecular dipole-dipole contribution to the fluorine relaxation rate is given by [92]

$$(1/T_{1F})_{DD}^{inter} = 32 \gamma_F^2 \gamma_D^2 h^2 N_D / (8\pi D_a b) + \gamma_F^4 h^2 N_F / (18\pi D r) \quad (IV-13)$$

where h is Planck's constant, N_D and N_F are the number densities of 2D and ^{19}F in the solution, D_a is the sum of the translational diffusion coefficient D of TFB and the translational diffusion coefficient of the solvent, r is the effective radius of TFB (0.282 nm), and b is the sum of r and the solvent radius. The first term in Eq. (IV-13) arises from interactions between ^{19}F on TFB and 2D on

solvent molecules, and is much larger than the second term which is due to dipolar interactions between ^{19}F nuclei on different TFB molecules. In this work the effective radii were taken to be $(3V/4\pi)^{1/3}$, where V is the van der Waals molecular volume [85]. The intermolecular dipolar contributions to the fluorine relaxation rates were estimated using the translational diffusion coefficients (See Table IV-1) of TFB. In the initial estimates of $(1/T_{1\text{F}})_{\text{DD}}^{\text{inter}}$, D_a was approximated as twice the translational diffusion coefficient of TFB, and, for all solutions except those in HMPA and DMF at the lower temperatures, the estimated intermolecular dipolar contributions were smaller than the experimental errors in $1/T_{1\text{F}}$. Translational diffusion coefficients for HMPA [93] and DMF [94] from the literature were used to obtain improved estimates of $(1/T_{1\text{F}})_{\text{DD}}^{\text{inter}}$ for TFB in these solvents.

The contribution due to motional modulation of anisotropic chemical shift interactions to the fluorine relaxation rate is given by [91]

$$(1/T_{1\text{F}})_{\text{ACS}} = (3/10)(\gamma_{\text{F}}H_0)^2\delta_z^2(1 + \eta^2/3)\tau_0 \quad (\text{IV-14})$$

where H_0 is the magnitude of the applied magnetic field, δ_z is the chemical shift anisotropy and η is the asymmetry parameter in the anisotropic chemical shift. δ_z and η are related to the principal values σ_{xx} , σ_{yy} , σ_{zz} of the chemical shift tensor by

$$\delta_{z'} = \sigma_{zz} - (\sigma_{xx} + \sigma_{yy} + \sigma_{zz})/3 \quad (\text{IV-15})$$

and

$$\eta = (\sigma_{xx} - \sigma_{yy})/\delta_{z'} \quad (\text{IV-16})$$

The values of $(1/T_{1F})_{\text{ACS}}$ were estimated using the principal values [95] $\sigma_{xx} = 223$ ppm, $\sigma_{yy} = 304$ ppm, $\sigma_{zz} = 365$ ppm and τ_θ determined from ^2D relaxation time measurements.

The spin-rotational contribution to the ^{19}F relaxation rate is related to the angular momentum correlation time τ_J , in the limit of rotational diffusion, by [42,96]

$$(1/T_{1F})_{\text{SR}} = (2k_B T/3\hbar^2) [C_z^2 I_{//} + (C_x^2 + C_y^2) I_{\perp}] \tau_J \quad (\text{IV-17})$$

where C_x , C_y , and C_z are the principal values of the spin-rotation interaction tensor, which have values [7] -7.35×10^3 , -1.48×10^4 , and $-2.45 \times 10^3 \text{ s}^{-1}$ respectively, and $I_{//}$ and I_{\perp} are the principal moments of inertia along the molecular symmetry axis and the axis perpendicular to the symmetry axis, with values [7] 9.76×10^{-38} and $4.88 \times 10^{-38} \text{ g cm}^2$, respectively. The angular momentum correlation time τ_J is related to the correlation times $\tau_{//}$ and τ_{\perp} for the components of the angular velocity along the molecular symmetry axis and the axis perpendicular to the symmetry axis by

$$\tau_J = [c_z^2 I_{//} \tau_{//} + (c_x^2 + c_y^2) I_{\perp} \tau_{\perp}] / [c_z^2 I_{//} + (c_x^2 + c_y^2) I_{\perp}] \quad (IV-18)$$

The relative magnitudes of $\tau_{//}$ and τ_{\perp} reflect the anisotropy in the modulation of the angular velocity components which is introduced into the FPL model [53]. These two correlation times $\tau_{//}$ and τ_{\perp} are closely related to the viscous drag coefficients of the retarding torques appearing in the rotational Langevin equation. In the ED model where only the anisotropy in the moments of inertia is taken into account, the two correlation times $\tau_{//}$ and τ_{\perp} are assumed to be equal.

The values of τ_J given in Table IV-1 were determined from $(1/T_{1F})_{SR}$ which was obtained by subtracting the estimated values of $(1/T_{1F})_{DD}^{intra}$, $(1/T_{1F})_{DD}^{inter}$, and $(1/T_{1F})_{ACS}$ from the measured values of $1/T_{1F}$. It can be seen from Table IV-1 that the spin-rotational contribution, $(1/T_{1F})_{SR}$, dominates the fluorine relaxation rate, $1/T_{1F}$, in most cases. However, in the case of HMPA solution, $(1/T_{1F})_{SR}$ is considerably smaller than $1/T_{1F}$ especially at lower temperatures. In this case, the relative contribution from the spin-rotation interactions increases slowly from 38% at 300K to 82% at 374K. On the other hand, the contributions from the modulation of anisotropic chemical shifts and intra- and intermolecular dipolar interactions are of comparable magnitude at all temperatures.

It is apparent from Table IV-1 that the values of τ_J are much

smaller than the values of τ_0 which means that the conditions for the rotational diffusion limit are realized in this work. Hence the use of Eq. (IV-17) for the determination of τ_J is justified. The uncertainties in τ_J are significantly greater than the errors in τ_0 because of the uncertainties incurred in estimating $(1/T_{1F})_{DD}^{inter}$ and $(1/T_{1F})_{ACS}$.

4. Discussion

A. Relationship between τ_0 and τ_J

It is appropriate to compare the relationship between τ_0 and τ_J obtained for TFB solutions with that predicted by theoretical models for molecular rotation in liquids. The reduced correlation times

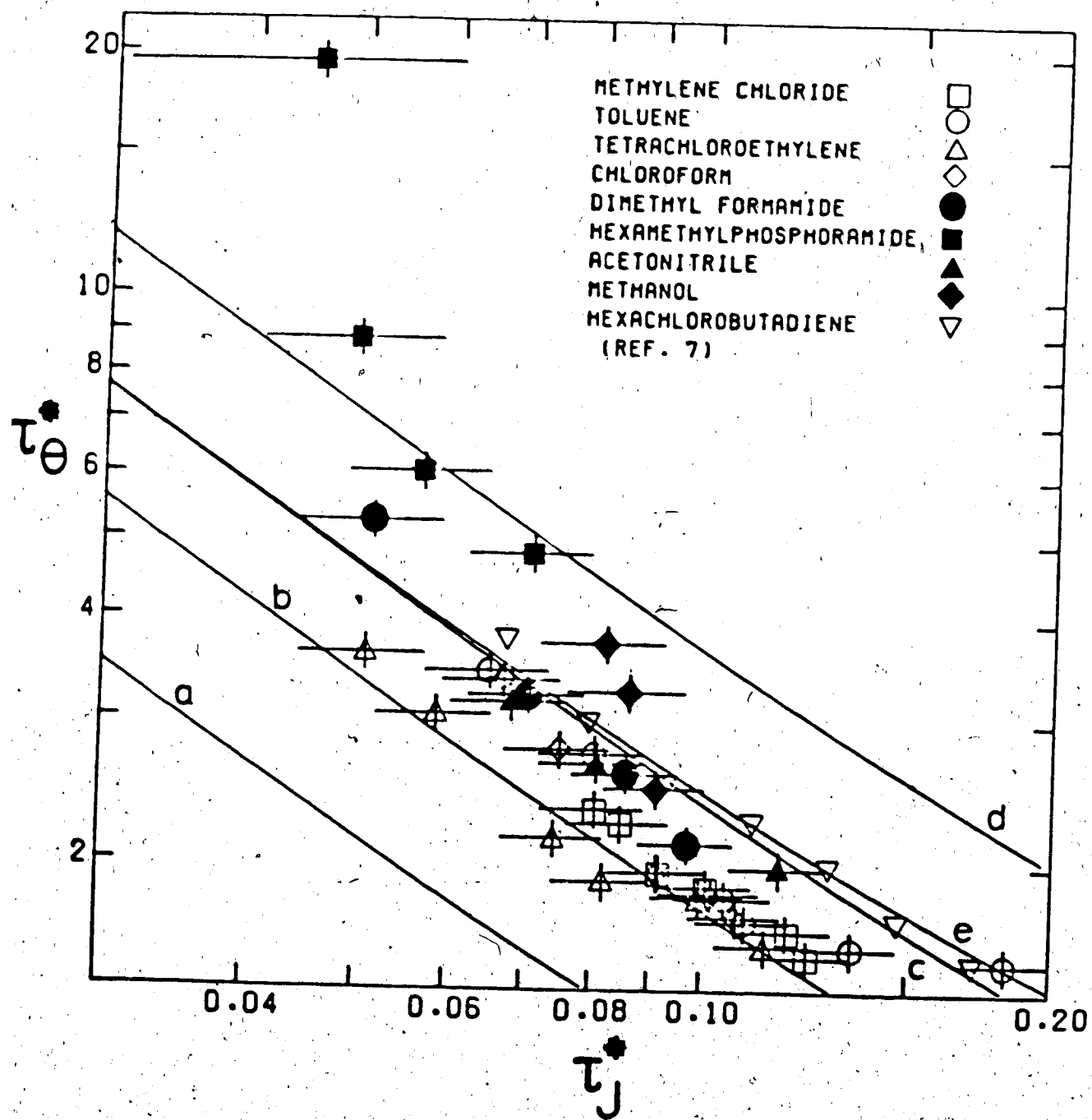
$$\tau_0^* = \tau_0 (k_B T / I_x)^{1/2} \quad (IV-19)$$

and

$$\tau_J^* = \tau_J (k_B T / I_x)^{1/2} \quad (IV-20)$$

are used to facilitate easy comparison between theory and experiment. In Fig. IV-1, the experimental variation of τ_0^* with τ_J^* is shown along with the theoretical curves for the EDJ and FPL models. For comparison, Bull's data [6] in hexachlorobutadiene are also shown in Fig. IV-1. In the FPL model, the anisotropy in the motional modulation of the angular velocity components is taken into

Fig. IV-1. Reorientational and angular momentum correlation times for 1,3,5-trifluorobenzene- d_3 in 0.15 mol fraction solutions compared with FPL (curve a - $\tau_{//}/\tau_{\perp} = 5$, b - $\tau_{//}/\tau_{\perp} = 2$, c - $\tau_{//}/\tau_{\perp} = 1$, d - $\tau_{//}/\tau_{\perp} = 0.2$) and EDJ curve (curve e) models.



account in addition to the anisotropy in the moments of inertia, so that each curve in Fig. IV-1 corresponds to a different $\tau_{//}/\tau_{\perp}$ ratio. The curve for the FPL model with the ratio $\tau_{//}/\tau_{\perp} = 1$ is almost identical to that for the EDJ model in the limit of rotational diffusion ($\tau_0 \gg \tau_J$), which is consistent with comparisons of the EDJ and FPL models for linear and spherical [56], and asymmetric top molecules [60]. It is shown in Fig. IV-1 that the experimental points for most solutions lie between the curves for the FPL model with $\tau_{//}/\tau_{\perp} = 1$ and $\tau_{//}/\tau_{\perp} = 2$ except for the solution in HMPA. It is clear that the measured correlation times for TFB in the different solvents do not all agree with the predictions of the EDJ model. The correlation time data does, however, show the $\tau_0^* \propto 1/\tau_J^*$ behaviour predicted by the FPL and EDJ models. In the limit $\tau_J^* \ll \tau_0^*$, the FPL model [53] predicts the relationship

$$\tau_0^* \tau_J^* \cong \left\{ \frac{1}{3} + \frac{3}{1 + (\tau_{//}/\tau_{\perp})} \right\} \{ C_x^2 + C_y^2 + 2C_z^2 (\tau_{//}/\tau_{\perp}) \} / \{ 8[C_x^2 + C_y^2 + 2C_z^2] \} \quad (IV-21)$$

so that the value of the ratio $\tau_{//}/\tau_{\perp}$ which best fits the experimental data for TFB in a particular solvent can be obtained from the average value of $\tau_0^* \tau_J^*$ for that solution. The values of $\tau_{//}/\tau_{\perp}$ obtained are given in Table IV-2. The data for HMPA solutions is incompatible with the FPL model for all positive values of $\tau_{//}/\tau_{\perp}$, and is incompatible with the EDJ model.

Table IV-2. Anisotropy Parameters of TFB, Hydrodynamic radius, and Properties of Solvents

Solvent	κ^a	b_{FR}^b	κ_W^c	$\tau_{\parallel}/\tau_{\perp}$	s	τ_0 (ps)	r_D (nm)	v_D^d (nm ³)	r_S^e (nm)	Dipole Moment ^f (D)
Tetrachloroethylene	0.16	0.13	0.16	2.0	-0.077	0.52	0.19	0.0954	0.283	0
Methylenechloride	0.19	0.16	0.19	1.7	-0.038	0.69	0.21	0.0566	0.238	1.60
Methanol	0.20	0.16	0.22	0.8	-0.026	0.24	0.16	0.0361	0.205	1.69
Toluene	0.21	0.19	0.16	1.2	-0.013	0.50	0.20	0.0978	0.286	0.36
Chloroform	0.23	0.17	0.18	1.4	0.013	0.22	0.21	0.0707	0.257	1.01
Acetonitrile	0.27	0.23	0.20	1.2	0.064	0.48	0.20	0.0471	0.224	3.92
HMPA	0.28	0.27	0.13	-9	0.077	-0.19	0.17	0.183	0.352	5.40
DMF	0.32	0.22	0.17	0.9	0.13	-0.48	0.20	0.0777	0.265	3.82

a from least squares fit to Eq. (IV-7).

b from least squares fit to Eq. (IV-7) with τ_0 replaced by τ_{FR} in Eq. (IV-8).

c calculated with Eq. (IV-5).

d van der Waals' volume of solvent.

e van der Waals' radius of solvent.

f Dipole moments and dielectric constants from Handbook of Physics and Chemistry (Chemical Rubber Co., 63rd Ed. 1983), Encyclopedia of Chemical Technology (Interscience, New York, 2nd Ed., 1966), Merck Index (Merck and Co., Inc., 10th Ed. 1983), and H. Mornant, Angew. Chem. Internat. Ed. 6, 1046 (1967).

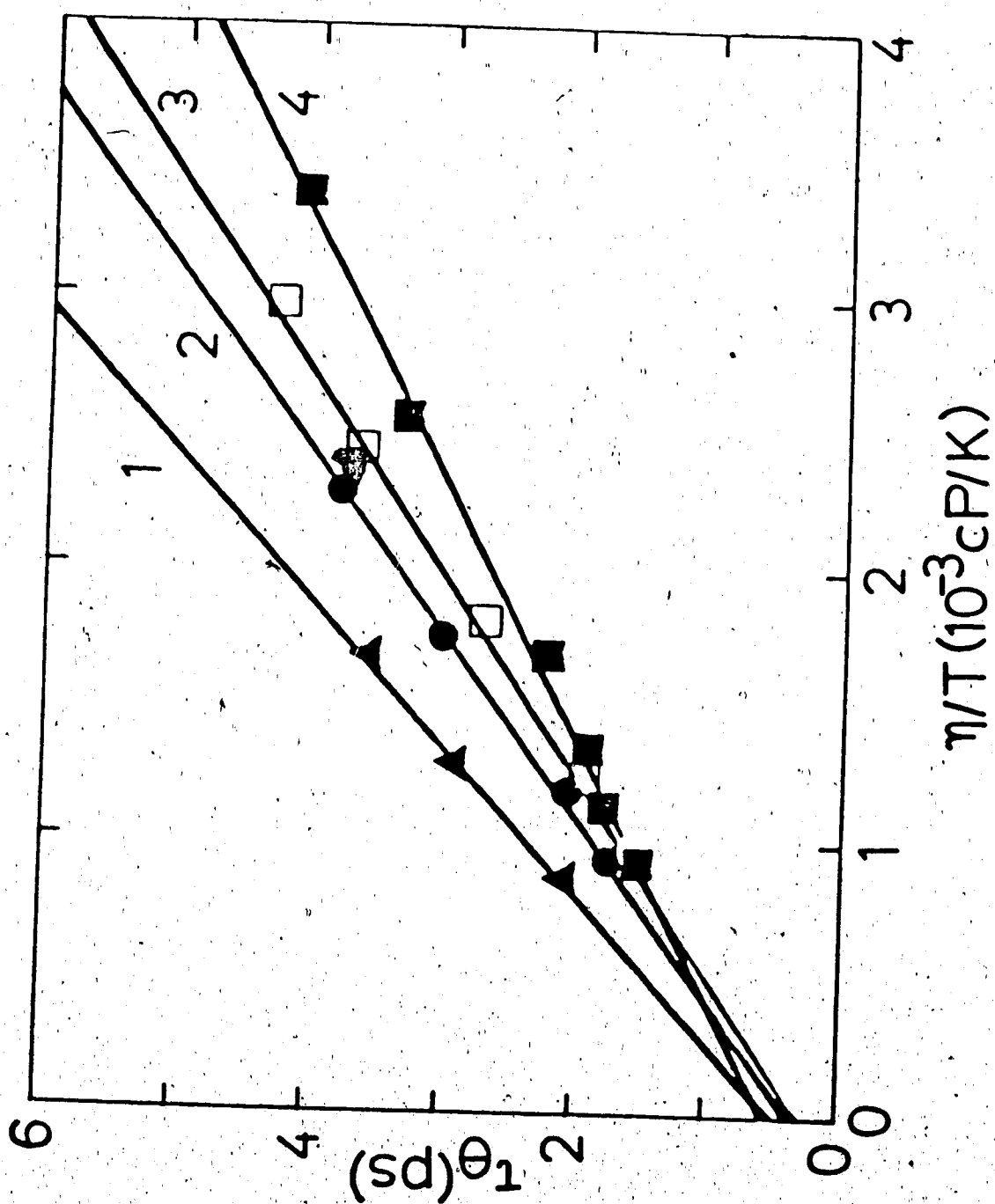
g Unable to obtain $\tau_{\parallel}/\tau_{\perp}$ in HMPA.

Although the magnitude of the frictional anisotropy, as characterized by $\tau_{\parallel}/\tau_{\perp}$, does not vary over a large range, it is clear from the data in Table IV-2 that the ratio $\tau_{\parallel}/\tau_{\perp}$ generally decreases with increasing solvent polarity, but there are exceptions (most notably methylene chloride and toluene) to this general trend. The observation that $\tau_{\parallel} \geq \tau_{\perp}$ for TFB in most solvents is not unexpected since rotation of the ring about the C_3 axis (τ_{\parallel}) should create less disruption of neighboring solvent molecules than rotations of the ring about the C_2 axes (τ_{\perp}). Although TFB does not have a net dipole moment, the C-F bond dipole moments may interact with dipole moments on neighboring solvent molecules, and these interactions should retard rotations of the ring about the C_3 axis as well as about the C_2 axes. When the solvent molecules have small dipole moments, molecular shape effects, as reflected by $\tau_{\parallel} > \tau_{\perp}$, determine the "friction" between solute and solvent molecules. On the other hand, if the solvent dipole moment is large, electrostatic interactions, as reflected by $\tau_{\parallel} \sim \tau_{\perp}$, dominate the frictional torques retarding the rotation of TFB.

B. Relationship between τ_0 , D and Solution Viscosity

We now wish to discuss the reorientational correlation times and the translational diffusion coefficients in terms of Eqs. (IV-7) and (IV-9). In Fig. IV-2, the reorientational correlation time τ_0 is plotted against η/T for TFB solutions in representative solvents. It is shown in Fig. IV-2 that τ_0 varies reasonably linearly with η/T .

Fig. IV-2. Viscosity-temperature dependence of reorientational correlation times for 1,3,5-trifluorobenzene in 0.15 mol fraction solutions. \blacktriangle - acetonitrile, \bullet - chloroform, \square - methanol, \blacksquare - tetrachloroethylene. Lines correspond to 1 - $\kappa = 0.27$, $\tau_0 = 0.48$; 2 - $\kappa = 0.23$, $\tau_0 = 0.22$; 3 - $\kappa = 0.20$, $\tau_0 = 0.24$; 4 - $\kappa = 0.16$, $\tau_0 = 0.52$.



The data were fit to Eq. (IV-7) and the values of the intercept τ_0 and the anisotropic interaction parameter κ which were obtained from the least squares analysis, using an effective hydrodynamic radius of 0.282 nm, are given in Table IV-2. κ has significant dependence on the solvent as found in earlier studies [8-13]. This is reflected by the difference in the slopes of the lines for different solvents as shown in Fig. IV-2. For the calculation of κ from the slope of the plot of τ_0 versus η/T , a reasonable value of the radius of TFB is required. There are several methods to determine the molecular radius. One method is to determine the effective radius from the van der Waals volume of a molecule, which was suggested by Edward [85]. In this method, the molecular volume is estimated by summing up the contributions from the atoms or groups of the molecule using the increments for the various atoms or groups which have been tabulated by Bondi [97] and Edward [85]. The van der Waals radius of TFB was estimated to be 0.282 nm. Another method which may be used to estimate the molecular radius is to use the theoretical expression [9]:

$$r^3 = (2/3)r_z^3(2 + \lambda^2)\lambda^3[\lambda + (\lambda^2 - 1)\tan^{-1}\lambda]^{-1}, \quad (\text{IV-22})$$

where the dimensionless structure factor, λ^2 , is given by

$$\lambda^2 = (r_x^2 - r_z^2)/r_z^2. \quad (\text{IV-23})$$

This expression has been obtained for a spheroidal particle with semiaxes $r_z < r_x = r_y$ which undergoes rotational diffusion motion. An effective radius of 0.291 nm was calculated from Eq. (IV-22), using $r_z = 0.185$ nm and $r_x = 0.347$ nm which were estimated from the corresponding values for the benzene ring [98] and by taking into account the difference between the C-H and C-F bond lengths. These values of r agree closely with the effective radius of C_6F_6 (0.280 nm) which has been determined by Sawyer et al. [89] for close-packed spheres at the melting point, assuming C_6F_6 to be a spherical molecule. The Stokes-Einstein equation [Eq. (IV-9)] can be also used to estimate the effective radius of a molecule from its translational diffusion coefficient as mentioned earlier. We examined the applicability of this equation to our molecular system using the measured values of the translational diffusion coefficient, D , and the solution viscosity, η , at various temperatures. It was found that the values of the effective radius of TFB determined from the Stokes-Einstein equation were in the range 0.16 to 0.21 nm (see r_D given in Table IV-2) and that these values were significantly smaller than those determined from the van der Waals volume or Eq. (IV-22). On the basis of the assumption that the size of TFB is very close to that of C_6F_6 , the value of the effective radius of TFB estimated from the van der Waals volume or Eq. (IV-22) seem to be more reasonable than that determined from the Stokes-Einstein equation. This implies that the Stokes-Einstein equation derived for the hydrodynamic fluid

with the "stick" boundary condition is probably not applicable to our molecular system, since the translational friction coefficient for cases intermediate between "slip" and "stick" boundary conditions will be smaller than the "stick" limit. Therefore we have not used the Stokes-Einstein equation for the estimation of the effective radius of TFB. Instead, we have used the van der Waals radius [85] of 0.282 nm for the effective radius, r , in Eq. (IV-7) to determine κ .

From Table IV-2, one can see that the values of κ lie in the range 0.16 to 0.32. These values are relatively small compared to 1 (the "stick" hydrodynamic case), which means that TFB experiences relatively weak anisotropic intermolecular interactions in the solvents studied in this work, and the boundary conditions appropriate to these solute-solvent systems lie closer to "slip" than to "stick". This result is compatible with the previous finding that the Stokes-Einstein equation for the translational motion, based on the hydrodynamic "stick" boundary condition, is not applicable to our solute-solvent systems.

The variation of κ with solvent may be correlated with some properties of solvents (see Table IV-2). Hwang et al. [9] have determined κ for dilute solutions of vanadyl acetylacetonate in various organic solvents and the values of κ obtained were in the range 0.48 to 0.85. They have analyzed the variation of κ in terms of the effects of solvent size and solvent dipole moment, and found that, in general, κ decreases with solvent size and increases with

solvent dipole moment. In this work, we tried to correlate the variation in κ with the molecular volumes (van der Waals volumes [85]) of the solvent molecules which are given in Table IV-2. It is very difficult to find a definite correlation between them. This might be due to the fact that the difference in the molecular volumes of the solute molecule (0.0942 nm^3) and the solvent molecules is not large and individual solvents have quite different dipole moments so that solvent polarity is more important than solvent size. In order to investigate the effect of solvent size on κ using the Wirtz theory [66], we have computed the values of κ_w defined in Eq. (IV-5) for the solute-solvent systems studied in this work and the results are included in Table IV-2. It can be seen from Table IV-2 that as a whole, κ_w and κ are of comparable magnitude except for the cases of the solvents with high dipole moment. In highly polar solvents, κ is considerably larger than κ_w . This result indicates that the Wirtz theory may account for the observed variations in κ in non-polar solvents, where molecular size effects are dominant, but it does not work well in polar solvents where strong electrostatic intermolecular interactions dominate. Secondly, we tried to correlate the variation in κ with the dipole moments of the solvent molecules, since the ease of reorientation of the C-F bond dipole moments is expected to reflect the strength of the anisotropic interactions between TFB and nearby solvent molecules. From Table IV-2, it can be seen that κ generally increases with the dipole moment of solvent molecules. This result is compatible with the results of others [9-12].

An interesting anomaly is the solution of TFB in toluene, a planar aromatic molecule. Since the dipole moment of toluene is very low, one might expect a small value of κ like that for the solvent tetrachloroethylene. However, the value of κ for toluene is relatively high and similar to that for the polar solvent methanol. This unusual result may indicate a specific interaction between aromatic solute molecule and aromatic solvent molecule. Hwang et al found that κ for vanadylacetylacetonate in toluene was much smaller than the value in chloroform, while we observe almost the same values of κ for TFB in these solvents.

It is interesting to note that the frictional anisotropy $\tau_{//}/\tau_{\perp}$ decreases with increasing κ . This can be rationalized by recognizing that for smaller κ , where interactions are weak, "molecular shape" effects make the larger contribution to the anisotropy of the intermolecular potential and rotation of the benzene ring about the C_3 axis is less hindered than rotation about the C_2 axes. On the other hand, when electrostatic interactions between bond dipoles on solute and solvent molecules make significant contributions to the anisotropy of the intermolecular potential, κ is larger. In this case, the difference between $\tau_{//}$ and τ_{\perp} is smaller because rotations about the C_3 and C_2 axes, all of which involve motion of a C-F bond dipole, are retarded by the electrostatic solvent-solute interactions.

Several investigators [21-25,78] have found that the zero viscosity intercept τ_0 might be associated with the free rotor

correlation time [see Eq. (IV-8)]. We have compared the values of τ_0 with the values of τ_{FR} in the temperature range studied in this work and found that the calculated values of τ_{FR} (0.8 ~ 0.9 psec) were somewhat higher than the values of τ_0 , but were of comparable magnitude except for the cases of DMF and HMPA. In those two cases, the values of τ_0 were found to be negative. We cannot explain the negative values of τ_0 , but it should be noted that the intercept τ_0 is not the "true" zero viscosity value of τ_0 , but an extrapolation of τ_0 from the region of relatively high viscosity, where retarding torques and intermolecular torques are important, to the limit of zero viscosity where inertial rotational motion is important. Since negative values of τ_0 are not allowed theoretically, we performed least squares analyses in which τ_0 was restricted to positive values but obtained values for κ which were similar to those given in Table IV-2. We also fit the experimental data to Eq. (IV-7) with τ_0 replaced by τ_{FR} [Eq. (IV-8)] and obtained the values for κ (denoted κ_{FR}) which are given in Table IV-2. One can see that κ_{FR} is slightly smaller than κ , but the general variation with solvent is not changed significantly.

It is useful to calculate the stickiness factor, S , defined in Eq. (IV-6) to investigate the contribution from non-geometrical anisotropic interactions to the rotational relaxation. The parameter f , which is the ratio of the rotational friction coefficients appropriate to the "slip" and "stick" boundary conditions, has been computed by Hu and Zwanzig [76], and represents a measure of the

geometrical contribution to the total anisotropic intermolecular interaction. Using $d_S = 0.370$ nm and $d_L = 0.694$ nm, one estimates a value of 0.22 for f [76]. We have calculated the stickiness factor for the solute-solvent systems studied in this work and the results are given in Table IV-2. According to the definition of the stickiness factor, its lower limit corresponding to $\kappa = 0$ is -0.28 and its upper limit corresponding to $\kappa = 1$ is 1 for TFB. The values of the stickiness factor in Table IV-2 are close to the lower limit. This means that all the solute-solvent systems of this work lie close to the "slip" boundary condition and the contribution from non-geometric anisotropic interactions to the rotational relaxation is not large.

5. CONCLUSION

The rotational motion of TFB in various solvents has been studied by nuclear relaxation measurements. The reorientational correlation time of this symmetric top molecule has been described by Eq. (IV-7) which involves the anisotropic interaction parameter, κ . The variation in κ with the solvent was due mainly to the difference in the dipole moments of various solvents and the effect of the solvent size relative to the solute size was not significant in the range of solvent molecular size studied in this work. Comparison of the experimental relationship between the reorientational and angular momentum correlation times with those predicted by the EDJ and FPL models showed that the

rotational motion of TFB was well described by the FPL model, but not by the EDJ model. The frictional anisotropy was not large, but was shown to vary significantly with solvent polarity.

References

1. T. C. Farrar, A. A. Maryott, and M. S. Malmberg, J. Chem. Phys. **54** (1971) 64.
2. K. T. Gillen, D. C. Douglass, M. S. Malmberg, and A. A. Maryott, J. Chem. Phys. **57** (1972) 5170.
3. R. A. Assink, J. DeZwaan, and J. Jonas, J. Chem. Phys. **56** (1972) 4975.
4. R. A. Assink and J. Jonas, J. Chem. Phys. **57** (1972) 3329.
5. J. DeZwaan, R. J. Finney, and J. Jonas, J. Chem. Phys. **60** (1974) 3223.
6. T. E. Bull, J. Chem. Phys. **59** (1973) 6173.
7. T. E. Bull, J. Chem. Phys. **62** (1975) 222.
8. R. E. D. McClung and D. Kivelson, J. Chem. Phys. **49** (1968) 3380.
9. J. Hwang, D. Kivelson, and W. Plachy, J. Chem. Phys. **58** (1973) 1753.
10. D. Hoel and D. Kivelson, J. Chem. Phys. **62** (1975) 1323.
11. D. Hoel and D. Kivelson, J. Chem. Phys. **62** (1975) 4535.
12. B. Kowert and D. Kivelson, J. Chem. Phys. **64** (1976) 5206.
13. M. Patron, D. Kivelson, and R. N. Schwartz, J. Phys. Chem. **86** (1982) 518.
14. T. E. Eagles and R. E. D. McClung, J. Chem. Phys. **59** (1973) 435.

15. T. E. Eagles and R. E. D. McClung, J. Chem. Phys. **61** (1974) 4070.
16. S. Sunder and R. E. D. McClung, Chem. Phys. **2** (1973) 472.
17. S. Sunder and R. E. D. McClung, Can. J. Phys. **52** (1974) 1209.
18. S. Sunder, K. E. Hallin, and R. E. D. McClung, J. Chem. Phys. **61** (1974) 2920.
19. R. Arndt and R. E. D. McClung, J. Chem. Phys. **69** (1978) 4280.
20. R. Arndt and R. E. D. McClung, J. Chem. Phys. **70** (1979) 5598.
21. G. R. Alms, D. R. Bauer, J. I. Brauman and R. Pecora, J. Chem. Phys. **58** (1973) 5570.
22. G. R. Alms, D. R. Bauer, J. I. Brauman and R. Pecora, J. Chem. Phys. **59** (1973) 5310.
23. D. R. Bauer, G. R. Alms, J. I. Brauman and R. Pecora, J. Chem. Phys. **61** (1974) 2255.
24. D. R. Bauer, J. I. Brauman and R. Pecora, J. Am. Chem. Soc. **96** (1974) 6840.
25. D. R. Bauer, J. I. Brauman and R. Pecora, Ann. Rev. Phys. Chem. **27** (1976) 443.
26. G. D. J. Phillies and D. Kivelson, J. Chem. Phys. **71** (1979) 2575.
27. D. Kivelson and P. A. Madden, Ann. Rev. Phys. Chem. **31** (1980) 523.
28. B. Cvikl, Phil. Mag. **28** (1973) 1353.
29. P. Debye, **Polar Molecules** (Reinhold, New York, 1929), pp. 77ff.

30. W. R. Hackleman and P. S. Hubbard, J. Chem. Phys. **39** (1963) 2688.
31. P. Rigny and J. Virlet, J. Chem. Phys. **47** (1967) 4645.
32. M. Bloom, F. Bridges and W. N. Hardy, Can. J. Phys. **45** (1967) 3533.
33. W. A. Steele, J. Chem. Phys. **38** (1963) 2404.
34. W. A. Steele, J. Chem. Phys. **38** (1963) 2411.
35. W. M. Noniz, W. A. Steele and J. A. Dixon, J. Chem. Phys. **38** (1963) 2418.
36. D. E. Woessner, J. Chem. Phys. **40** (1964) 2341.
37. H. Shimizu, J. Chem. Phys. **43** (1965) 2453.
38. R. G. Gordon, J. Chem. Phys. **44** (1966) 1830.
39. R. E. D. McClung, J. Chem. Phys. **51** (1969) 3842.
40. R. E. D. McClung, J. Chem. Phys. **55** (1971) 3459.
41. M. Fixman and K. Rider, J. Chem. Phys. **51** (1969) 2425.
42. R. E. D. McClung, J. Chem. Phys. **57** (1972) 5478.
43. J. C. Leicknam, Y. Guissani and S. Bratos, J. Chem. Phys. **68** (1978) 3380.
44. T. E. Bull, J. Chem. Phys. **81** (1984) 3181.
45. C. Dreyfus and T. Nguyen Tan, J. Chem. Phys. **62** (1975) 2492.
46. R. E. D. McClung, Adv. Mol. Relaxation Process **10** (1977) 83.
47. P. S. Hubbard, Phys. Rev. **131** (1963) 1155.
48. P. S. Hubbard, Phys. Rev. **A6** (1972) 2421.
49. G. T. Evans, J. Chem. Phys. **65** (1976) 3030.
50. G. T. Evans, J. Chem. Phys. **67** (1977) 2911.

51. J. G. Powles and G. Rickayzen, *Mol. Phys.* **33** (1977) 1207.
52. R. E. D. McClung, *J. Chem. Phys.* **73** (1980) 2435.
53. R. E. D. McClung, *J. Chem. Phys.* **75** (1981) 5503.
54. S. Perry, V. H. Schiemann, M. Wolfe and J. Jonas, *J. Phys. Chem.* **85** (1981) 2805.
55. T. W. Zerda, J. Schroeder and J. J. Jonas, *J. Chem. Phys.* **75** (1981) 1612.
56. G. Levi, J. P. Marsault, F. Marsault-Heraïl and R. E. D. McClung, *J. Chem. Phys.* **73** (1980) 2443.
57. J. P. Marsault, F. Marsault-Heraïl, and G. Levi, *J. Chem. Phys.* **62** (1975) 893.
58. K. T. Gillen, J. H. Noggle and T. K. Leipert, *Chem. Phys. Lett.* **17** (1972) 505.
59. P. S. Hubbard, *Phys. Rev.* **A9** (1974) 481.
60. D. H. Lee and R. E. D. McClung, *Chem. Phys.* (in press 1986).
61. N. Bloembergen, E. M. Purcell and R. V. Pound, *Phys. Rev.* **73** (1948) 679.
62. H. M. McConnell, *J. Chem. Phys.* **25** (1956) 709.
63. D. Kivelson, *J. Chem. Phys.* **33** (1960) 1094.
64. R. Wilson and D. Kivelson, *J. Chem. Phys.* **44** (1966) 154.
65. A. Spornol and K. Wirtz, *Z. Naturforsch.* **8A** (1953) 522.
66. A. Gierer and K. Wirtz, *Z. Naturforsch.* **8A** (1953) 532.
67. R. W. Mitchell and M. Eisner, *J. Chem. Phys.* **33** (1960) 86.
68. R. W. Mitchell and M. Eisner, *J. Chem. Phys.* **34** (1961) 651.
69. H. Shimizu, *J. Chem. Phys.* **37** (1962) 765.

70. W. B. Moniz and H. S. Gutowsky, J. Chem. Phys. **38** (1963) 1155.
71. R. Wilson and D. Kivelson, J. Chem. Phys. **44** (1960) 4440.
72. F. Perrin, J. Phys. Radium **5** (1934) 497.
73. L. D. Favro, Phys. Rev. **119** (1960) 53.
74. D. E. Woessner, J. Chem. Phys. **37** (1962) 647.
75. D. Kivelson, M. G. Kivelson and I. Oppenheim, J. Chem. Phys. **52** (1970) 1810.
76. C. Hu and R. Zwanzig, J. Chem. Phys. **60** (1974) 4354.
77. F. J. Bartoli and T. A. Litovitz, J. Chem. Phys. **56** (1972) 413.
78. M. Fury and J. Jonas, J. Chem. Phys. **65** (1976) 2206.
79. C. R. Wilke, Chem. Eng. Progr. **45** (1949) 218.
80. P. V. Cheng and H. K. Schachman, J. Polymer Sci. **16** (1955) 19.
81. W. Z. Plachy and D. Kivelson, J. Chem. Phys. **47** (1967) 3312.
82. L. G. Longworth, J. Am. Chem. Soc. **75** (1953) 5705.
83. L. G. Longworth, J. Phys. Chem. **67** (1963) 689.
84. M. Ihnat and D. A. I. Goring, Can. J. Chem. **45** (1967) 2353.
85. J. T. Edward, J. Chem. Ed. **47** (1970) 261.
86. T. C. Farrar and E. D. Becker, **Pulse and Fourier Transform NMR** (Academic Press, New York, 1971).
87. H. Y. Carr and E. M. Purcell, Phys. Rev. **94** (1954) 630.
88. D. E. Woessner, Rev. Sci. Instrum. **31** (1960) 1146.
89. D. L. Hogenboom, K. Krynicki and D. W. Sawyer, Mol. Phys. **40** (1980) 823.
90. P. K. Bhattacharyya and B. P. Dailey, J. Chem. Phys. **63** (1975) 1336.

91. A. Abragam, **The Principles of Nuclear Magnetism** (Clarendon, Oxford, 1961).
92. Y. Ayant, E. Belorizky, J. Alizon and J. Gallice, *J. Physique* **36** (1975) 991.
93. B. K. John, Ph.D. dissertation, University of Alberta, 1984.
94. A. Fratiello, *Mol. Phys.* **7** (1964) 565.
95. H. Raber and M. Mehring, *Chem. Phys.* **26** (1977) 123.
96. C. H. Wang, *J. Magn. Reson.* **9** (1973) 75.
97. A. Bondi, *J. Phys. Chem.* **68** (1964) 441.
98. G. Rudakoff and K. L. Oehme, *Chem. Phys. Lett.* **54** (1978) 342.

CHAPTER V

GENERAL DISCUSSION

In this thesis, the theoretical formulation of the FPL model [1-8] for the rotational dynamics of asymmetric top molecules in liquids and applications of the FPL [8] and EDJ [9,10] models to symmetric and asymmetric top molecules have been presented.

The FPL model is a frictional model in which the molecules experience some intermolecular torques at all times and the fluctuations in the intermolecular torques are relatively weak so that a large number of fluctuations in the torques are required to bring about a substantial change in the angular velocity of the molecule. In the EDJ model, on the other hand, the molecules are assumed to rotate freely except during instantaneous "collisions", and each "collision" causes a large random change in the angular momentum of the molecule. In addition, for symmetric and asymmetric top molecules a new feature has been introduced into the FPL model: the anisotropy in the motional modulation of the angular velocity components which is referred to as frictional anisotropy. Numerical calculations of the FPL reorientational correlation functions, correlation times and spin-rotation functions have shown that these properties are sensitive to the frictional anisotropy.

From the comparison of the reorientational correlation times and spin-rotation functions computed using the FPL model for the case of an isotropic friction tensor with the corresponding correlation times and functions computed using the EDJ model, it was found that the predictions of the two models were almost identical in the limit of rotational diffusion although the basic physical pictures in the FPL and EDJ models are very different. However, the two models were found to predict significantly different behavior in the region where free rotation and precessional effects become important.

The applications of the FPL and EDJ models to the asymmetric top molecules fluorobenzene- d_5 and chlorine dioxide have been presented in Chapter III. The theoretical relationships between the reorientational correlation times and the angular momentum correlation times have been compared with the experimental results obtained from the nuclear relaxation studies of C_6D_5F neat liquid [11]. It was found that the rotational motion of C_6D_5F is better described in terms of the FPL model by incorporating frictional anisotropy than in terms of the EDJ model. The degree of frictional anisotropy was found to be considerable and largely determined by molecular shape effects rather than by electrostatic interactions due to the molecular dipole moment. In the case of the other asymmetric top molecule, ClO_2 [12], the experimental ESR linewidths in several solvents have been compared with the ESR linewidths predicted by the FPL model. It was found that the agreement between theory and experiment was good in strongly interacting solvents, but the

agreement was poor in very weakly interacting solvents. It must be noted, however, that in very weakly interacting solvents, the angular momentum correlation times obtained from the FPL model fit of the observed linewidth data were long ($\tau_x^* > 1$), and that the validity of the FPL model is questionable in this region.

The application of the EDJ and FPL models to the description of rotational motion of 1,3,5-trifluorobenzene- d_3 (TFB), a symmetric top molecule, has been presented in Chapter IV. The theoretical relationships between the reorientational correlation times and the angular momentum correlation times predicted by the two models have been compared with the relationship between the correlation times obtained from nuclear relaxation studies of 0.15 mole fraction solutions of TFB in various solvents. It was found that the rotational motion of this symmetric top molecule in most solutions was well described in terms of the FPL model with frictional anisotropy, as reflected by $\tau_{\parallel}/\tau_{\perp}$, in the range 1 to 2 (τ_{\parallel} and τ_{\perp} are the correlation times for the angular velocity components along the axes parallel to and perpendicular to the molecular symmetry axis). On the other hand, the observed variations of the reorientational correlation times with the angular momentum correlation times in most solutions did not agree with the predictions of the EDJ model, although the correlation time data showed the inverse proportionality between the reorientational correlation times and the angular momentum correlation times predicted by the EDJ model. This result and the result from the application to the asymmetric top molecule,

C_6D_5F , indicate that the effect of frictional anisotropy is important in the description of the rotational motion of symmetric and asymmetric top molecules.

The viscosity and temperature dependence of the reorientational correlation times of TFB in various solvents has been analyzed in terms of a modified Debye equation [13-19]. The values of the anisotropic interaction parameter, κ [12,20], were found to be relatively small compared to 1 (the "stick" hydrodynamic case), which means that TFB experiences relatively weak anisotropic intermolecular interactions in the solvents studied in this work, and the boundary conditions appropriate to these solute-solvent systems lie closer to "slip" than to "stick". The anisotropic interaction parameter, κ , of TFB shows significant dependence on the solvent. This solvent dependence of κ has been analyzed in terms of solvent size and solvent dipole moment and it was found that the variation of κ with solvent was attributed mainly to the variation in the dipole moment of the solvent molecules. Hence one may conclude that the solvent dipole moment is a decisive factor for determining κ when the solute and the solvent are of comparable size for a given solute.

It was found that the degree of frictional anisotropy generally decreased as κ and the solvent dipole moment increased. This was interpreted in terms of the effects of molecular shape of TFB and electrostatic interactions between C-F bond dipole moments and solvent dipole moments. When the solvent dipole moment is small, molecular shape effects make a large contribution to the anisotropy

of the intermolecular potential and rotation of the benzene ring about the C_3 axis (τ_{\parallel}) is less hindered than rotation of the ring about the C_2 axis (τ_{\perp}) so that $\tau_{\parallel} > \tau_{\perp}$. On the other hand, when the solvent dipole moment is large, electrostatic interactions between bond dipoles on solute and solvent molecules make significant contributions to the anisotropy of the intermolecular potential and both rotations about C_3 and C_2 axes involving motion of the C-F bond dipole are retarded by the electrostatic interactions so that $\tau_{\parallel} \sim \tau_{\perp}$.

References

1. M. Fixman and K. Rider, J. Chem. Phys. **51** (1969) 2425.
2. P.S. Hubbard, Phys. Rev. **A6** (1972) 2421.
3. P.S. Hubbard, Phys. Rev. **A8** (1974) 1429.
4. G.T. Evans, J. Chem. Phys. **65** (1976) 3030.
5. G.T. Evans, J. Chem. Phys. **67** (1977) 2911.
6. J.G. Powles and G. Rickayzen, Mol. Phys. **33** (1977) 1207.
7. R.E.D. McClung, J. Chem. Phys. **73** (1980) 2435.
8. R.E.D. McClung, J. Chem. Phys. **75** (1981) 5503.
9. R.E.D. McClung, J. Chem. Phys. **57** (1972) 5478.
10. T.E. Bull, J. Chem. Phys. **81** (1984) 3181.
11. R.A. Assink and J. Jonas, J. Chem. Phys. **57** (1972) 3329.
12. R.E.D. McClung and D. Kivelson, J. Chem. Phys. **49** (1968) 3380.
13. G.R. Alms, D.R. Bauer, J.I. Brauman, and R. Pecora, J. Chem. Phys. **58** (1973) 5570.
14. G.R. Alms, D.R. Bauer, J.I. Brauman, and R. Pecora, J. Chem. Phys. **59** (1973) 5310.
15. D.R. Bauer, G.R. Alms, J.I. Brauman, and R. Pecora, J. Chem. Phys. **61** (1974) 2255.
16. D.R. Bauer, J.I. Brauman, and R. Pecora, J. Am. Chem. Soc. **96** (1974) 6840.
17. G.D.J. Phillies and D. Kivelson, J. Chem. Phys. **71** (1979) 2575.
18. D. Kivelson and P.A. Madden, Ann. Rev. Phys. Chem. **31** (1980) 523.

19. M. Furry and J. Jonas, J. Chem. Phys. 65 (1976) 2206.
20. D. Kivelson, M.G. Kivelson, and I. Oppenheim, J. Chem. Phys. 52 (1970) 1810.

APPENDIX I

EDJ MODEL FOR ASYMMETRIC TOP MOLECULES

Bull [1] and Leicknam et al. [2] have discussed the EDJ model for asymmetric top molecules. Bull's results have been used in Chapters II and III of this thesis, so it is appropriate to give brief derivations of these important results in this appendix.

A. EDJ reorientational correlation times

In the EDJ model, we can define a general diffusion trajectory by defining the angular momentum vectors $J_1, J_2, J_3, \dots, J_n$ of the molecule during the n successive diffusive steps, and the times $t_1, t_2, t_3, \dots, t_{n-1}$ at which each "collision" occurs. Suppose that at time zero, the molecular frame (the principal coordinate system) is related to the laboratory frame by the Euler angles Ω_0 . The angular momentum vector J_1 is fixed in space and its orientation is described by the Euler angles Ω_1 with respect to the molecular frame at time zero. We can construct a "J" frame in which the z axis lies along the direction of the angular momentum vector. During $0 < t < t_1$, the transformation from the "J" frame to the molecular frame is given by $D^{(j)}[\Delta\Omega(t)]$, where $\Delta\Omega(t)$ represents the Euler angles which describe the reorientation of the molecule during the first diffusive step. Hence, for the first step, the transformation

from the laboratory frame to the molecular frame is given by

$$D^{(j)}[\Omega(t)]_1 = D^{(j)}[\Omega_0] D^{(j)}[\Omega_1] D^{(j)}[\Delta\Omega(t)] \quad (\text{AI-1})$$

At the first collision (time t_1) the angular momentum is randomized and its orientation with respect to the molecular frame at time t_1 is specified by the Euler angles Ω_2 . During the second diffusive step, the transformation from the "J" frame to the molecular frame is described by $D^{(j)}[\Delta\Omega(t-t_1)]$. Hence the transformation from the laboratory frame to the molecular frame is given by

$$D^{(j)}[\Omega(t)]_2 = D^{(j)}[\Omega_0] D^{(j)}[\Omega_1] D^{(j)}[\Delta\Omega(t_1)] D^{(j)}[\Omega_2] D^{(j)}[\Delta\Omega(t-t_1)] \quad (\text{AI-2})$$

This process continues and the general transformation relating the laboratory components of a spherical tensor of rank j to its components in the molecular frame during the n -th diffusive step will be given by

$$D^{(j)}[\Omega(t)]_n = D^{(j)}[\Omega_0] \prod_{i=1}^n \{ D^{(j)}[\Omega_i] D^{(j)}[\Delta\Omega(t_i - t_{i-1})] \} \quad (\text{AI-3})$$

In this equation, we have made the identifications $t_0 \equiv 0$ and $t_n = t$.

In order to calculate the reorientational correlation times, we must evaluate the ensemble average $\langle D_{mk}^{(j)}[\Omega_0] D_{mk}^{(j)}[\Omega(t)] \rangle$. This ensemble average is over all possible trajectories and must involve

averages over (i) the number of "collisions" experienced by the molecule up to time t , (ii) the times at which the "collisions" occurred, (iii) the angular momentum in each diffusive step, and (iv) the initial molecular orientation.

The probability that a molecule undergoes $n-1$ "collisions" between time zero and time t , on the time intervals t_1 to t_1+dt_1 , t_2 to t_2+dt_2 , ..., t_{n-1} to $t_{n-1}+dt_{n-1}$, is

$$dP_{n-1}[t_1, t_2 \dots t_{n-1} | t] = dt_1 dt_2 \dots dt_{n-1} \tau_J^{-(n-1)} \exp(-t/\tau_J). \quad (AI-4)$$

with an average time τ_J between "collisions". Therefore

$$\begin{aligned} \langle D_{mk}^{(j)*} [Q_0] D_{mk}^{(j)} [Q(t)] \rangle = \\ \sum_{n=1}^{\infty} \tau_J^{-(n-1)} \exp(-t/\tau_J) \int_0^t dt_{n-1} \int_0^{t_{n-1}} dt_{n-2} \dots \int_0^{t_2} dt_1 \\ \times \langle D_{mk}^{(j)*} [Q_0] D_{mk}^{(j)} [Q(t)]_n \rangle \end{aligned} \quad (AI-5)$$

Here $D^{(j)} [Q(t)]_n$ is given by Eq. (AI-3), and one obtains

$$\begin{aligned} \langle D_{mk}^{(j)*} [Q_0] D_{mk}^{(j)} [Q(t)]_n \rangle = \sum_{a_1 \dots a_n} \langle D_{mk}^{(j)*} [Q_0] D_{mk}^{(j)} [Q_0] \rangle_{Q_0} \\ \times \langle \{ D^{(j)} [Q_1] D^{(j)} [Q(t_1)] \}_{a_1 a_2} \rangle_{J_1} \times \dots \\ \times \langle \{ D^{(j)} [Q_n] D^{(j)} [Q(t_n - t_{n-1})] \}_{a_n k'} \rangle_{J_n} \end{aligned} \quad (AI-6)$$

The subscripted brackets denote ensemble averages over the variables indicated.

The ensemble average over the initial orientation Q_0 is independent of all other averages and, in the absence of any strong applied perturbations, all orientations are equally probable so that

$$\langle D_{mk}^{(j)*}(Q_0) D_{ma_1}^{(j)}(Q_0) \rangle_{Q_0} = (2j+1)^{-1} \delta_{k,a_1} \quad (AI-7)$$

Hence the reorientational correlation function $G_{kk'}^{(j)}(t)$ is given by

$$\begin{aligned} G_{kk'}^{(j)}(t) &= \frac{\langle D_{mk}^{(j)*}(Q_0) D_{mk'}^{(j)}(Q(t)) \rangle}{\langle |D_{mk}^{(j)}(Q_0)|^2 \rangle} \\ &= \sum_{n=1}^{\infty} \tau_J^{-(n-1)} \exp(-t/\tau_J) \int_0^t dt_{n-1} \dots \int_0^{t_2} dt_1 \\ &\quad \times \delta_{k,a_1} \sum_{a_2 \dots a_n} \prod_{i=1}^n \langle D_{a_i}^{(j)}(Q_1) D_{a_{i+1}}^{(j)}(\Delta Q(t_1 - t_{i-1})) \rangle_{a_1 a_{i+1}} J_1 \end{aligned} \quad (AI-8)$$

The reorientational correlation time, which is the zero frequency Fourier transform of reorientational correlation function, is given by

$$\tau_{\theta}^{jkk'} = \int_0^{\infty} G_{kk'}^{(j)}(t) dt = \sum_{n=1}^{\infty} \tau_J^{-(n-1)} \int_0^{\infty} \exp(-t/\tau_J) dt \int_0^t dt_{n-1} \dots \int_0^{t_2} dt_1$$

$$\begin{aligned}
 & \times \delta_{k,a_1} \sum_{a_2 \dots a_n} \prod_{i=1}^n \langle \{D^{(j)}[\Omega_i] D^{(j)}[\Delta\Omega(t_i - t_{i-1})]_{a_i a_{i+1}} \rangle_{J_i} \\
 & = \sum_{n=1}^{\infty} \tau_J^{-(n-1)} \delta_{k,a_1} \sum_{a_2 \dots a_n} \prod_{i=1}^n \int_0^{\infty} d(t_i - t_{i-1})
 \end{aligned}$$

$$\langle \{D^{(j)}[\Omega_i] D^{(j)}[\Delta\Omega(t_i - t_{i-1})]_{a_i a_{i+1}} \rangle_{J_i} \exp\{-(t_i - t_{i-1})/\tau_J\} \quad (\text{AI-9})$$

If we introduce $A_{kk'}$, which is defined as

$$A_{kk'} = \int_0^{\infty} d\tau \langle \{D^{(j)}[\Omega] D^{(j)}[\Delta\Omega(\tau)]\}_{kk'} \rangle_J \exp(-\tau/\tau_J) \quad (\text{AI-10})$$

then $\tau_{\theta}^{jkk'}$ can be written as

$$\tau_{\theta}^{jkk'} = A_{kk'} + \frac{1}{\tau_J} \sum_{a_2} A_{ka_2} A_{a_2 k'} + \frac{1}{\tau_J^2} \sum_{a_2, a_3} A_{ka_2} A_{a_2 a_3} A_{a_3 k'} + \dots$$

$$\tau_{\theta}^{jkk'} = \{ \lambda [1 - \frac{1}{\tau_J} A]^{-1} \}_{kk'} \quad (\text{AI-11})$$

where λ is the unit matrix, since the series in Eq. (AI-9) is a geometric series. Eq. (AI-9) is the result used in Eqs. (II-51) and (III-6) of Chapters II and III.

B. EDJ spin-rotational relaxation

The spin-rotation interaction is described by Eq. (AI-11). This Hamiltonian can be written as

$$H_{SR} = I_x \omega_x C_x S_x + I_y \omega_y C_y S_y + I_z \omega_z C_z S_z \quad (\text{AI-12})$$

where ω_x , ω_y , and ω_z are not in reduced units.

When ω and S are expressed in terms of spherical tensor components, then one obtains

$$\begin{aligned} H_{SR} = & (S_+ \omega_{+1} + S_- \omega_{-1}) \left(\frac{1}{2} I_x C_x - \frac{1}{2} I_y C_y \right) + S_0 \omega_0 I_z C_z \\ & + (S_+ \omega_{-1} + S_- \omega_{+1}) \left(-\frac{1}{2} I_x C_x - \frac{1}{2} I_y C_y \right) \end{aligned} \quad (\text{AI-13})$$

We can construct the irreducible spherical tensors, T_{Lk} , from the product of S and ω [3].

$$T_{Lk} = \sum_{k'} C(11L; k', k-k', k) S_{k'} \omega_{k-k'} \quad (\text{AI-14})$$

where $C(11L; k', k-k', k)$ are the Clebsch-Gordan coefficients. In terms of these irreducible tensor components, H_{SR} can be rewritten as

$$H_{SR} = \sum_{L,k} I_z C_k^{(L)} T_{Lk} \quad (\text{AI-15})$$

where the $C_k^{(L)}$ are given by

$$C_{\pm 2}^{(2)} = \frac{1}{2}(I_x C_x - I_y C_y)/I_z$$

$$C_0^{(2)} = \frac{2}{\sqrt{6}}[I_z C_z - \frac{1}{2}(I_x C_x + I_y C_y)]/I_z$$

$$C_0^{(0)} = \frac{-1}{\sqrt{3}}[I_x C_x + I_y C_y + I_z C_z]/I_z \quad (\text{AI-16})$$

No other spherical tensor components are involved in the spin-rotation interaction.

From Eq. (AI-14) and Eq. (AI-15),

$$H_{SR} = \sum_{L,k} I_z C_k^{(L)} \sum_{k'} C(11L; k', k-k', k) S_k \omega_{k-k'} \quad (\text{AI-17})$$

Since \mathbf{S} is quantized in the laboratory coordinate system, it is convenient to transform S_k into the corresponding components S_m in the laboratory coordinate system as follows:

$$S_k = \sum_m S_m D_{mk}^{(1)} [Q(t)]_n \quad (\text{AI-18})$$

where $D^{(1)} [Q(t)]_n$ is the transformation from laboratory to molecular frames at time t during the n -th diffusive step and is given by Eq.

(AI-3).

From Eq. (AI-17) and Eq. (AI-18),

$$H_{SR} = \sum_m S_m \sum_{L,k,k'} D_{mk}^{(1)} [Q(t)]_n I_z C_k^{(L)} C(11L; k', k-k', k) \omega_{k-k'}$$

$$= \sum_m S_m V_m(t) \quad (AI-19)$$

In order to determine the spin-rotational relaxation rate, we must evaluate the ensemble average $\langle V_m(t) V_m^*(0) \rangle$. In the ED model each collision randomizes the angular momentum. Hence we need to consider the ensemble average only for the first diffusive step (i.e. $n = 1$ in Eq. (AI-18) and Eq. (AI-3)) so that $V_m(t)$ becomes

$$\begin{aligned} V_m(t) &= \sum_{L,k,k'} D_{mk}^{(1)}[\Omega(t)]_1 I_z C_k^{(L)} C(11L; k', k-k', k) \omega_{k-k'} \\ &= \sum_{L,k,k'} \{ D^{(1)}[\Omega_0] D^{(1)}[\Omega_1] D^{(1)}[\Delta\Omega(t)] \}_{mk} \\ &\quad \times I_z C_k^{(L)} C(11L; k', k-k', k) \omega_{k-k'} \\ &= \sum_{L,k,k'} \{ D^{(1)}[\Omega_0] D^{(1)}[\Omega_1] \}_{m\ell} D_{\ell k}^{(1)}[\Delta\Omega(t)] \\ &\quad \times I_z C_k^{(L)} C(11L; k', k-k', k) \omega_{k-k'} \end{aligned} \quad (AI-20)$$

The components of the angular velocity in the molecular coordinate system are given by

$$\begin{aligned} \omega_1 &= J \left[\frac{1}{2} D_{0,1}^{(1)}[\Delta\Omega(t)] \left(\frac{1}{I_x} + \frac{1}{I_y} \right) + \frac{1}{2} D_{0,-1}^{(1)}[\Delta\Omega(t)] \left(\frac{1}{I_y} - \frac{1}{I_x} \right) \right. \\ &\quad \left. + \delta_{1,0} D_{1,0}^{(1)}[\Delta\Omega(t)] \left(\frac{1}{I_z} - \frac{1}{I_y} \right) \right] \end{aligned} \quad (AI-21)$$

where J is the magnitude of the angular momentum. Note that

$$D_{\ell, k}^{(1)}[\Delta\Omega(t)] D_{0, k-k}^{(1)}[\Delta\Omega(t)] \\ = \sum_N C(11N; \ell 0 \ell) C(11N; k', k-k', k) D_{\ell, k}^{(N)}[\Delta\Omega(t)] \quad (\text{AI-22})$$

and

$$\sum_{k'} C(11L; k', k-k', k) C(11N; k'', k-k', k) = \delta_{N,L} \quad (\text{AI-23})$$

Using Eqs. (AI-20), (AI-21), (AI-22), and (AI-23), one obtains

$$V_m(t) = \sum_{\ell} \{ D^{(1)}[\Omega_0] D^{(1)}[\Omega_1] \}_{m\ell} \sum_{L, K} J C_k^{(L)} \left\{ \frac{1}{2} \left(\frac{I_z}{I_x} + \frac{I_z}{I_y} \right) \right. \\ \times C(11L; \ell 0 \ell) D_{\ell, k}^{(L)}[\Delta\Omega(t)] \\ \left. + \left(1 - \frac{I_z}{I_y} \right) C(11L; k, 0, k) D_{00}^{(1)}[\Delta\Omega(t)] D_{\ell k}^{(1)}[\Delta\Omega(t)] \right. \\ \left. + \frac{1}{2} \left(\frac{I_z}{I_y} - \frac{I_z}{I_x} \right) \sum_{k'} C(11L; k', k-k', k) D_{0, k'-k}^{(1)}[\Delta\Omega(t)] D_{\ell k}^{(1)}[\Delta\Omega(t)] \right\} \\ = \sum_{\ell} \{ D^{(1)}[\Omega_0] D^{(1)}[\Omega_1] \}_{m\ell} \sum_{L, k} C_k^{(L)} w_{\ell k}^{(L)}(t) \quad (\text{AI-24})$$

Here we have defined $w_{\ell k}^{(L)}(t)$ to represent the time dependent part.

Then,

$$\begin{aligned}
\langle v_m(t) v_m^*(0) \rangle &= \sum_{\lambda, \lambda'} \langle \{ D^{(1)} [Q_0] D^{(1)} [Q_1] \}_{m\lambda} \{ D^{(1)} [Q_0] D^{(1)} [Q_1] \}_{m\lambda}^* \rangle \\
&\times \sum_{L, L', k, p} C_k^{(L)} C_p^{(L')*} \langle w_{\lambda k}^{(L)}(t) w_{\lambda p}^{(L')*}(0) \rangle \exp(-t/\tau_J) \\
&= \frac{1}{3} \sum_{\lambda} \sum_{L, L', k, p} C_k^{(L)} C_p^{(L')*} \langle w_{\lambda k}^{(L)}(t) w_{\lambda p}^{(L')*}(0) \rangle \exp(-t/\tau_J)
\end{aligned}
\tag{AI-25}$$

Hence the spin-rotational contribution to the spin relaxation time is

$$\begin{aligned}
\frac{1}{T_1} &= \frac{2}{\hbar^2} \int_0^\infty \langle v_1(t) v_1^*(0) \rangle dt \\
&= \frac{2}{3\hbar^2} \sum_{L, L', k, p} C_k^{(L)} C_p^{(L')*} \int_0^\infty \sum_{\lambda} \langle w_{\lambda k}^{(L)}(t) w_{\lambda p}^{(L')*}(0) \rangle \exp(-t/\tau_J) dt \\
&= \frac{2}{3\hbar^2} \tau_J I_z k_B T \sum_{L, L', k, p} C_k^{(L)} C_p^{(L')*} F_{k,p}^{(L, L')}
\end{aligned}
\tag{AI-26}$$

where $F_{k,p}^{(L, L')}$ are spin-rotation factors defined as

$$F_{k,p}^{(L, L')} = (\tau_J I_z k_B T)^{-1} \int_0^\infty \sum_{\lambda} \langle w_{\lambda k}^{(L)}(t) w_{\lambda p}^{(L')*}(0) \rangle \exp(-t/\tau_J) dt
\tag{AI-27}$$

Eq. (AI-26) is the result used in Eqs. (II-53) and (III-8) in Chapters II and III.

References

1. T.E. Bull, J. Chem. Phys. **81** (1984) 3181.
2. J.C. Leicknam, Y. Guissani, and S. Bratos, J. Chem. Phys. **68** (1978) 3380.
3. M.E. Rose, **Elementary Theory of Angular Momentum** (Wiley, New York, 1957) Chap. IV.

APPENDIX II

INSTRUMENTATION FOR NMR EXPERIMENTS

Nuclear spin relaxation times and translational diffusion coefficients were measured using a Bruker SXP 4-100 pulsed NMR spectrometer. This spectrometer is operated under the control of a Nicolet 1180 minicomputer along with a Nicolet 293A pulse programmer. It has four independent radio frequency (rf) channels which can be gated on or off by the Nicolet 293A pulse programmer. The phase of the rf pulse can be adjusted independently in each of the four channels. Tuning the spectrometer to the required operating frequency is carried out by adjusting two variable capacitors on the high power amplifier and on the NMR probe arm. The signal detection part of the spectrometer consists of a preamplifier, an rf filter with adjustable bandwidth (0.1-100 kHz), and a detector which can be operated in phase sensitive or diode detection mode. When it is operated in the diode detection mode, the detector gives a signal which is proportional to the square root of the sum of the squares of the absorption and dispersion signals. The signal in the diode detection mode is not affected by moderate changes in magnetic field or operating frequency. Phase sensitive detection mode has the advantage of linearity of response over the full dynamic range of the detector and better signal-to-noise ratio, particularly at low signal intensities.

The pulse lengths corresponding to 90° and 180° tip angles were determined by adjusting control knobs on the Nicolet 1180 minicomputer. Using a [pulse-acquire-wait] sequence, the diode-detected signal should be a maximum for a 90° pulse and it should be a minimum for a 180° pulse. The spectrometer was tuned before determination of the pulse lengths. In the experiments requiring rf pulses of different phases, the relative phases of the pulses on each pulse channel were adjusted manually by observing the FID in the phase sensitive detection mode after a 90° pulse.

The temperature of the sample was controlled by a Bruker B-ST temperature control unit which controlled the sample temperature to ± 0.5 K. A Doric Trendicator 400 digital thermometer with a copper-constantan thermocouple was used to measure the temperature. The sample was allowed to equilibrate at each temperature for 15-20 minutes after inserting it into the probe.

A. Measurement of T_1

T_1 measurements were made using the $180^\circ - \tau - 90^\circ$ pulse sequence. This pulse sequence can be represented by $[180^\circ - \tau_0 - 90^\circ]$ -sample-wait- $[180^\circ - (\tau_0 + \Delta) - 90^\circ]$ -sample-wait- $[180^\circ - (\tau_0 + 2\Delta) - 90^\circ]$..., where τ_0 and Δ are the initial delay and the increment to the delay, respectively. The "wait" time is five times the approximate T_1 value. Typically about ten τ values were used such that $\tau_0 + 10\Delta \approx 3T_1$. The initial value τ_0 was chosen as 0.8 times the approximate T_1 value. The FID after the 90° pulse was detected in the diode

detection mode and digitized. The intensity of the magnetization, $M(\tau)$, was determined by integrating the initial part of the FID. The total acquisition time for the complete FID was in the range of 10-40 ms. The signal intensity $M(\tau)$ was fit to

$$M(\tau) = A_1 + B_1 \exp(-\tau/T_1) \quad (\text{AII-1})$$

using a non-linear least squares analysis algorithm [1] with A_1 , B_1 , and T_1 as variable parameters. The computer program was designed to make repetitive T_1 measurements and to calculate the variance and the standard deviation. The diode detection mode was used for signal acquisition since it was insensitive to moderate variations in the magnetic field over the period of time required to carry out the repetitive T_1 measurements.

B. Measurement of translational diffusion coefficients

The translational diffusion coefficients of TFB in various solvents were measured by the stationary field gradient spin echo technique [2-4]. The amplitude of the spin echo from equivalent spins is modulated by diffusion of spins along a magnetic field gradient in the sample. The effective T_2 relaxation time, $T_{2\text{eff}}$, in the presence of a field gradient is affected by the diffusion coefficient D . Hence, for the experimental determination of D , the transverse relaxation time is measured both in the presence, and in the absence of a magnetic field gradient, using the Carr-Purcell-

Meiboom-Gill (CPMG) pulse sequence [3,5]. The CPMG pulse sequence can be represented by $90^\circ_x - \tau/2 - [180^\circ_y - \tau]_n$. This pulse sequence minimizes the cumulative effect of inaccuracies in setting the 180° pulse length by applying the 180° pulses along the y axis, i.e. at 90° phase difference relative to the initial 90° pulse. The 90°_x pulse creates transverse magnetization which is allowed to dephase for a time period $\tau/2$. The 180°_y pulse is applied and refocusses the dephased magnetization components. At time $\tau/2$ after the 180°_y pulse, a spin echo is formed and detected. A train of spin echoes is formed by successive 180°_y pulses and τ delays. The amplitude $M(t)$ of the spin echo at time t in the absence of a magnetic field gradient is given by [2]

$$M(t) = A_2 + B_2 \exp(-t/T_2) \quad (\text{AII-2})$$

where A_2 , B_2 and T_2 are fitting parameters. In the presence of a magnetic field gradient of magnitude G , the amplitude of the spin echo at time t is [2,4]

$$M(t) = A_3 + B_3 \exp[-t/T_{2\text{eff}}] \quad (\text{AII-3})$$

where A_3 , B_3 and $T_{2\text{eff}}$ are fitting parameters and

$$1/T_{2\text{eff}} = 1/T_2 + \gamma^2 G^2 D \tau^2 / 3 \quad (\text{AII-4})$$

where γ is the magnetogyric ratio of the spin of interest and D is the translational diffusion coefficient. The translational diffusion coefficient D was determined from Eq. (AII-4) with the field gradient G obtained from calibration using C_6F_6 (see below).

At the beginning of the experiment, the relative phases of the 90° and 180° pulses were adjusted using the rf phase control knobs on the NMR spectrometer and the pulse lengths were optimized by adjusting the control knobs on the Nicolet 1180 minicomputer. The signal was detected in the phase sensitive detection mode at the maximum of the spin echo amplitude. In the first part of the experiment, the normal T_2 of ^{19}F on TFB was measured in the absence of a magnetic field gradient. The value of T_2 was determined by fitting to Eq. (AII-2) using a non-linear least squares analysis program [1]. In the second part of the experiment, T_{2eff} was measured in the presence of a static magnetic field gradient. A magnetic field gradient was generated by passing current through a pair of copper coils mounted on the aluminum side plates on both sides of the probe. The current to the coils was supplied by a filtered D.C. power supply (Model D-6127, Electro Products Laboratories Inc.) and was gated on or off under computer control in synchronization with the CPMG pulse sequence using programmable level line 7 of the Nicolet 293A unit. The current passing through the coils was monitored with a Simpson digital multimeter (Model 461). The magnetic field gradient was calibrated using C_6F_6 whose translational diffusion coefficients are known [6].

References

1. D.W. Marquardt, R.G. Bennett, and E.J. Burrell, J. Molec. Spectroscopy **7** (1961) 269.
2. T.C. Farrar and E.D. Becker, **Pulse Fourier Transform NMR** (Academic Press, New York, 1971).
3. H.Y. Carr and E.M. Purcell, Phys. Rev. **94** (1954) 630.
4. D.E. Woessner, Rev. Sci. Instrum. **31** (1960) 1146.
5. S. Meiboom and D. Gill, Rev. Sci. Instrum. **29** (1958) 688.
6. D.L. Hogenboom, K. Krynicky, and D.W. Sawyer, Mol. Phys. **40** (1980) 823.